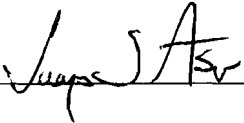AN ABSTRACT OF THE THESIS OF

Juliet A. Wallace for the Master of Science in Physical Sciences presented on July 7th, 2000.

Title: Temporal Studies of Deciduous Forests in Northeastern Kansas Using Landsat Thematic Mapper Images

Abstract Approved: _____

Committee Members: Dr. James Aber

Dr. Rodney J. Sobieski

Dr. Firooza Pavri

Eight years of Landsat Thematic Mapper (TM) data were used to assess vegetation changes in two temperate deciduous forests located on the Fort Leavenworth Military Reservation in northeastern Kansas, U.S.A. The primary forests are an upland oak-hickory hardwood forest and a floodplain cottonwood-sycamore forest.

Normalized Difference Vegetation Index (NDVI) and the ratio of TM band 5 to band 4 (moisture stress index) were used to detect changes in health and vigor of the forests. NDVI data indicate a one- to two-year lag in the full response of the forests to changes in precipitation during the drought years from 1987 to 1989. The forests also display different responses at the start of the drought, with the cottonwood forest experiencing increased NDVI and the hardwood forest experiencing a decline.

Principal component analysis (PCA) and image differencing were employed to determine the time and location of NDVI changes. The data indicate that the edges of the forests have experienced the greatest variations in NDVI over the study period. All edges of the hardwood forest were affected, while the northern edge of the cottonwood forest was most affected. PCA was also successful in isolating the spectral responses of different forest stands within the floodplain forest.

The band 5:4 ratios indicate greatest stress in both forests in 1989 and values are generally consistent with precipitation data. In 1988, opposite responses were observed, with increased stress in the hardwood forest and decreased stress in the cottonwood forest. This result is consistent with NDVI data. In addition, the raw band 5:4 ratios for each forest display different spectral responses, which may be useful in differentiating similar types of forests on remotely sensed images.

Temporal Studies of Deciduous Forests in Northeastern Kansas

Using Landsat Thematic Mapper Images

————————————————————————

A Thesis

Presented to

The Physical Sciences Department

Emporia State University

————————————————————————

In Partial Fulfillment

Of the Requirements for the Degree

Master of Science, Physical Sciences
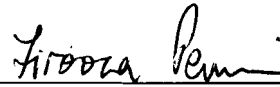
Earth Science Concentration
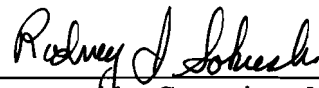
————————————————————————

By

Juliet A. Wallace

July 7, 2000
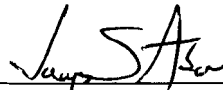
Approved by Major Advisor
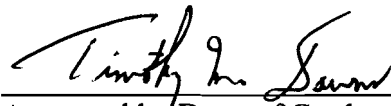Dr. James Aber

Approved by Committee Member
Dr. Firooza Pavri

Approved by Committee Member
Dr. Rodney J. Sobieski

Approved by Division Chair
Dr. DeWayne Backhus

Approved by Dean of Graduate
Studies And Research
Dr. Timothy M. Downs

Acknowledgments

I would like to express my most sincere gratitude to Dr. James Aber for his guidance and support throughout. I would also like to thank committee members Dr. Rodney J. Sobieski and Dr. Firooza Pavri who provided valuable insights and comments. My thanks to Matt Nowak, forester at the Fort Leavenworth Military Reservation, for his assistance on usage of the forests.

I would also like to express appreciation to the Physical Sciences Division of Emporia State University, and Dr. Aber for the opportunity to undertake this program under the Kansas NASA EPSCoR grant.

TABLE OF CONTENTS

List of Tables

List of Figures

Chapter 1

Introduction

1.1 Change detection

The need to monitor changes in the environment over the long term is paramount for

maintaining healthy Earth systems. Vegetation is one of the key indicators of such

change, and many temporal studies are being conducted globally in an effort to

understand the causes and effects of environmental degradation.

This study examines changes in two temperate deciduous forest stands located in

northeastern Kansas, United States. Eight years of Landsat Thematic Mapper imagery

from the 10-year period between 1987 and 1997 are used. During this time, a severe

drought was experienced in 1988-1989 and severe flooding occurred in 1993. The

Normalized Difference Vegetation Index (NDVI) (Rouse *et al.*, 1974) is one of the most

commonly used vegetation indices for determining the extent and health of vegetation

cover and is utilized in this study as the primary indicator of vegetation growth and vigor.

The techniques employed in this study compare yearly NDVI for each forest. Time series

analysis employing principal component analysis and image differencing techniques were

used to assess varying temporal changes. In addition, ratios of band 5 to band 4 for

Landsat TM images were used in the analyses, based on the premise that decreased leaf

water content results in increased reflectance in band 5 (Tucker, 1980). All data were

compared with precipitation, temperature, Palmer Drought Severity Index (PDSI) and available tree-ring data.

1.2 Location

The study forests are located in the Fort Leavenworth Military Reservation in northeastern Leavenworth County, Kansas, USA (Fig.1). The study area lies between latitudes 39° 20' N and 39° 25' N and longitudes 94° 55' W and 95° 00' W. Both forests are comprised of deciduous stands, but exist in different environments. The first area is located on limestone bedrock in the upland area west of the Missouri River, in the western part of the military reservation. The second area lies on the floodplain of the Missouri River, east of the Sherman Army Airfield. For this study, the two forest areas are called the hardwood and cottonwood forests for the upland and floodplain areas respectively.

1.3 Description of forests

Freeman *et al.* (1997), identified two forest stands on each site. Fig. 2 shows the location of these forest stands. Forest A is described by Freeman *et al.* (1997) as a white oak - shagbark hickory forest. It is a 150 to 200 year-old mature forest, which consists predominantly of drought resistant species of oak including white oak, northern red and bur oaks. Bitternut and shagbark are the common hickory species. Other hardwoods
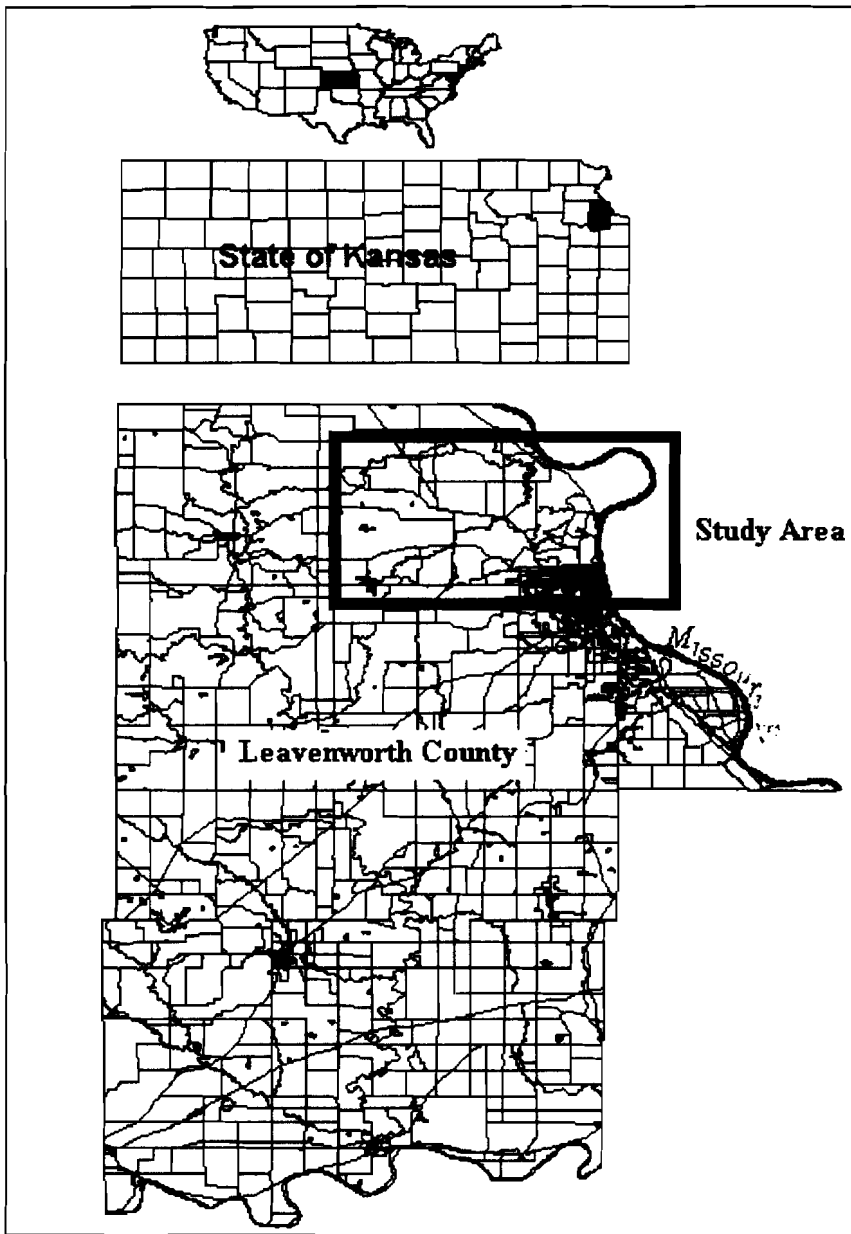
Fig. 1. Location map of study area.
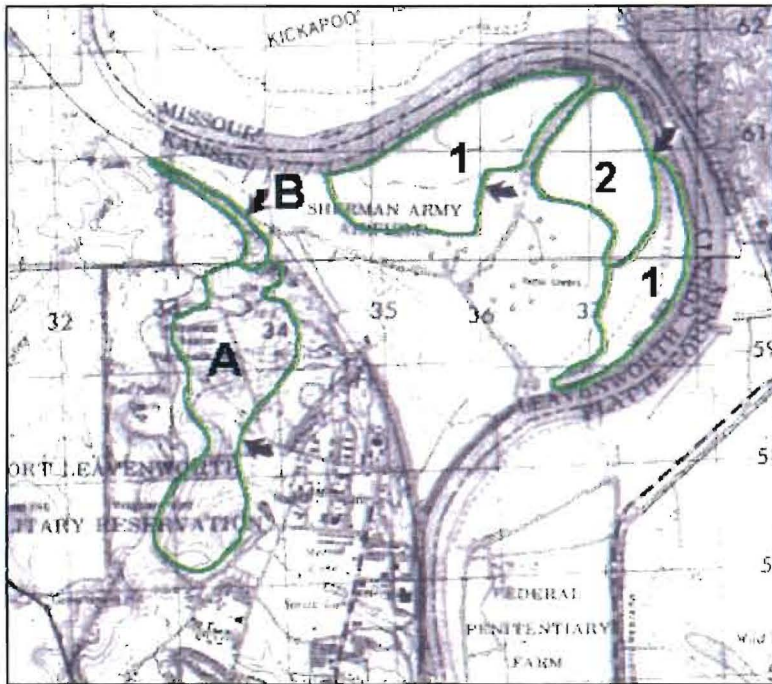
Fig. 2. Modified from Freeman *et al.*, 1997. Upland forest area showing two forest stands. **A** - *Quercus alba-Carya ovata/Ostrya virginiana* (white oak - shagbark hickory) forest. **B** - *Acer saccharum-Tilia americana-Quercus rubra/Ostrya virginiana* (maple-basswood) forest. Floodplain of the Missouri River with two forests. **1** - *Populus deltoides - Platanus occidentalis* (cottonwood - sycamore) Floodplain forest. **2** - *Carya illinoensis - Celtis laevigata* (pecan - sugarberry) floodplain forest.

include American elm, green ash, box elders, backbrush, hackberry, basswood, pecan, silver maple, sycamore and walnut. Understory species include cluster sanicle, large flowered tickclover and wood nettle (Fig. 3). This forest is located on approximately 400 hectares and varies in altitude from approximately 240 to 325 meters (800 to 1070 feet). Small tracts of tallgrass prairie are found in open areas within the forest. The forest outlined by Freeman *et al.* (1997) is contained in the eastern three-quarters of the oak-hickory forest studied. Fig. 4 shows a digital orthophoto quarter quadrangle (DOQQ) and a digital elevation model of the forests.

Forest B is defined by Freeman *et al.* (1997) as a maple-basswood forest. It occupies approximately 18 hectares and consists primarily of northern red oak, basswood and sugar maple with pawpaw as the dominant understory tree.

The floodplain area supports two forest types on approximately 550 hectares, in the large meander. Forest 1 occurs as two stands of cottonwood-sycamore floodplain forest. The southern stand is a mature to old-growth forest while the northern stand is an early to mid-successional forest. The dominant overstory is the plains cottonwood. Boxelder, red mulberry, green ash and American elm are also common.

A high quality pecan-sugarberry forest separates these cottonwood-sycamore stands. Mature to old-growth pecans are the dominant overstory species. Boxelder, red mulberry, American elm, green ash and hackberry are also present. Sugarberry is not present but is replaced by hackberry.

Fig. 3.

Above: Upland oak-hickory hardwood forest.

Below: Understory of forest. Pictures taken July, 1999.
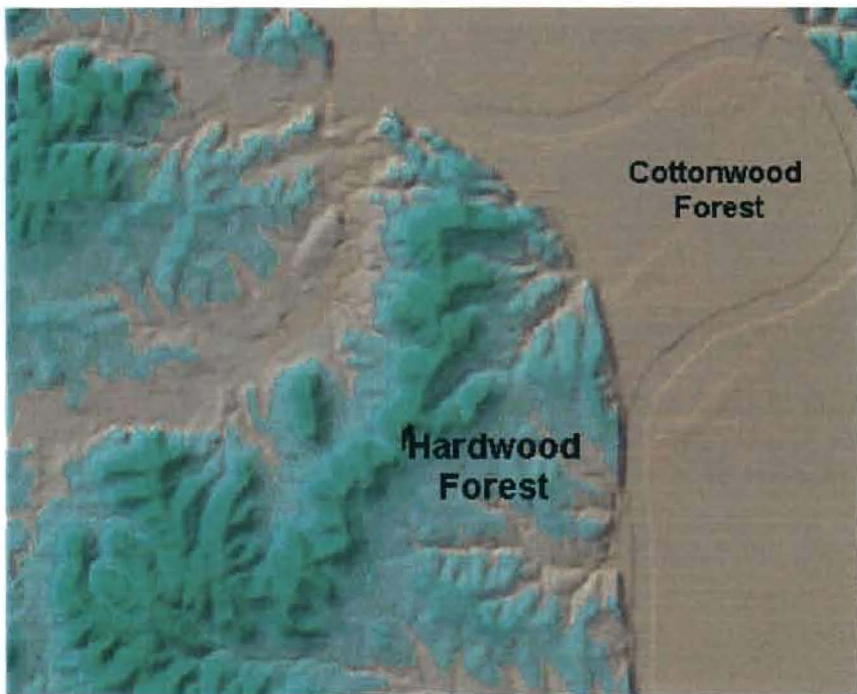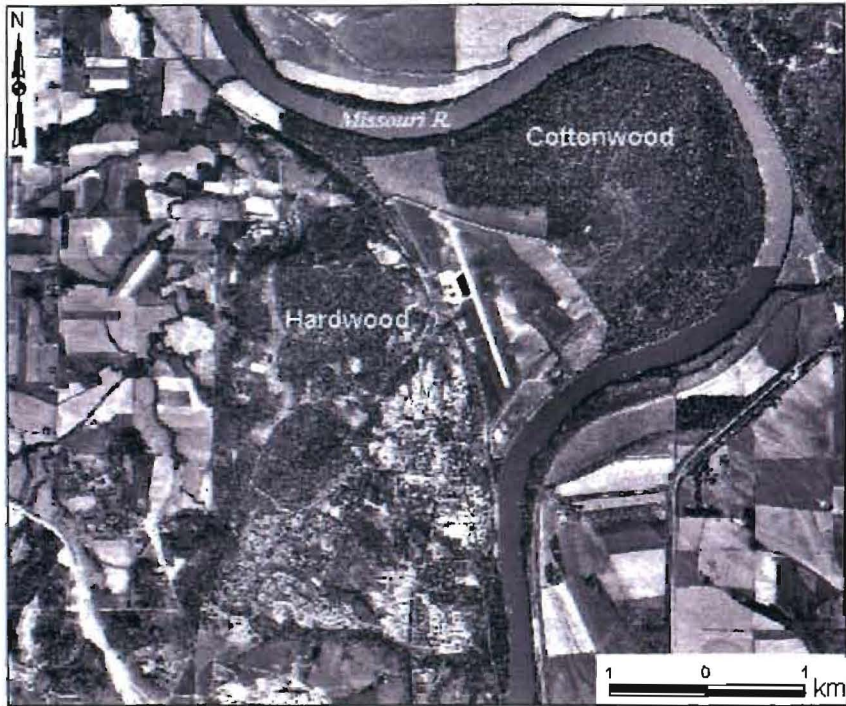
Fig. 4.

Above: 1-meter digital orthophoto quadrangle of the study forests.

Below: Digital elevation model of the forests.

The floodplain forests are located at an altitude of 235 meters (770 feet) and are separated from the airfield by levees. The forest floor is swampy with open, waterlogged areas (Fig. 5) and is an important ecosystem for a wide variety of plants and a number of migrating and nesting bird species, including the bald eagle. These forests are believed to be the largest old-growth stands remaining in the lower Missouri River valley (Freeman *et al.*, 1997)

This cottonwood riparian forest evolved on a dynamic river system that floods periodically. Arcuate terraces are evidence of the development of this meander, as the Missouri River migrated. Water settles in the depressions between the terraces. This area was completely inundated by the flooding of the Missouri River in 1993. The river crested at 14.9 meters, 5.3 meters above flood stage (Lott, 1994). New trees now flourish on the flooded areas.

These forests are not subject to logging or other large-scale destructive activity. The floodplain forest is largely undisturbed, although it is in close proximity to the airfield at the western boundary. The upland hardwood forest is subject to moderate human activity as it houses several structures such as a skeet shooting range, lodge, scout camp sites, sanitary landfill, and trails which are actively used.

The study area lies on the western edge of the eastern temperate deciduous forest zone (Fig. 6) and could play an important role in early identification of long-term changes to the overall vegetation of this ecosystem.

Fig. 5.

Above: Cottonwood forest east of Sherman Army Airfield.

Below: Understory of the cottonwood forest. Pictures taken July, 1999.
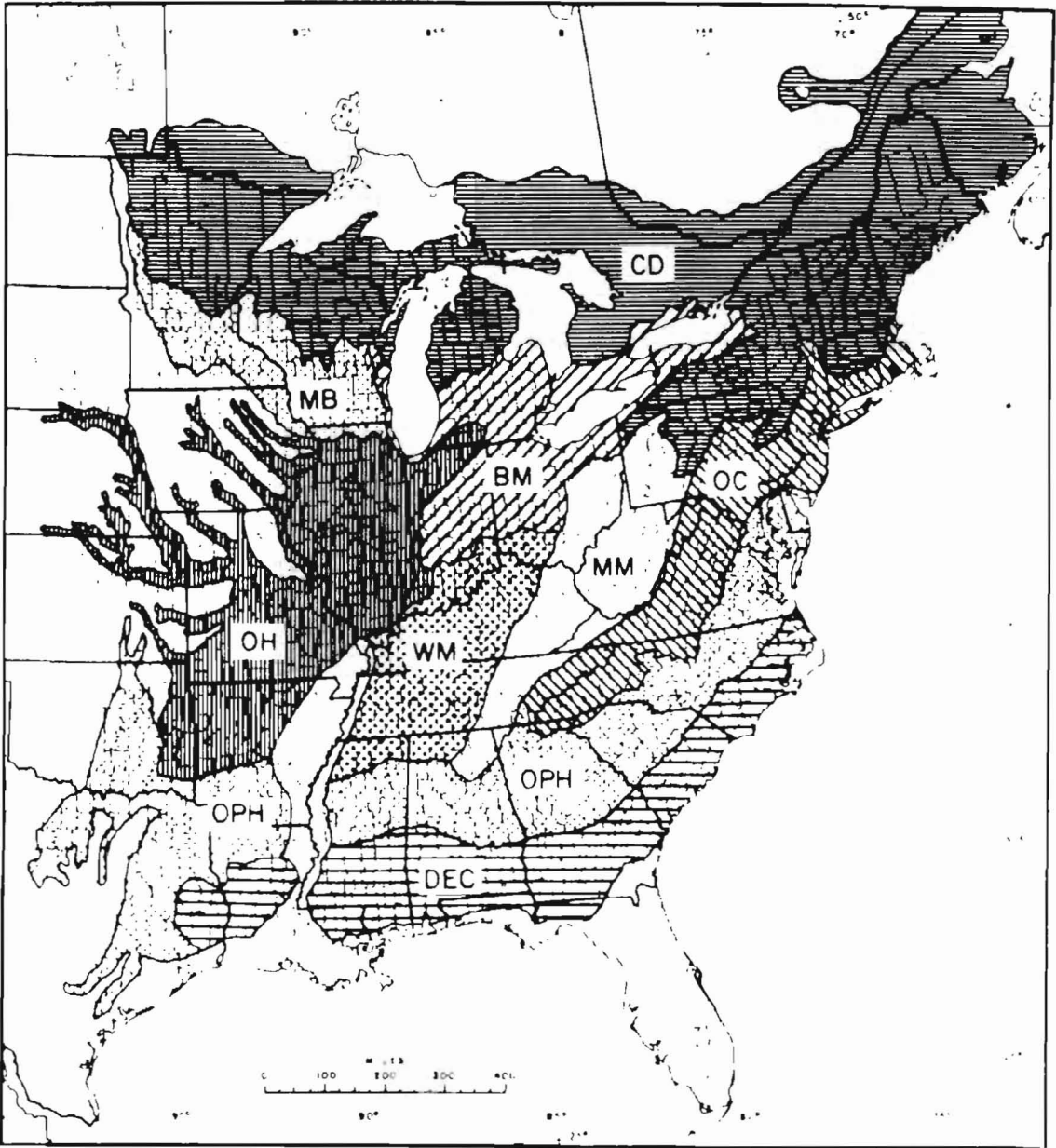
Fig. 6. Main vegetation forest zones of the eastern U.S. and southern Canada.

CD- Coniferous, Deciduous; MB-Maple. Basswood; OH- Oak, Hickory; BM- Beech.

Maple; WM- Western Mesophytic; MM- Mixed Mesophytic; OC- Oak, Chestnut; OPH-

Oak, Pine, Hickory; DEC- deciduous and evergreen dicots, conifer.

From: North American Terrestrial Vegetation (Barbour and Billings, 1988).

1.4 Climate

This area of Kansas experiences a continental climate with distinct seasons. Mean annual temperature is 12.2 °C (54.0°F), with average daily maximum and minimum temperatures of 19.3 °C (66.6°F) and 7°C (44.5°F) respectively. Average annual precipitation is approximately 90 cm (35 inches) (NCDC, 1999). Highest monthly precipitation is generally received in May and June and the growing season lasts from April to October. The average annual precipitation (January to December) for the study area over the 10-year period from 1987 to 1997 was 74 cm (29 inches).

1.5 Geology

The study area lies in the glaciated region of northeastern Kansas. The exposed formations belong to the Shawnee and Douglas Groups of Pennsylvanian age, and alluvium and glacial sediments of Quaternary age (Fig. 7). The hardwood forest sits on a ridge that extends from Government Hill in the south to Hancock Hill in the north. This ridge is part of the Oread Escarpment, a prominent feature that is capped by limestones of the Oread Formation. This is a 45-foot thick sequence of limestones and shales which forms the base of the Shawnee Group in this area. This sequence is underlain by the Lawrence and Stranger formations of the Douglas Group. Both formations comprise a 220-foot thick sequence of shales, sandstones and thin limestones. Quaternary loess and glacial drift overlie most upland areas (KGS, 1999). The dominant soils belong to the Knox Complex which are well drained silt-loams formed in loess (Fig. 8). The lowland

cottonwood and pecan forests are underlain by Holocene alluvial deposits of the Missouri

River. The dominant soil type is the poorly drained Onawa silty clay loam (Fig. 8).
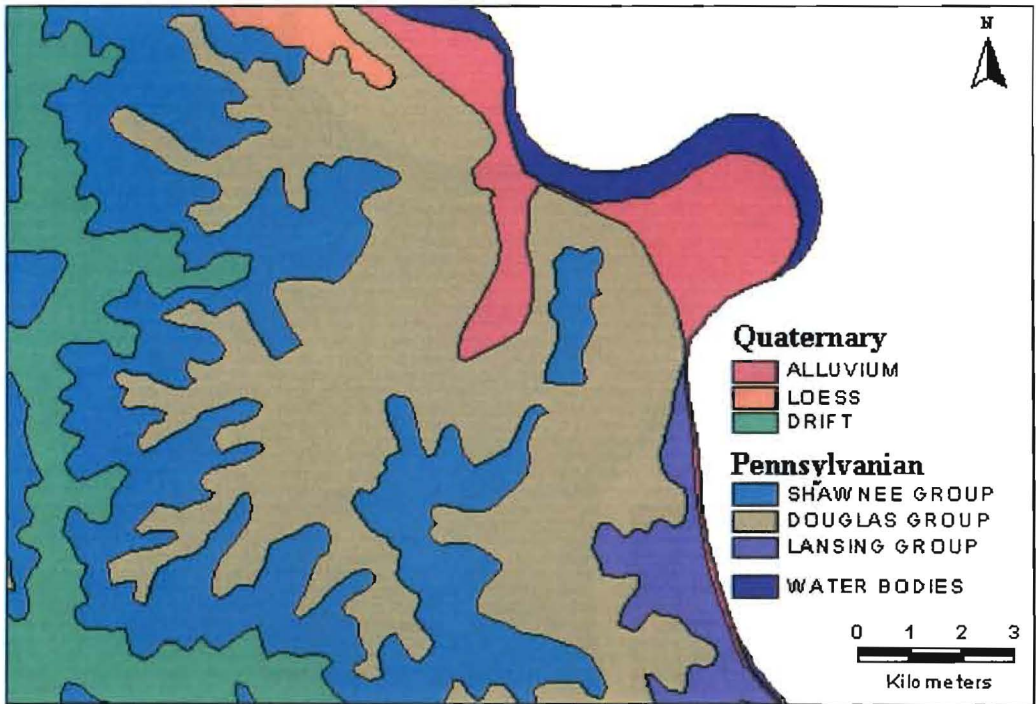
Fig. 7. Generalised geology of the study area (DASC, 1999).

	Eu EUDORA COMPLEX,
	Gc GOSPORT COMPLEX
	Gs GOSPORT-SOGN COMPLEX
	Hy HAYNIE SILT LOAM
	Kh KNOX SILT LOAM
	Km KNOX SILTY CLAY LOAM
	Kn KNOX COMPLEX
	La LADOGA SILT LOAM
	Mc MARSHALL SILT LOAM
	On ONAWA SILTY CLAY LOAM
	Oo ONAWA SOILS
	Sa SARPY-HAYNIE COMPLEX
	W WATER
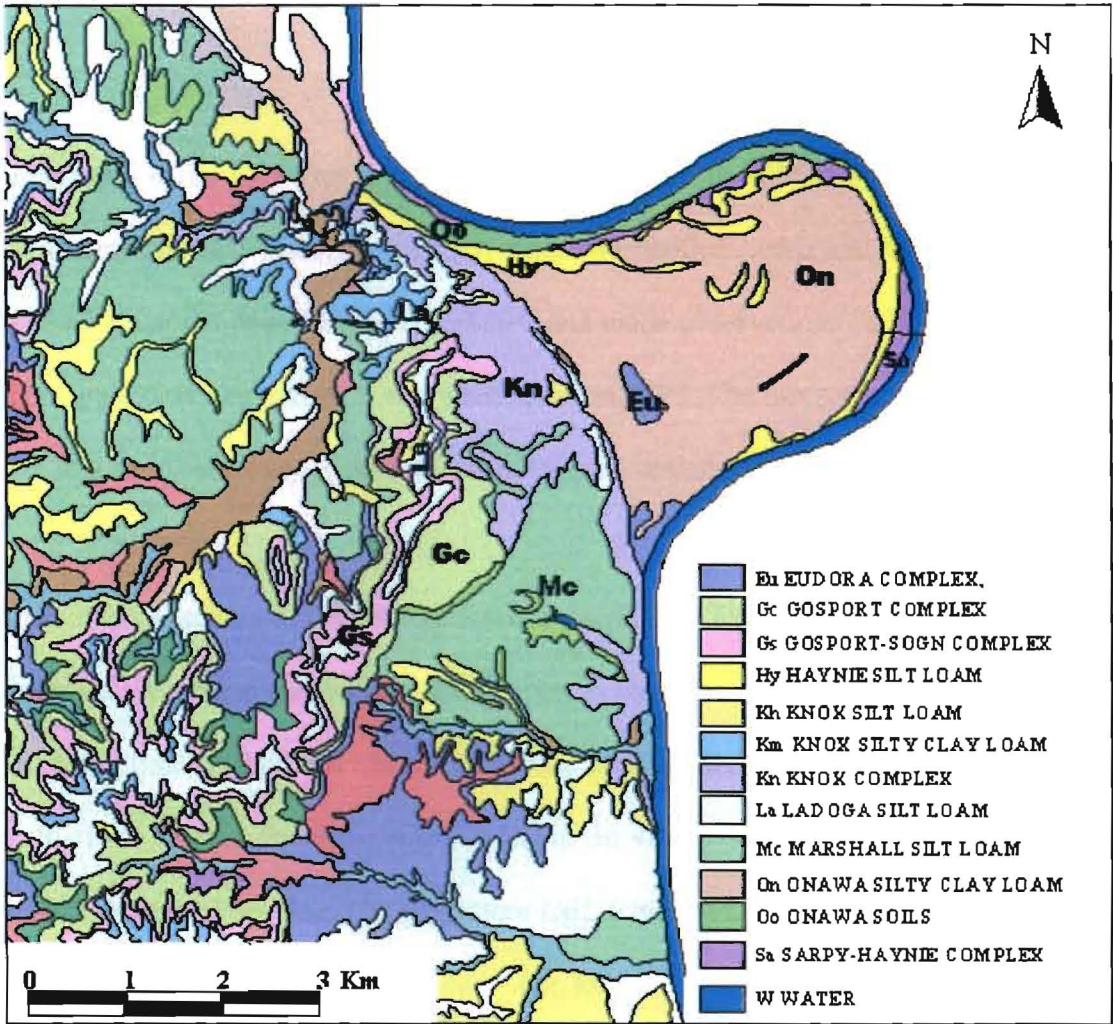
Fig. 8. Soil map of the study area (DASC, 1999).

Chapter 2

Previous Work

The natural vicinity of what is now the Fort Leavenworth Military Reservation has been documented in early American history, when Meriwether Lewis and William Clark traveled along the Missouri River in 1804, and made observations of the flora and fauna in the area. Fort Leavenworth was established in 1827. The forests have matured since then and have been largely maintained in their natural state.

An ecological survey of the reservation was carried out by Brumwell (1951). He described the upland oak-hickory association in the areas of Government Hill to North Hill consisting of large size trees with a small area of hard maple confined entirely to the north of the region. For the lowland forest in the vicinity of Sherman field, he described an oak-pecan-hickory forest in the eastern half, fringed on the exterior with a cottonwood-elm-sycamore association. The forests were also documented in further work on vegetation in Kansas by Kuchler (1974).

Detailed mapping of the biota of the Fort Leavenworth Military Reservation was carried out by the State Biological Survey of Kansas (Freeman *et al.*, 1997). This work provides a detailed inventory of plant and animal species on the installation, with the natural vegetation communities including the upland and floodplain forests.

Since 1996, satellite imagery and other forms of remote sensing have been used for temporal studies of the forests on the reservation, as part of the NASA EPSCoR program (Experimental Program to Stimulate Competitive Research) investigating the effects of climate on vegetation in parts of Kansas. The present study was also conducted under the EPSCoR program. Previous work included analysis of Landsat TM imagery for the years 1987, 1988, 1990 and 1994 by Wilkins (1997). Wilkins examined NDVI changes in the upland oak-hickory forest over these years, and compared these with climatic variables of tree-ring width and precipitation. The study identified a time lag of one to two years between decreased precipitation during the drought of 1988 and decreased NDVI in 1990.

Tree-ring widths are highly correlated with moisture availability in soils. Narrow rings are produced when trees are stressed from moisture deprivation (Fritts, 1976). Tree-rings have been used in climate reconstruction in many areas including the U.S. Great Plains (Stockton and Meko, 1975, Blasing and Duvick, 1984; Cook *et al.*, 1988). For this study, tree-ring data were obtained from work completed by Nang (1998). Twenty-nine tree-ring cores were obtained from fifteen oak trees in the upland oak-hickory forest. These data were significantly correlated with precipitation and Palmer Drought Severity Index (PDSI), indicating that the forest immediately responds in growth to increased precipitation, though this may not be immediately evident in NDVI values. These studies suggest that NDVI values should be used cautiously in relating forest health to current annual climatic conditions (Aber *et al.*, 1998).

The upland oak-hickory forest was also part of a study of the relationship between NDVI and tree productivity, conducted by Wang *et al.* (1999 a). Results of this study suggest that tree-ring widths are best correlated with NDVI from mid- May to late June/early July. This study also reports a one-year lag between NDVI increase and the resulting growth in height for white ash trees at the Kansas Ecological Reserve, though there is a strong same-year correlation between NDVI and diameter growth. Other studies investigating the spatial and temporal relationships between NDVI and precipitation and temperature in the Central Great Plains, have also been carried out by Wang *et al.* (1999 b, c). Temporal studies indicate that NDVI shows most significant correlation with rainfall for a 15-month period which includes the current eight-month growing season plus the previous seven months. This was attributed to storage of moisture from precipitation of the previous winter season, in the soil. Correlations for the forests were lower that those of croplands or grassland.

Studies of NDVI and precipitation have been conducted worldwide and are significant to this study. Davenport and Nicholson (1990) studied diverse vegetation types in East Africa and reported that NDVI was sensitive to rainfall in dry areas but a significant lag was evident in wet forest areas. NDVI for eastern coastal forests was highest in 1985, the driest of the three years studied, though there was very heavy rainfall late in 1984. An overall best correlation was achieved for the current month plus two previous months, and this correlation was lowest for the forest areas.

Principal component analysis (PCA) has been used successfully to monitor multitemporal changes in vegetation in many studies. The method has been employed with NDVI in temporal studies of vegetation in Africa, to detect seasonal changes as well as underlying global patterns of climate change (Eastman *et al.*, 1995). Muchoney and Haack (1994) used PCA to study insect defoliation of mixed oak-pine forests in Virginia, using SPOT imagery. Townshend *et al.* (1985) used PCA with NDVI data from AVHRR imagery over Africa and North America to examine seasonal and annual changes, as well as changes related to the northern and southern hemispheres. Byrne, Crapper and Mayo (1980) worked with MSS images to monitor landcover changes over an area of southern Australia. Lu Jiaju (1988) used PCA with Landsat TM data to detect landcover changes in southern Sweden. Eastman and Fulk (1993) also used multitemporal NDVI data for Africa to examine short and long-term changes.

Image differencing has often been used for detection of changes in vegetation. Jano *et al.* (1998) used this method with difference vegetation index (DVI) images to detect vegetation decline due to destruction by birds in Manitoba, Canada. Green *et al.* (1994) used differencing of vegetation index images and band 7 from Landsat TM data for detection and monitoring landuse changes in Oregon, USA. The technique was also used by Cohen *et al.* (1998) to assist in mapping forest clearcuts in Oregon Cascade Range, and Bauer *et al.* (1994) combined PCA with differencing for change detection of Minnesota forest resources.

The moisture stress index (MSI), defined as the ratio of TM band 5: band 4, has been used in several studies to detect declining health of vegetation. Early work (Gates *et al.*, 1965 and others) identified the primary factors affecting leaf reflectance as chlorophyll, as well as water content. Allen *et al.* (1968) reported that the absorption of radiation in the 0.7 to 2 micron range was considerably reduced for a dehydrated cotton leaf. Stochastic modeling of leaf radiation by Tucker (1980) showed a strong correlation between decreased water content and increased reflectance in the mid-infrared range. Tucker's results led to the conclusion that the mid-infrared range between 1.55 and 1.75 microns, was the region most suited for remote sensing of plant canopy water status. Similar conclusions were reached from experiments conducted by Carter (1991), using leaves representing aquatic, broadleaved deciduous trees, grasses and coniferous tree species. It was determined that the direct absorption of radiation by water content in the leaves had the most influence on the reflectance from the leaves and this effect was greatest in the 1.3 to 2.5 micron range. Work with rye grass and oats (Cibula *et. al.*, 1992) also showed significant increases in leaf reflectance in the TM range for bands 5 and 7, with decreasing leaf water content. Poorest responses occurred in the near-infrared region, corresponding to Landsat TM band 4.

The Landsat TM band 5 : band 4 ratio has been used to detect moisture stress in several instances. Pinder and McLeod (1999) used this ratio to detect changes in reflectance of longleaf pine (*Pinus palustris*) in South Carolina, USA. These changes correlated with decreased rainfall and tree-ring data, though the correlations were not very high with coefficients between 0.4 and 0.6. Rock *et al.* (1986) also used the MSI to study

coniferous forest damage caused by aging and possibly environmental pollution, in

Vermont, USA.

Chapter 3

Methods

3.1 Pre-processing Landsat TM data

Complete 7-band sets of Landsat TM images for the years 1987, 1988, 1989, 1990, 1991, 1992, 1994 and 1997 were acquired from the EROS Data Center for this study. The study area is included on Landsat location row 33, path 27 (Fig. 9 and Table 1) and is situated in the north of this image (Fig. 10). *Idrisi* software from Clark Labs in Worcester, Massachusetts, was used for all processing of the images.

Landsat scenes for the month of July were selected for this study. During July, vegetation is in full growth and rainfall is high, providing the best conditions for healthy vegetation. In addition, the high sun position minimizes shadows on the images. The use of images from approximately the same time of year ensures that growing conditions are generally the same and reduces the variables such as, stages of vegetation growth, canopy development, sun angles, shadows and soil moisture content. All images, except for July 1989, and to a lesser extent that for July 1992, were cloud free over the study area.

To prepare the images for analysis, several pre-processing procedures were required. These were:

1. Convert raw images to a format compatible with *Idrisi* software.

2. Window the study area from the total scene.

3. Perform haze correction.
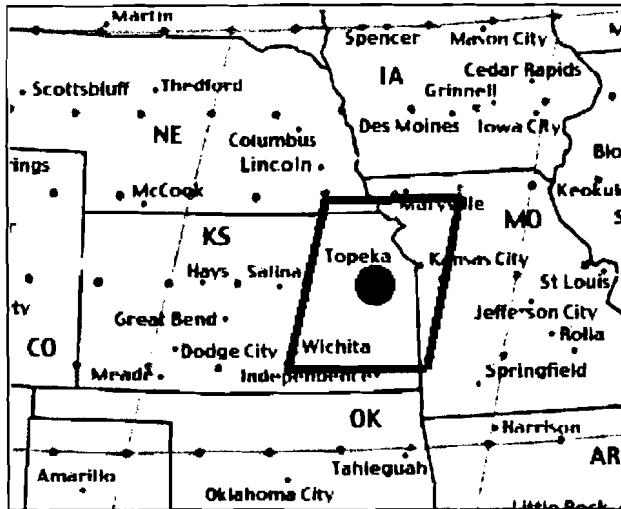
Fig. 9. Location of Landsat TM: Row 33, Path 27. Taken from NASA, 1999.

Path 27 Row 33	Latitude DD MM SS	Longitude DDD MM SS
Center	38 55 00 N	095 29 41 W
Upper Left	39 49 30 N	096 21 25 W
Upper Right	39 30 28 N	094 10 14 W
Lower Left	38 18 27 N	096 47 57 W
Lower Right	37 59 49 N	094 39 28 W
D = degrees, M = minutes, S = seconds		

Table 1. Latitude and longitude coordinates for Landsat TM image path 27, row 33. Taken from NASA, 1999.
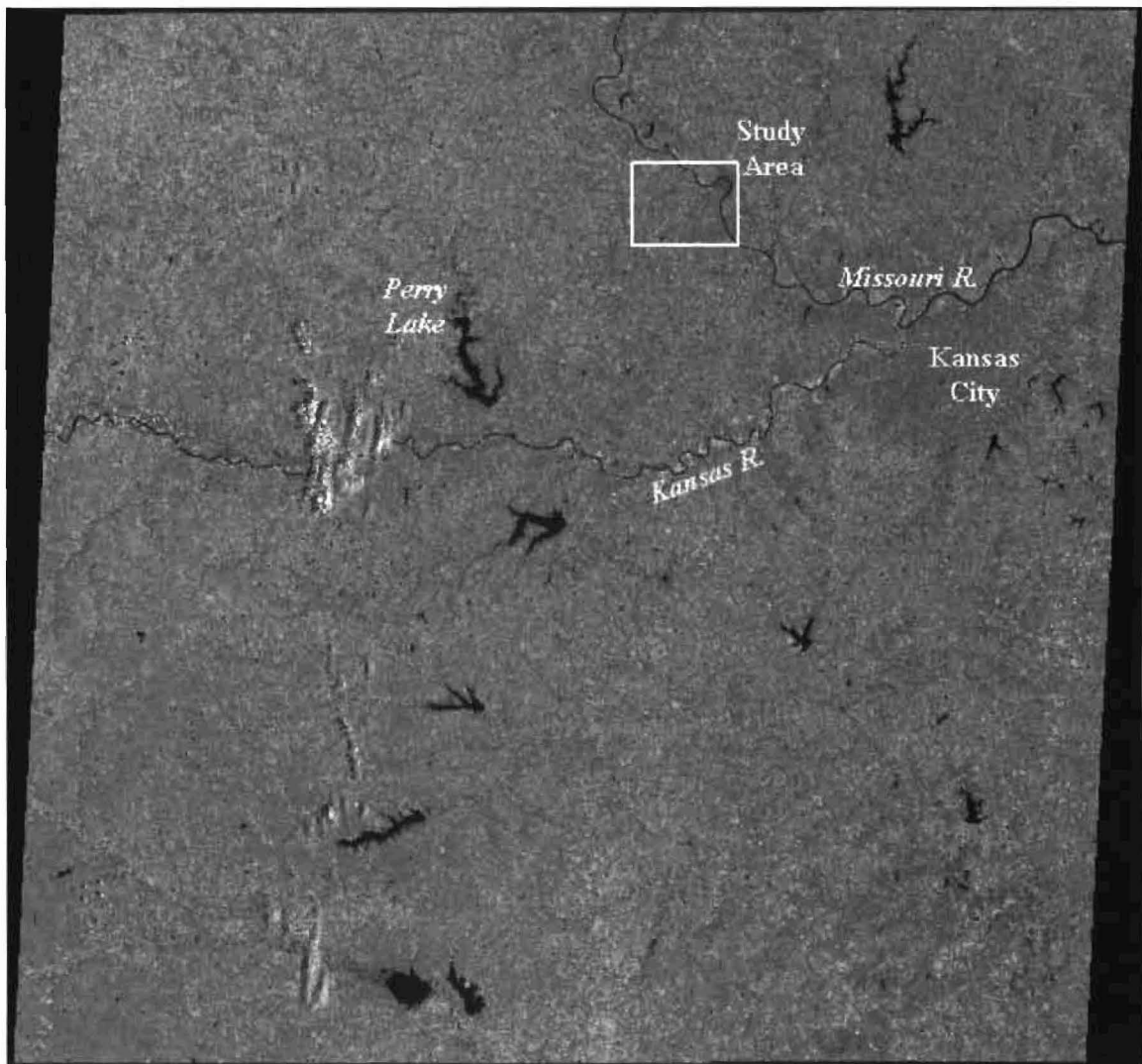
Fig. 10. Full Landsat TM scene for row 33 path 27, showing study area in the north. This image shows band 5 (mid-infrared) for July 23, 1987.

4. Georeference the images to a known coordinate system.

5. Window the georeferenced images to remove background zero values.

6. Remove cloud cover from 1989 image.

All images, except that for 1994, were in band sequential (bsq) format with the 7 bands separate. This format is readily readable by *Idrisi*, but the file extension must be changed to "img" and a documentation file created from header information. The 1994 image was in band interleaved by line (bil) format and was a simple import into *Idrisi*. Examples of a header and a documentation file are shown in Appendix 1.

Using information gleaned from the header file, documentation files were created for each band of each dataset using *Idrisi*'s DOCUMENT module. Data type was set to byte and file type to binary, the format of the raw data. The reference system was set to plane, an arbitrary system indicating that the raw data reference system was not known. Reference units were set to kilometers and resolution rounded to 0.03 km. Unit distance was set to 1 indicating that 1 kilometer on the image represents an equivalent distance on the ground. Minimum and maximum values were set to 0 and 255 respectively - the full range of byte-binary numerical values. Minimum x and y values were set to 0, and maximum x and y were calculated for each dataset using the formulae:

*Max x = No. of columns * Resolution*

*Max y = No. of rows * Resolution*

To focus on the study area, full scenes were then windowed to a size of 700 columns by 500 columns to include the study area. Following the original procedure by Wilkins (1997), the window was selected using the middle left cell of the old missile site located in the interior of the hardwood forest (Fig. 11). From the column value at this point, 400 was subtracted to determine upper left column of the window. From the row value, 200 was subtracted to determine the upper left row. The lower right column/row values were determined by adding 699 to the upper left column and 499 to the upper left row. For example, in the 1997 scene, the location of the "missile" pixel was determined to be column 4298, row 1228. The upper left corner for the window was determined to be column 3898, row 1028 and the lower right at column 4597, row 1527. The windowed area was used for further preprocessing. The six reflective TM bands (excluding band 6, the thermal band) were used for additional work.

The next step was to perform haze correction of the images. Haze results from atmospheric scattering of electromagnetic radiation by particles in the atmosphere. These include atmospheric gas particles, extraneous suspended particles, clouds and water droplets. The result of this scattering is to increase the overall brightness of the image, so that a clear water body, which should have a value of 0 in the infrared band, may have a much higher reflectance value. Bands in the visible light and low infrared range (bands 1 to 4) are most affected by haze as these shorter wavelengths are more easily scattered by atmospheric particles. There was some degree of haze in all images. Haze reduction was achieved by reducing the lowest pixel value to 1, following the procedure of Avery and
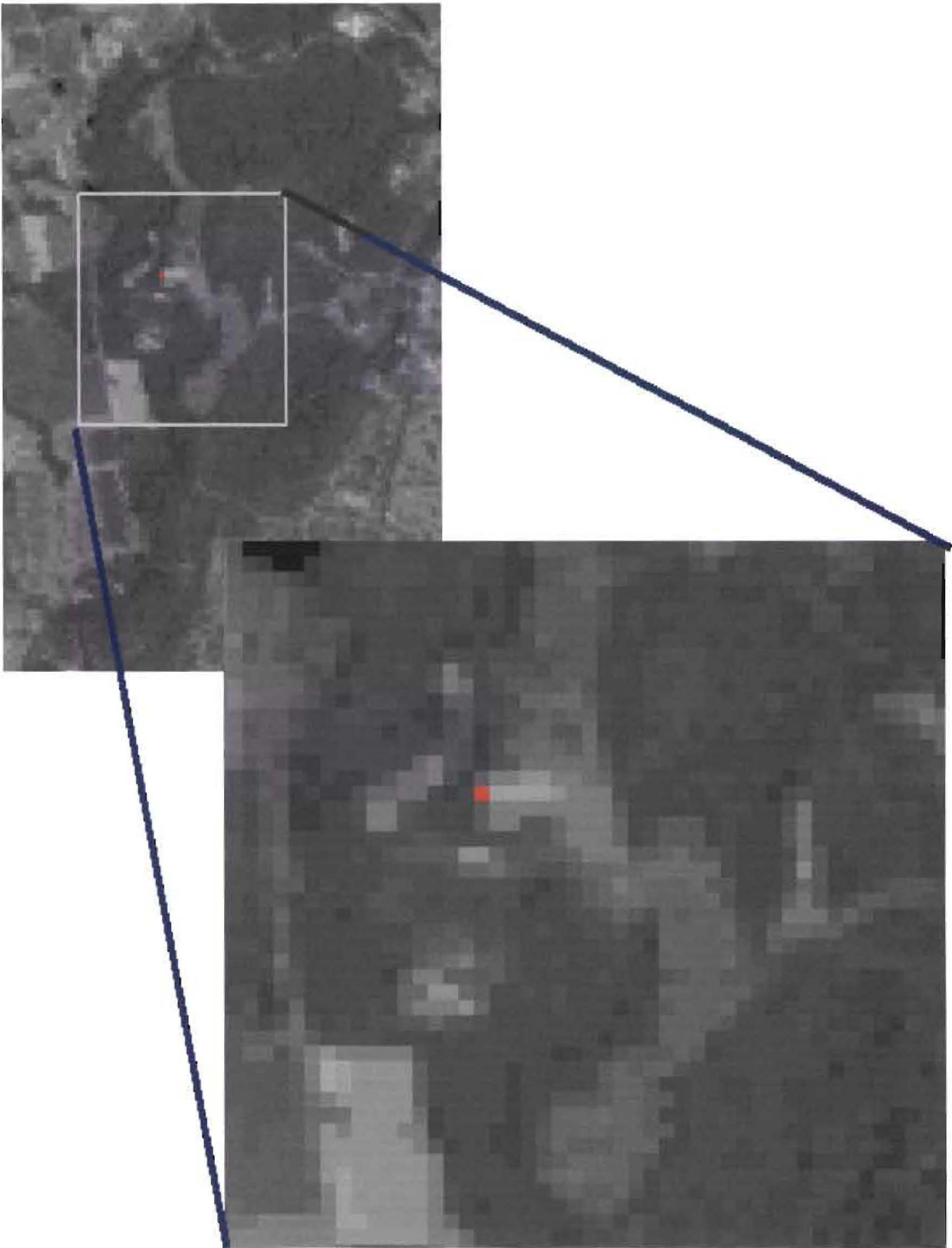
Fig. 11. Landsat TM Band 5 showing missile site pixel (in red) in the hardwood forest which was used as the point of reference for selecting study window.

Berlin (1992). The SCALAR function in *Idrisi* was used to perform this mathematical process.

As the raw data were assigned an arbitrary reference system, it was necessary to georeference the images to a real-world projection and coordinate system. This was done by relating points on the image to coordinates of selected control points on the ground. The georeferencing process warps or "rubber-sheets" the original image to the new coordinates. In this case, control points (Table 2 and Fig. 12), were determined by Global Positioning System (GPS) readings on site (Wilkins, 1997) and from digital topographic maps (DASC, 1999). Control point parameters were UTM projection, Zone 15 and NAD27 datum, which are standard map conventions in the United States. Each image was georeferenced individually using these parameters.

Georeferencing was accomplished with the RESAMPLE module of *Idrisi*. A correspondence file was prepared, listing the "old" x and y coordinates of the selected control points as indicated on each image, and the desired "new" x and y coordinates based on GPS and topographic maps (Appendix 2). *Idrisi* uses this information to generate a new grid and assigns new values based on one of two statistical methods. The first is the nearest neighbor method that assigns to the new cell, the value of the nearest old cell. The resampled image therefore contains only values that were contained in the original scene. The other method is bilinear interpolation that assigns to the new cell, the weighted average of the 4 nearest neighbors on the old grid. The output values are

Table 2

Control Points used for resampling raw images to UTM Zone 15 reference system

Points 1-10 were obtained from GPS readings (Wilkins, 1997). Points 11-13 were

determined from 24K County digital raster maps downloaded from the DASC website.

Point	Easting Km E	Northing Km N	Description	Source
1	0332.840	4357.995	Southwest corner of parking lot, skeet shooting range	GPS
2	0332.758	4358.725	Bell Point, southwest corner of large storage/parking area	GPS
3	0332.746	4357.513	South end ridge, northeast corner water tank	GPS
4	0335.355	4358.549	Airport runway, center of south end	GPS
5	0334.762	4360.249	Airport runway, center of north end	GPS
6	0335.820	4359.953	Service Area east of airport, northwest corner of parking lot	GPS
7	0333.051	4360.251	Northwest corner of fort, Coffin Rd	GPS
8	0333.293	4359.133	Circular tanks, east side of ridge top	GPS
9	0334.880	4355.844	Southeast corner of Warehouse Rd	GPS
10	0333.373	4355.055	Federal Prison, southeast corner parking lot	GPS
11	0330.379	4362.602	Southeast corner of cemetery in Kickapoo, Kansas	24K County DRG
12	0328.372	4358.286	Road junction, west of Salt Creek Valley	24K County DRG
13	0322.620	4355.415	Road junction, northwest of Stellmans Lake	24K County DRG
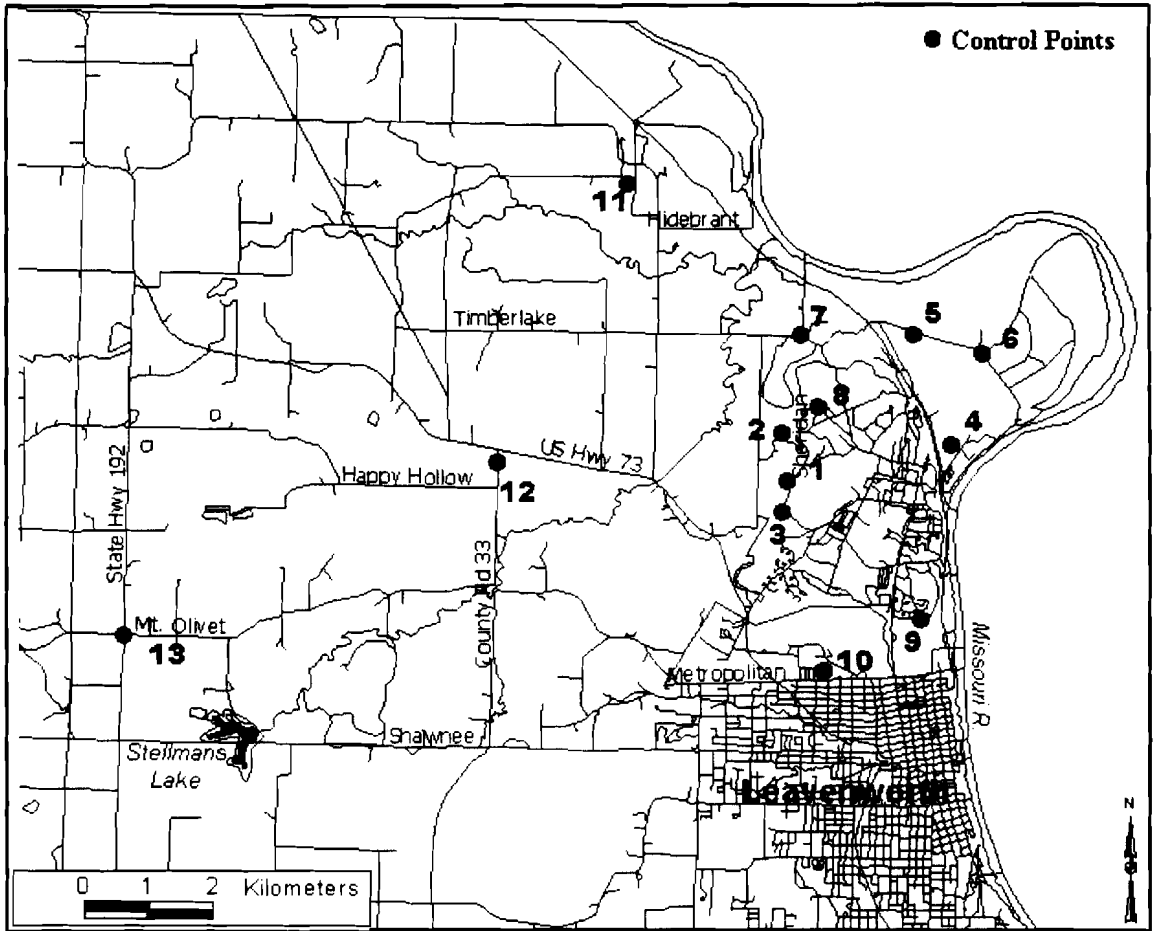
Fig. 12. Location of ground control points used for the resampling process.

therefore modified from the original. The nearest neighbor method was used for processing in this study. The parameters for the resampling process were as follows:

Reference System: US27TM15

Reference Units: km

Resampling Type: Nearest Neighbor

Mapping Function: Linear

Minimum x: 319.6 km E

Maximum x: 342.5 km E

Minimum y: 4348.0 km N

Maximum y: 4366.9 km N

Number of columns: 763

Number of rows: 630

The maximum and minimum x and y coordinates represent the desired boundary of the resampled output. Number of rows and columns were determined using the formulae:

No. of columns = (Max x - Min x)/Resolution = (342.5 - 319.6) / 0.03 = 763

No. of rows = (Max y - Min y)/Resolution = (4366.9-4348.0)/0.03 = 630

Using these parameters, macro files were created to batch process the resample procedure for each band of each image. An example of the batch file created for this process is given in Appendix 3.

With each resample procedure, an error in location is generated. The RMS error for each

image band is calculated by the software and a value of less than 0.5 is considered

acceptable (*Idrisi,* 1997). The values in this procedure ranged from 0.043 to 0.051 except

for the cloud covered 1989 image with a RMS of 0.078. All values were well within

acceptable limits (Appendix 2).

The resampled output images were rotated with respect to the original images, as a result

of alignment with the UTM-grid system in the rubber-sheeting process. The rotated

images were further windowed to remove the background zero values (Fig. 13).

Landsat TM July 1987 Band 5 - RESAMPLED

Window from Resampled Image - 1987 July Image, Band 5

Fig. 13.

Above: Image is rotated after the resampling process.

Below: The rotated image is windowed to produce the image that is used for all further processing and analyses.

3.2 Normalized Difference Vegetation Index (NDVI)

With the pre-processing complete, the next step was to isolate each forest, hardwood and cottonwood. The forests were isolated from the image representing the year of most vigorous vegetation. These isolated forest stands were then used as "masks" for all other years. To determine the image with the most vigorous vegetation cover, NDVI was calculated for each dataset. For Landsat TM data, NDVI is calculated using the red and near-infrared bands, with the formula (Rouse *et al.*, 1974 in *Idrisi*, 1997)

$$NDVI = \frac{Band\ 4 - Band\ 3}{Band\ 4 + Band\ 3}$$

The result is a slope-based vegetation index that has proved to be a good indicator of vegetation vigor, particularly in areas of good vegetation cover. Values range from -1 representing unvegetated surfaces, to +1 representing full vegetation cover.

3.2.1   Calculating NDVI

Calculating NDVI was a simple process for all images except the 1989 image, which had scattered cloud cover and associated shadows. For all other images, the VEGINDEX function of *Idrisi* was used with band 4 as the near-infrared and band 3 as the red band. The results of the VEGINDEX module are NDVI images with pixel values between -1 and +1, in real binary format. These images were enhanced by stretching the values between 0 and 255 and converting to byte binary format. This was done using the steps outlined below.

- Add 1 to the raw NDVI images to eliminate negative values

- Multiply the result by 120 to stretch the values between 0 and 255

- Convert to byte binary format.

Steps 1 and 2 were accomplished with the image calculator and step 3 with the

CONVERT module of *Idrisi*. This process was completed for each July dataset.

The images and corresponding histograms for each year are shown in Figs. 14 to 29. The

minimum, maximum, mean and standard deviation for NDVI values for each year are

shown in Table 3 with corresponding graph in Fig. 30. The results indicate that of the 8

years, 1987 had the best vegetation index, as Wilkins (1997) had observed earlier. The

dataset for this year was therefore chosen for isolating the forests. These images, with

further processing for 1989 as described below, were used in conjunction with the

isolated forest masks for temporal analyses.

3.2.2 Calculating NDVI for 1989 image

The standard false-color composite shown in Fig. 31 shows the extent of the cloud cover

and shadows on the 1989 image. Isolating the clouds and shadows was achieved by two

methods. The first and more accurate method used ISOCLUST for unsupervised

classification. Six bands (not including band 6) were used with the standard false-color

composite shown in Fig. 31. Twelve clusters were used and this image was then

reclassified to produce the isolated clouds and shadows in Fig. 32. Clouds and shadows
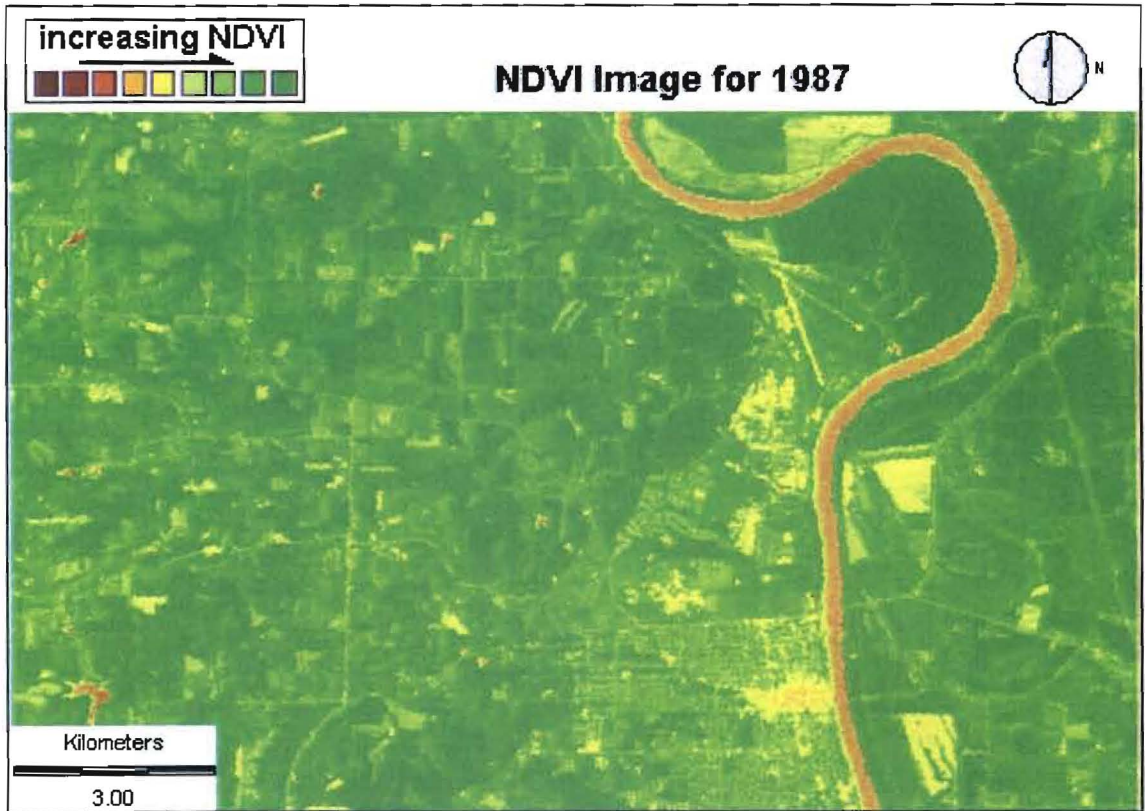
Fig. 14. NDVI image for July 1987.
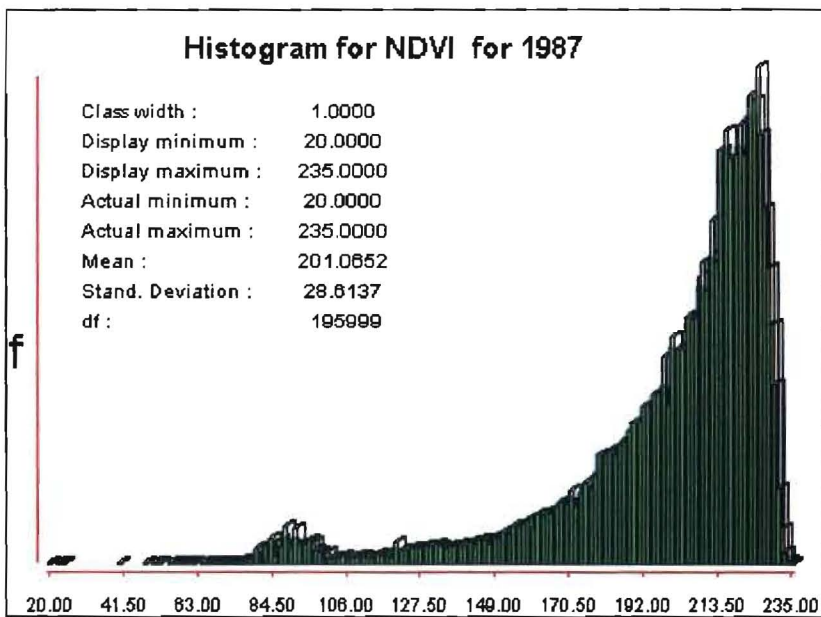
Fig. 15. Histogram for July 1987 NDVI.
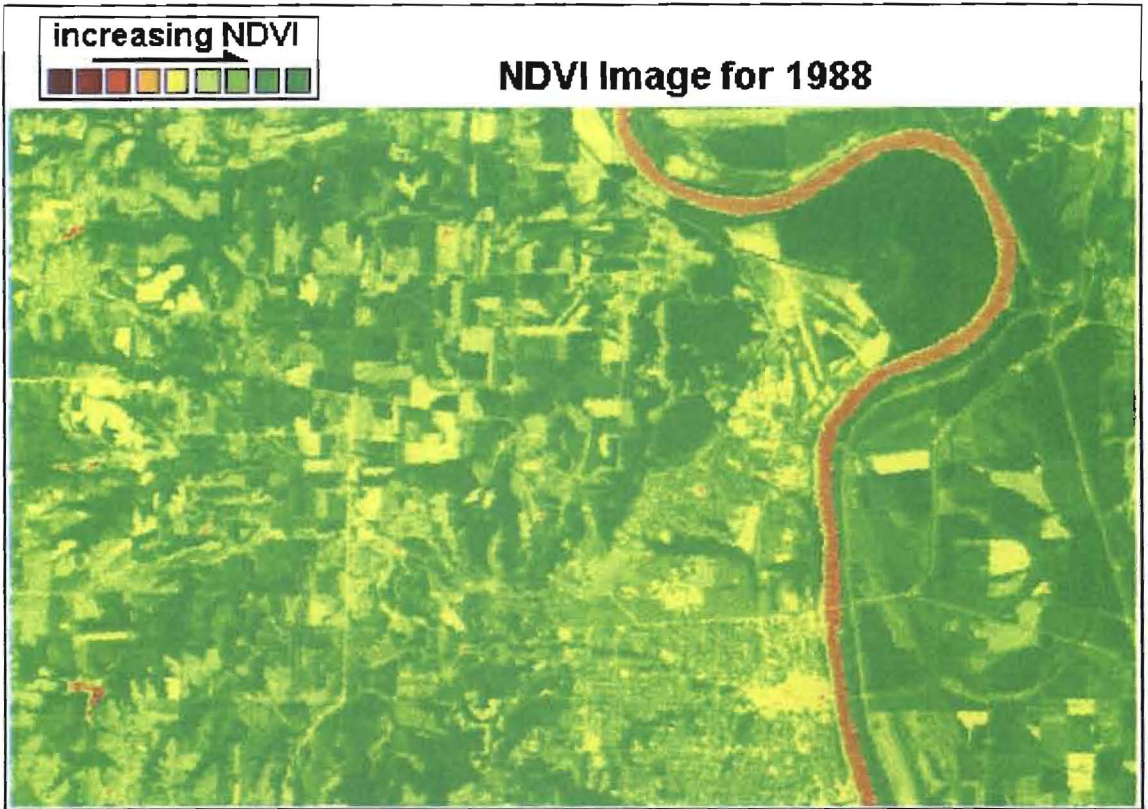
Fig. 16. NDVI image for July 1988.
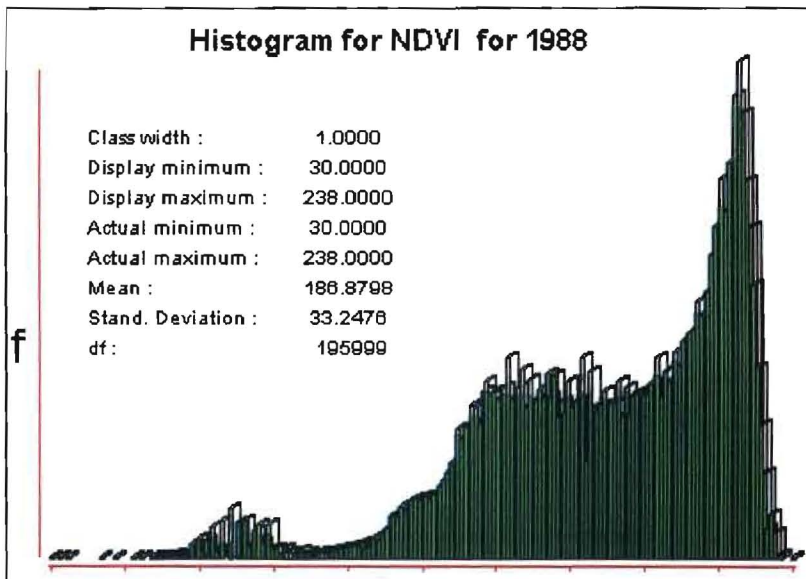
Fig. 17. Histogram for July 1988 NDVI.
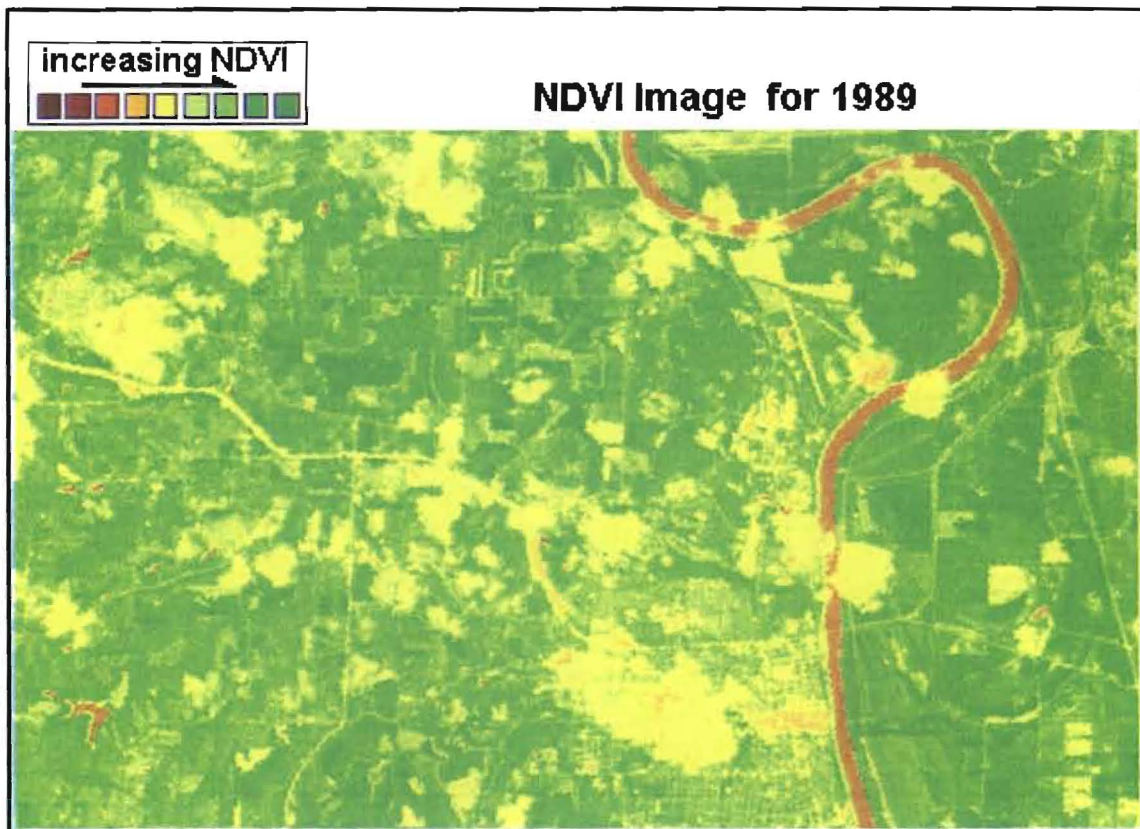
Fig. 18. NDVI image for July 1989. Clouds are scattered over the scene.
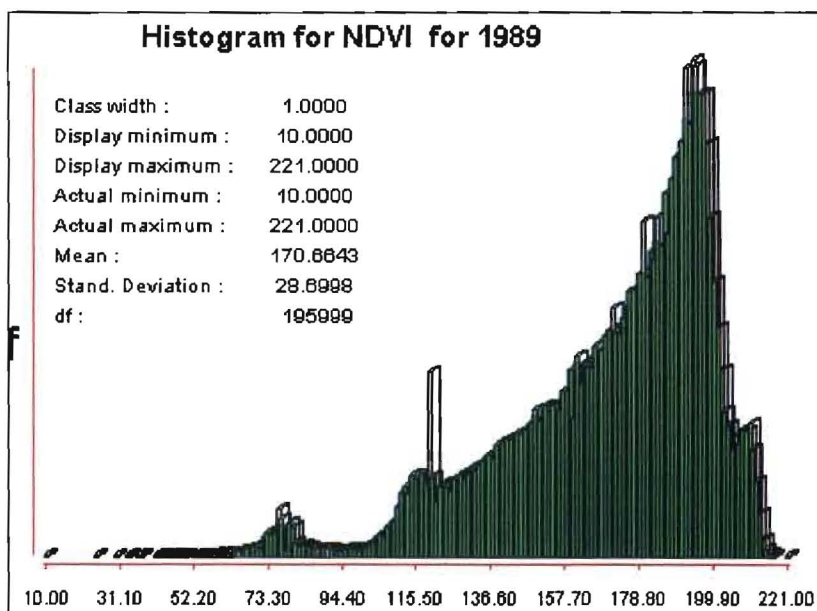
Fig. 19. Histogram for July 1989 NDVI.
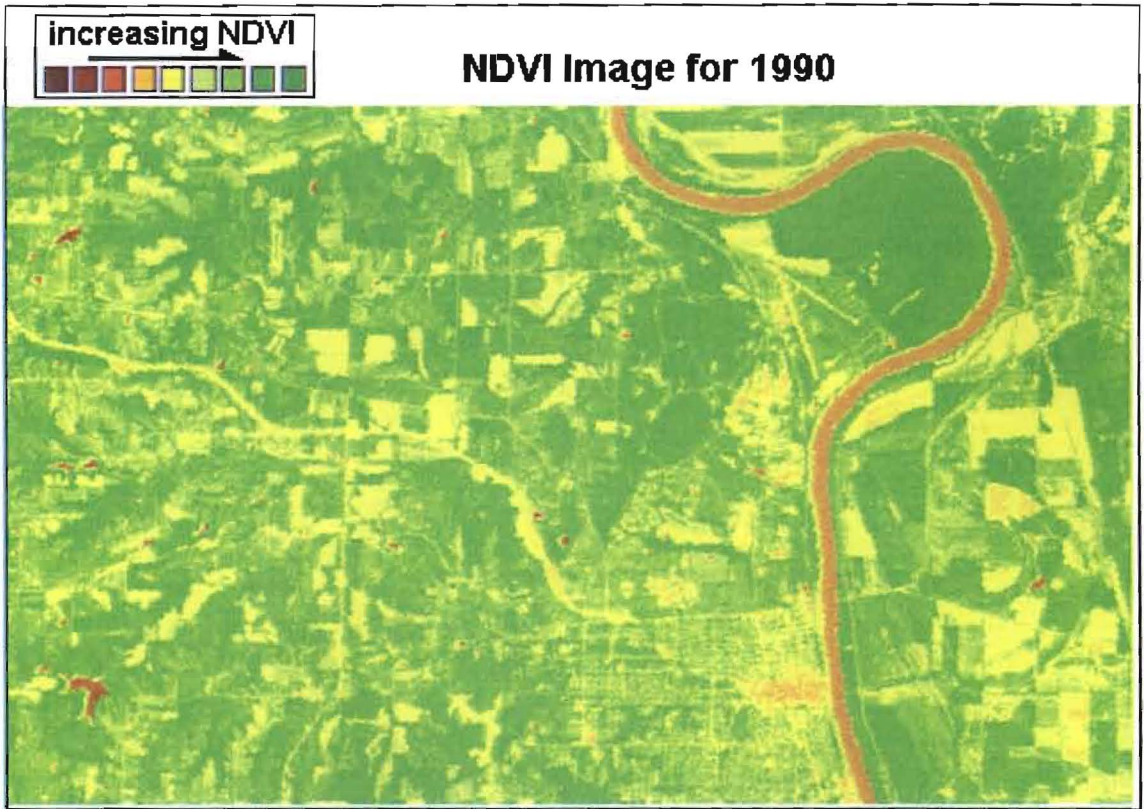
Fig. 20. NDVI image for July 1990.
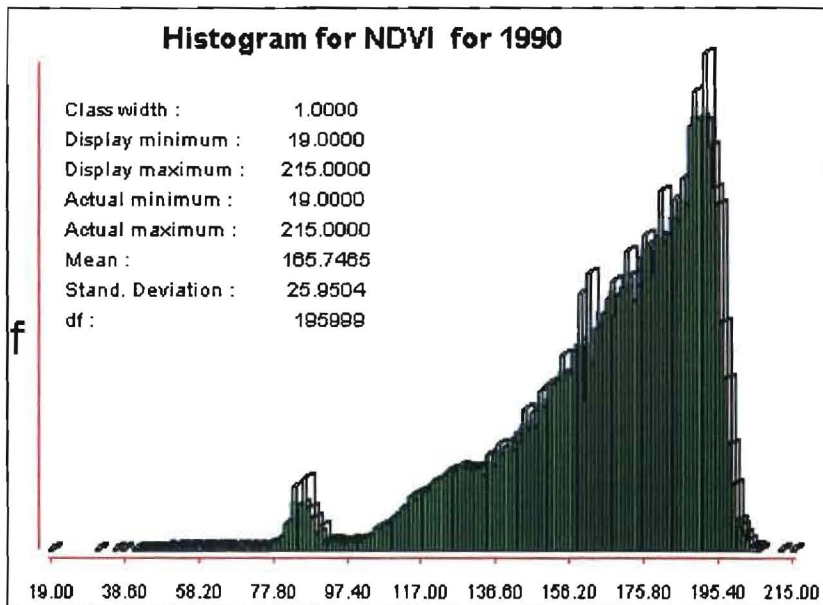
Fig. 21. Histogram for July 1990 NDVI.
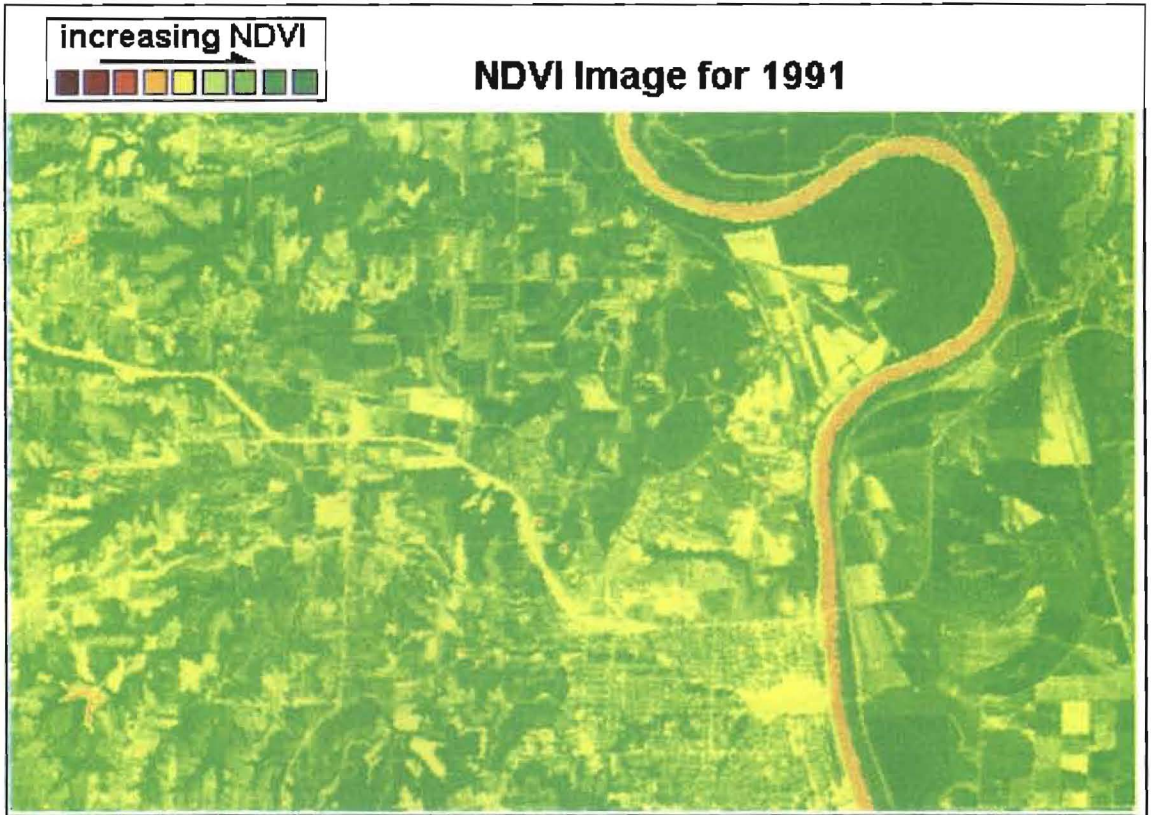
Fig. 22. NDVI image for July 1991.

Histogram for NDVI for 1991	
Class width :	1.0000
Display minimum :	11.0000
Display maximum :	237.0000
Actual minimum :	11.0000
Actual maximum :	237.0000
Mean :	173.4464
Stand. Deviation :	25.0101
df :	195999
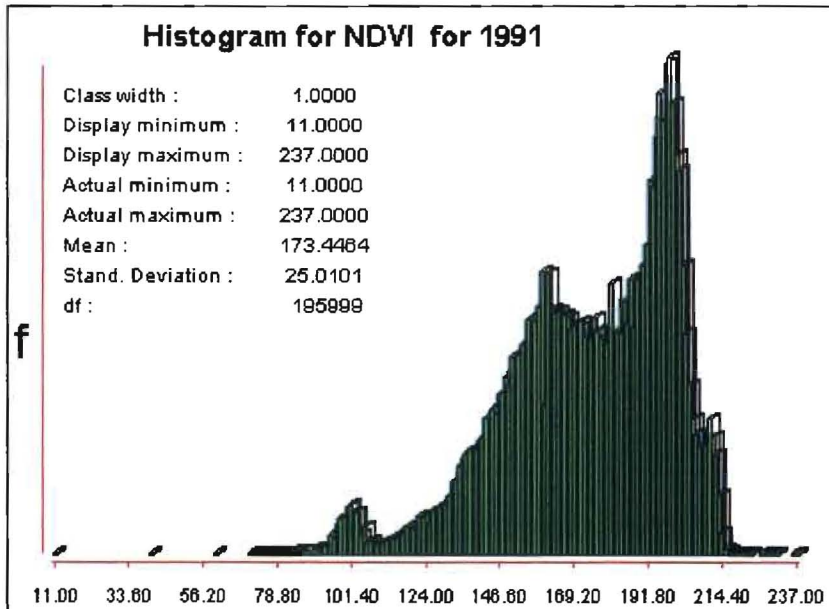
Fig. 23. Histogram for July 1991 NDVI.
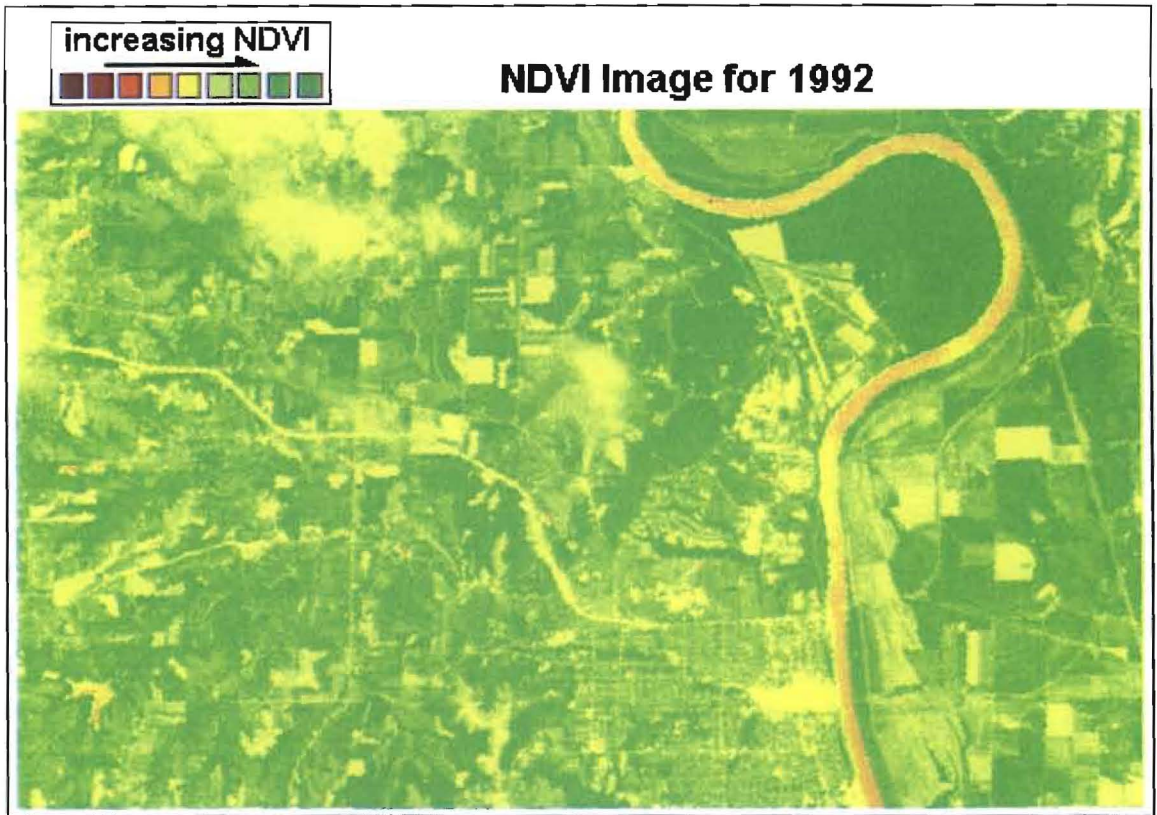
Fig. 24. NDVI image for July 1992.
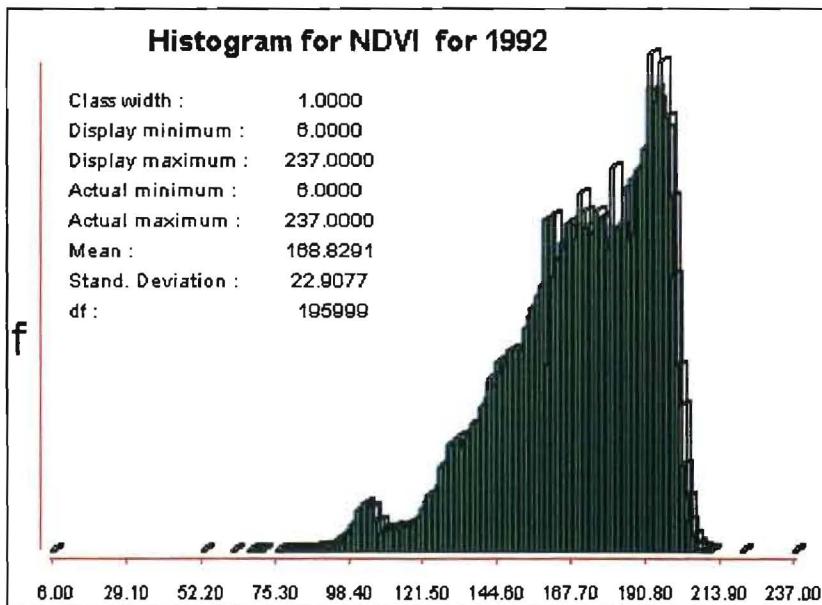
Fig. 25. Histogram for July 1992 NDVI.
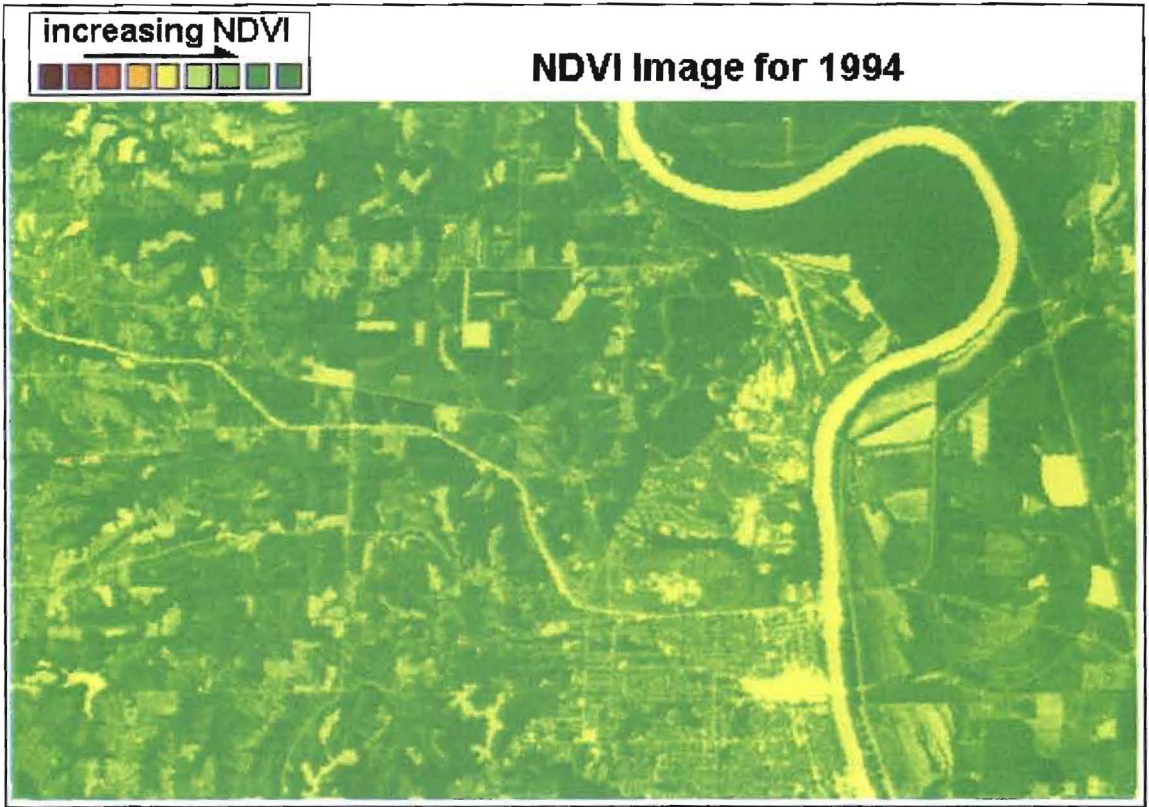
Fig. 26. NDVI image for July 1994.
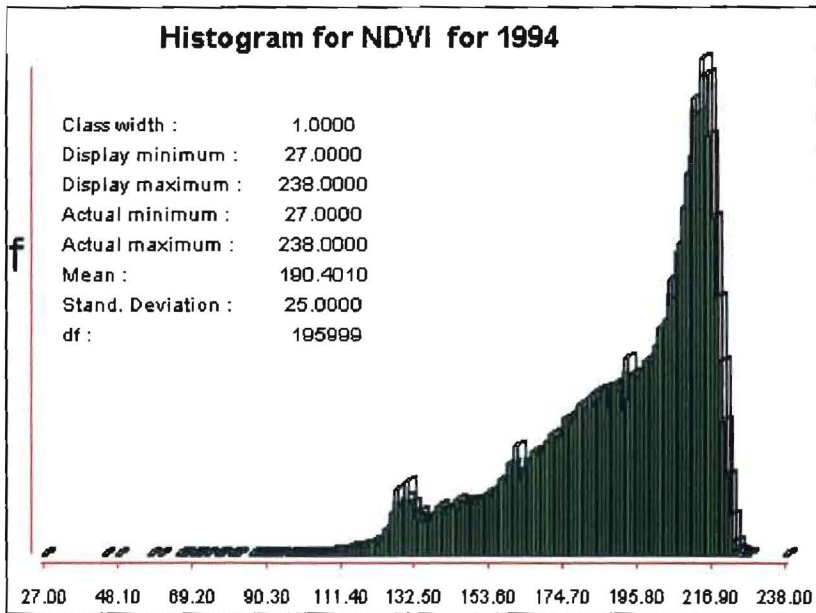
Fig. 27. Histogram for July 1994 NDVI.
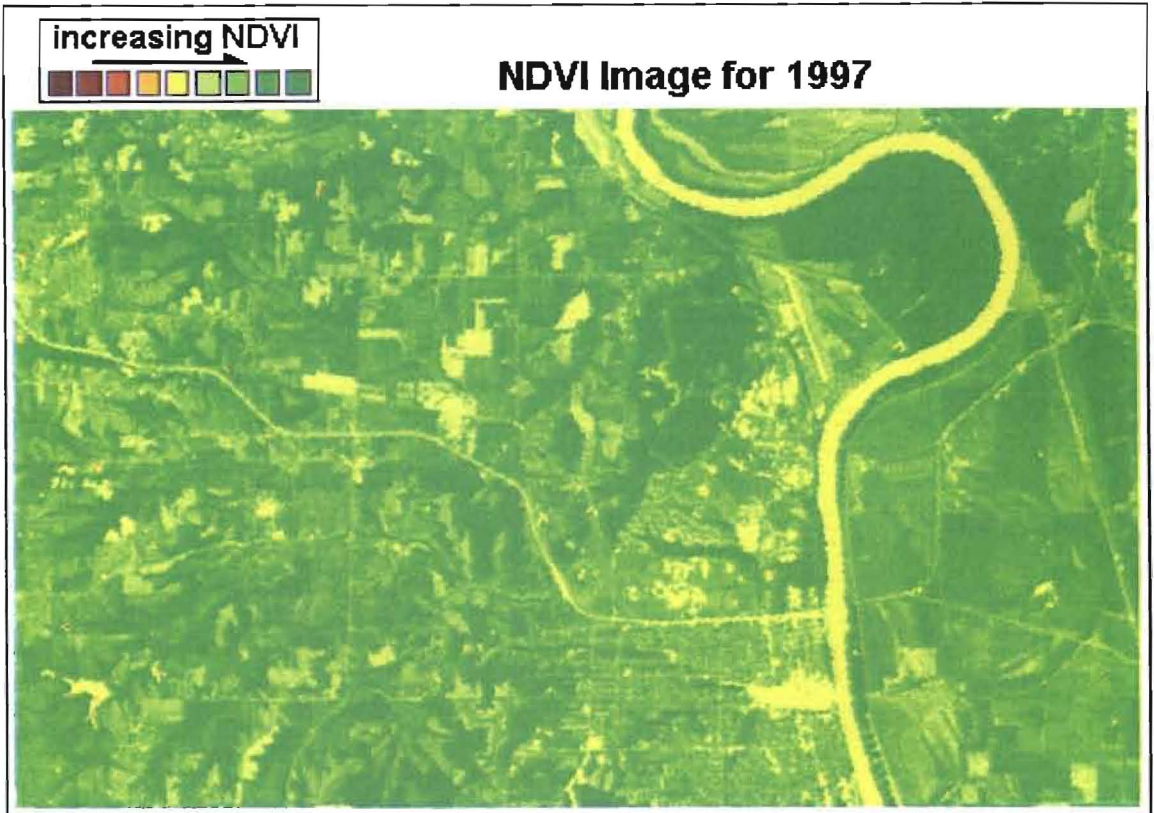
Fig. 28. NDVI image for July 1997.
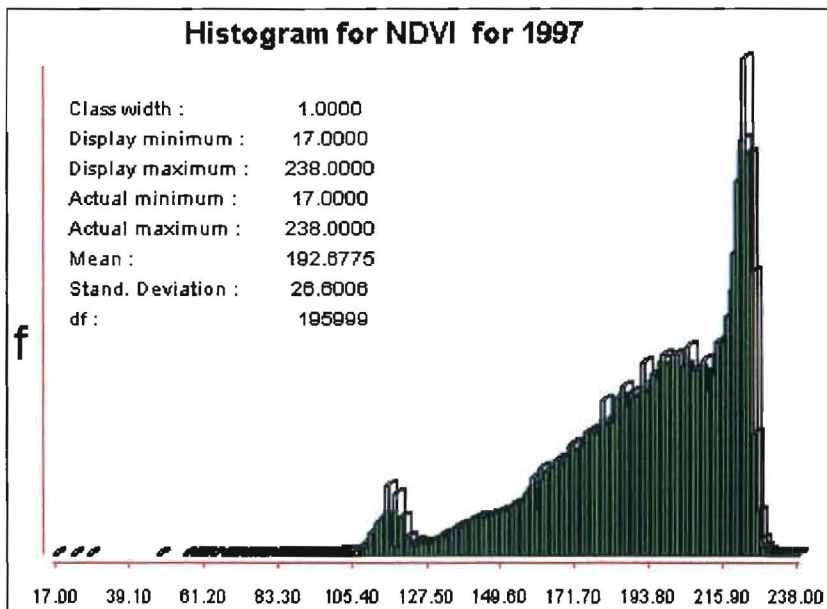
Fig. 29. Histogram for July 1997 NDVI.

Year	Min	Max	Mean	Relative % 1987=100%	SD
1987	20	235	201.1	100	28.6
1988	30	238	186.9	92.9	33.2
1989	10	221	179.2	89.1	21.1
1990	19	215	165.7	82.4	26.0
1991	11	237	173.4	86.2	25.0
1992	6	237	168.8	84.0	22.9
1994	27	238	190.4	94.7	25.0
1997	17	238	192. 7	95.8	26.6

Table 3.   Minimum. maximum. mean and standard deviation for

NDVI values for whole images.
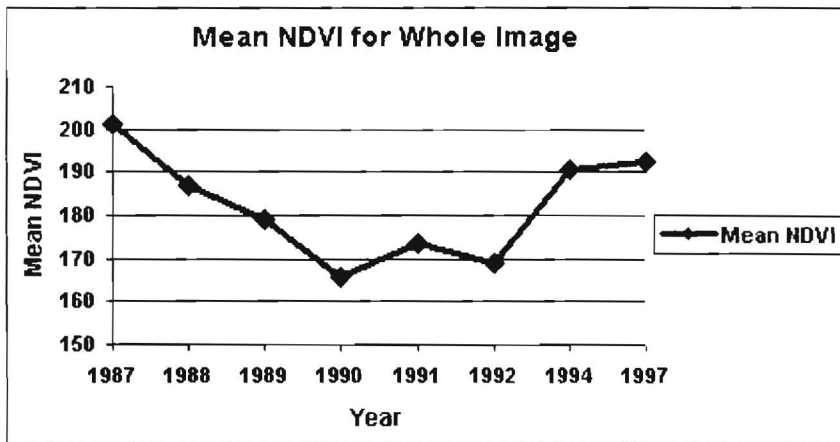
Fig. 30.   Graph of mean NDVI for images.
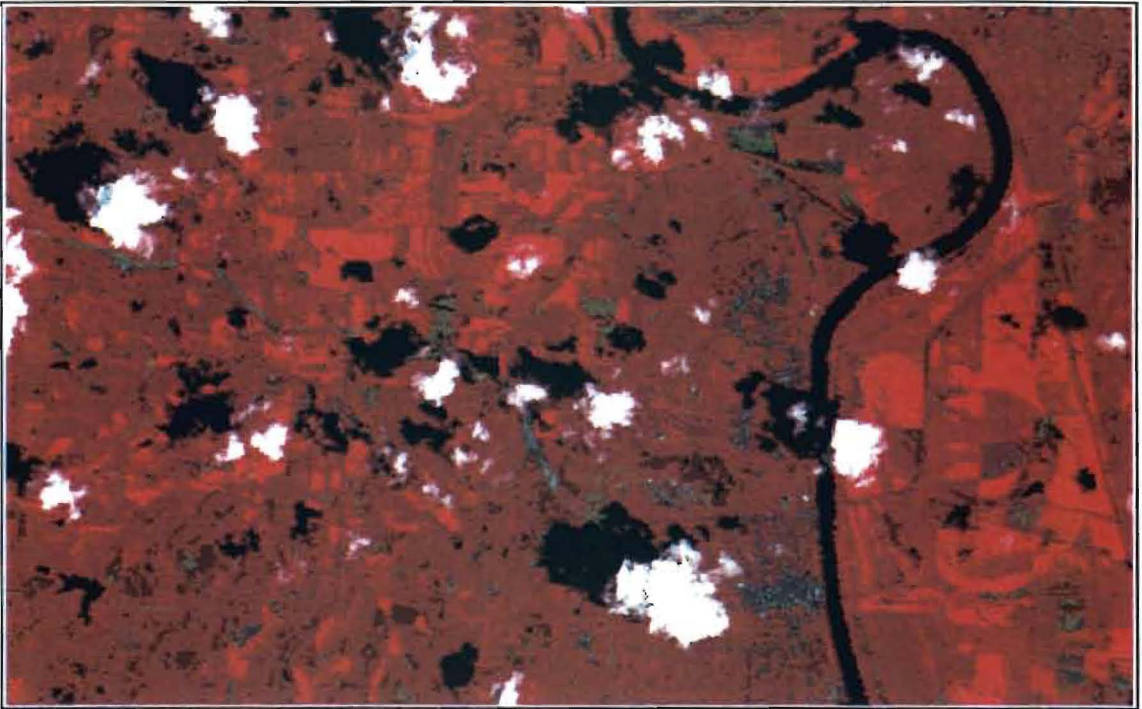
Fig. 31. Landsat TM standard false color composite (bands 2,3,4 - BGR) for July 1989, showing cloud cover over the study area.
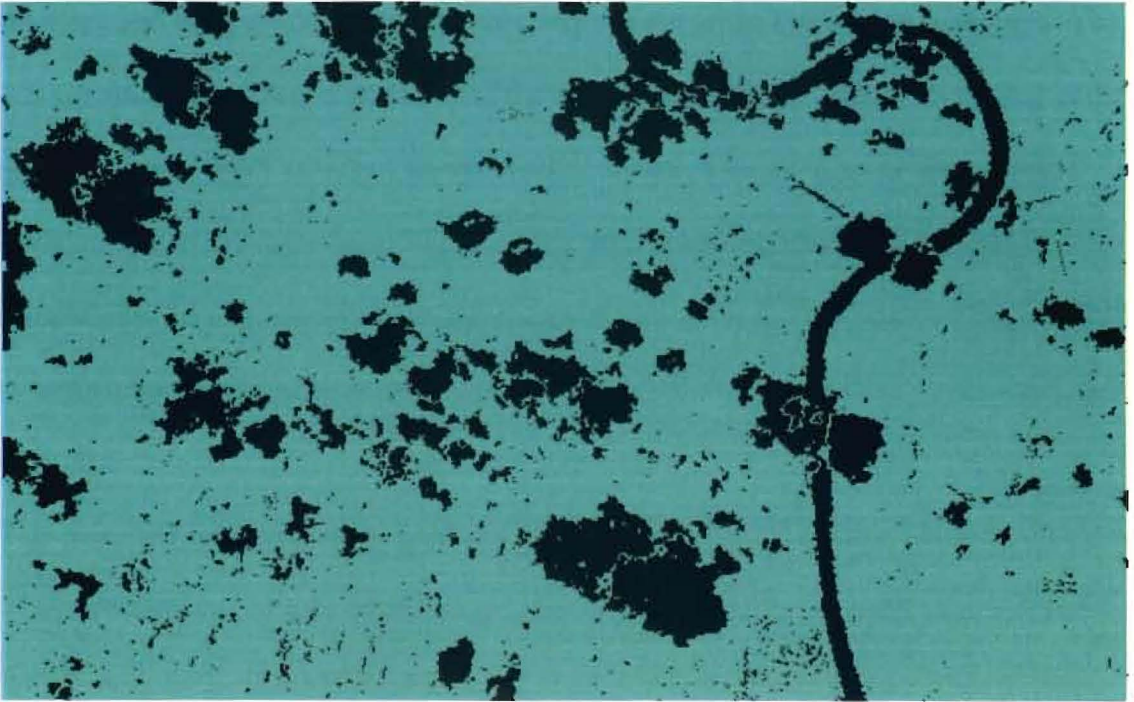
Fig. 32. ISOCLUST clusters reclassed to isolate clouds and shadows (black) from the image.

are black and have a value of 0. All other features are green and have a value of 1. The process also isolated water bodies with the clouds and shadows. These silty water bodies generally have NDVI values of 85-90 in other images. These values are 3-4 standard deviations from the respective NDVI means, so it is not expected that the removal of these additional features will have significant effect on the overall mean NDVI for 1989, in comparison to the other images.

This reclassed image was then used as a mask in the QUERY module. This module uses a mask to remove portions of an image. The output product is not itself an image but the "valid" or non-cloud/shadow values exist in tabular form. Statistical analyses of these values were used to determine a NDVI mean for the cloud/shadow-free portion of the image. A value of 179.2 with a standard deviation of 21.1 was obtained. For the cloud-covered image, the NDVI mean was 170.7 and standard deviation was 28.7.

This process works well for obtaining the mean and standard deviation of the image as a whole. However, the NDVI values for the separate forest areas were obtained by multiplying (OVERLAY) the respective 1987 forest masks by the NDVI image for each year. Because the image is lost in the QUERY process, it was not possible to use this method for calculating the NDVI values for the forests for 1989. Instead, a direct reclassification of the 1989 NDVI image was done (Fig. 33). All cloud and shadow pixel values were assigned a value of 0. In the process of removing the clouds and shadows with this classification, some non-cloud features were also removed.

1989 NDVI Image Reclassed to Remove Clouds
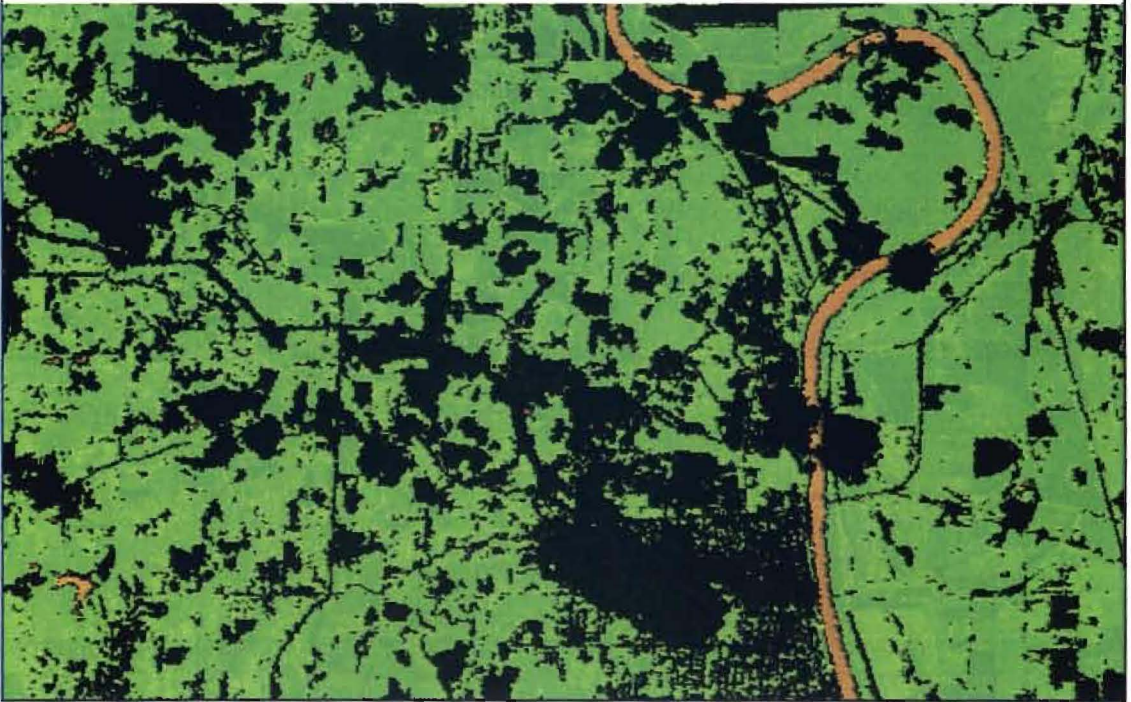
Fig. 33. NDVI image reclassed so that cloud and shadow pixels are set to 0 (black) This method also removes other low NDVI features such as roads.

Other low NDVI pixels such as roads, parts of the city of Leavenworth and the airstrips were eliminated, as well. The effect of this may be to increase slightly the NDVI mean by removing some low values.

3.3 Isolating the forests

Isolating the forests was accomplished with an unsupervised classification technique using the ISOCLUST module of *Idrisi*. This module uses an iterative self-organizing cluster analysis (*Idrisi*, 1999). This is an unsupervised classification technique in which the user selects the number of clusters to be derived from the image. The module randomly selects these clusters and uses an iterative routine to assign pixels to a cluster based on the minimum distance to the mean. A new mean is calculated for each cluster and reassignment of pixels occurs. The process is repeated until there is no significant change in the mean location of the clusters.

Using the 1987 image set, ISOCLUST was used with TM bands 3, 4, 5 and 7 plus a standard false-color composite created with bands 2, 3 and 4 assigned colors blue, green and red, respectively. Fifteen clusters were selected based on the histogram presented (Fig. 34) and the default number of three iterations was selected. Of the 15 clusters produced, clusters 1 and 3 belonged to the forests under study (Fig. 35). These were combined and assigned a value of 1 using the RECLASS function. All other clusters were reassigned a value of 0 (Fig. 36).
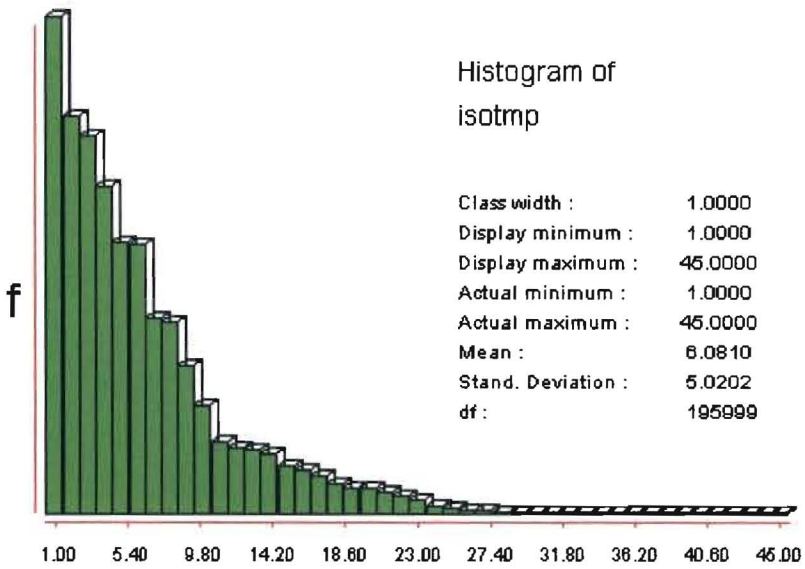
Fig. 34. Histogram showing breaks in the data used for the ISOCLUST

classifier. Fifteen clusters were selected for classification.
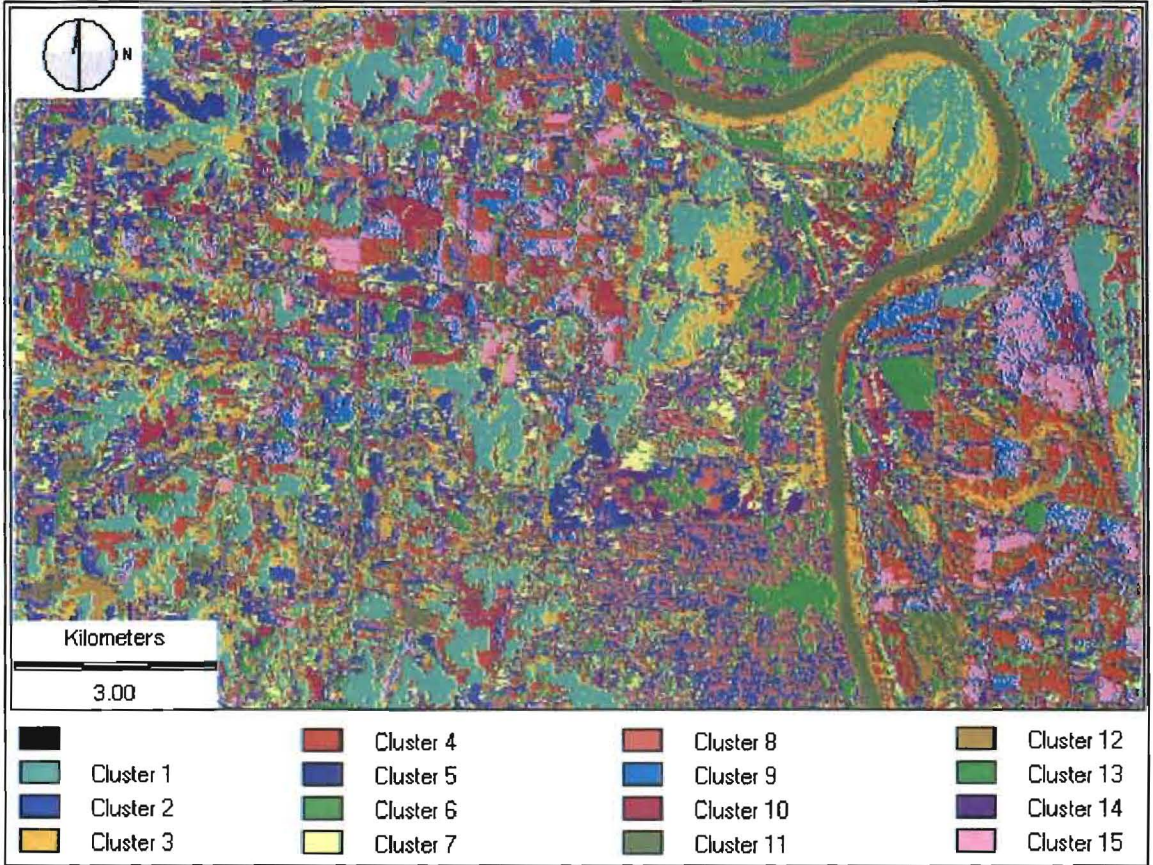
Fig. 35. The 15 clusters that were produced from the July 1987 image by the ISOCLUST

module are shown. Clusters 1 and 3 are forests.

Reclassified - All forests in green

Fig. 36. Clusters reclassified to separate all forests in the study area. Forests are shown in green.

The resulting image was further processed to separate the two individual forest stands of interest in this study. This was done with the GROUP module that joins contiguous pixels with the same value to form separate classes (Fig. 37). The hardwood and cottonwood forests were grouped separately. This image was reclassed twice, first to isolate the hardwood forest by assigning a value of 1 to that forest and 0 to all others. The same procedure was carried out for the cottonwood forest. The isolated forest stands are shown in (Figs. 38 and 39).
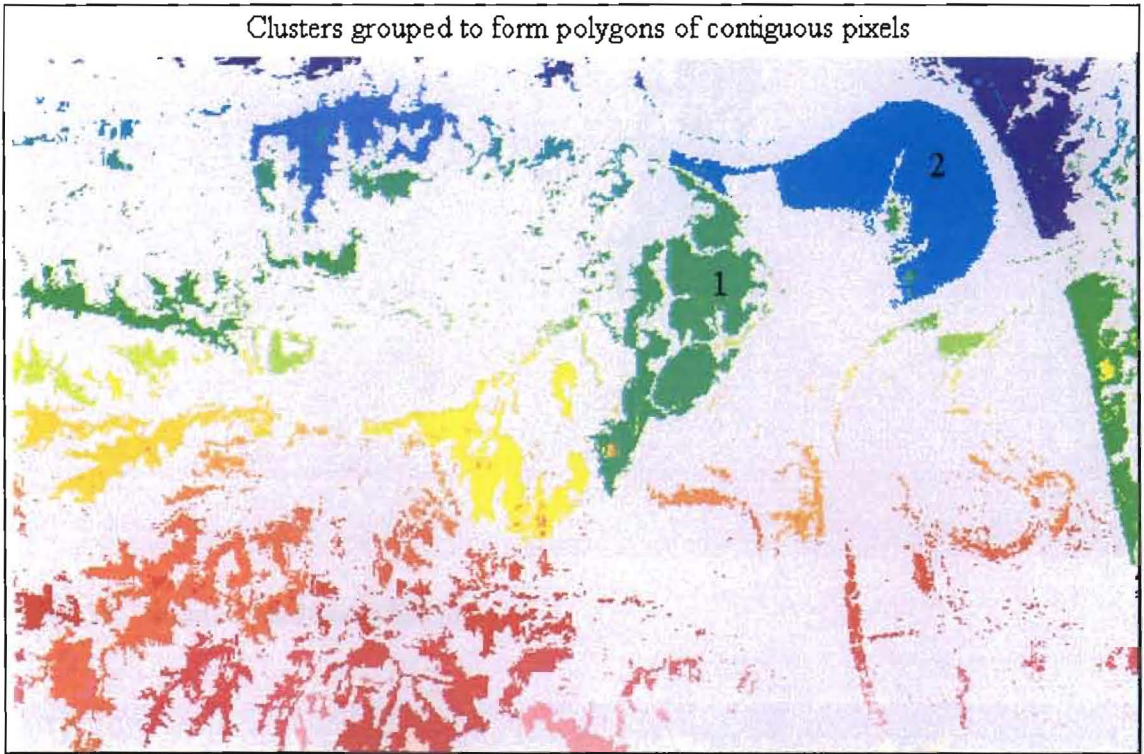
Fig. 37. Forests were grouped to create polygons of contiguous pixels. The hardwood forest is shown in green right-center of the image (1). The cottonwood forest is shown in pale blue, upper right (2).

Fig. 38. Isolated hardwood forest.
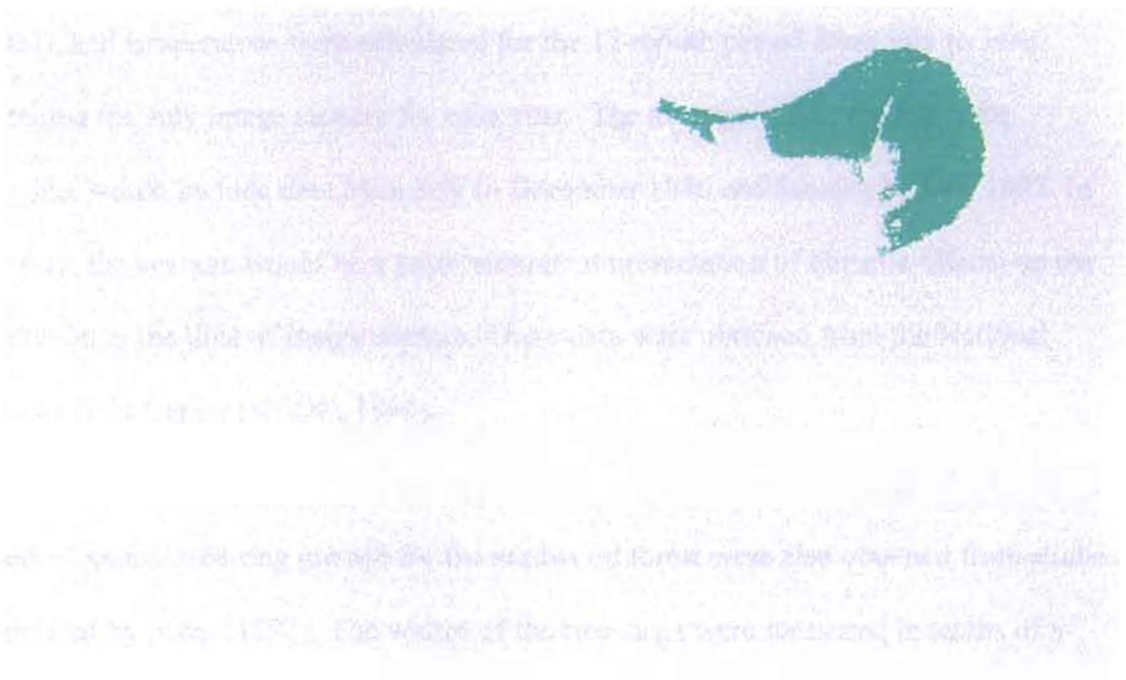
Fig. 39. Isolated cottonwood forest.

3.4 Calculating mean NDVI for the forests

With the forests isolated and the NDVI calculated for each image, the NDVI for each forest, for each year, was then determined. This was achieved by multiplying each forest mask with the NDVI image for successive years, using the *Idrisi* OVERLAY module. The result of this was to force all NDVI values outside the mask to zero, and represent only the NDVI values for the forests.

3.5 Climatic variables

In addition to the Landsat TM images, data on several climatic variables were obtained for the study region. Average values for precipitation, Palmer Drought Severity Index (PDSI), and temperature were calculated for the 12-month period from July to June, preceding the July image capture for each year. The average values for 1987, for example, would include data from July to December 1986 and January to June 1987. In this way, the average would be a more accurate representation of climatic effects on the vegetation at the time of image capture. These data were obtained from the National Climate Data Center (NCDC, 1999).

Residual annual tree-ring growth for the hardwood forest were also obtained from studies completed by Nang (1998). The widths of the tree-rings were measured in tenths of a millimeter.

3.6 Principal Component Analysis (PCA)

The PCA transformation is a multivariate statistical technique used for separating a dataset into uncorrelated linear combinations or components. Each component has little variance but together they represent all the data in the original dataset. If there is significant intercorrelation within the data, the first few components will account for a large part of the variance.

In *Idrisi*, the Time Series Analysis (TSA) module performs principal component analysis. This module uses standardized variables with components based on the correlation matrix (Singh and Harrison, 1985). The effect of this is to give equal weight to each image used (Eastman, 1995). The technique can be used for data compression, where several datasets are combined to give most of the information in a few components. In this study, the technique was used to assess change detection in the forests based on spectral variation over time.

As previously indicated, 1989 is an important year in these studies because of the low rainfall experienced at that time. However, the cloud cover on this image creates a problem of pixel contamination. In carrying out these analyses, PCA was performed separately on a dataset which included the July 1989 image and a dataset without the 1989 NDVI image. A discussion of this is provided in Appendix 4. The results show that there is no significant difference between the components generated from each dataset, except that with the 1989 image, component 2 represents clouds and shadows. On this

57

basis, it was decided to omit the 1989 NDVI image from the PCA analysis. The 1992

image also had slight cloud cover at the extreme western edge of the hardwood forest and

this image was omitted as well. As a result, six NDVI images were used for

multitemporal PCA analysis of each forest. These were NDVI images for the years 1987,

1988, 1990, 1991, 1994 and 1997. A time series file was prepared, listing the images to

be used in the multitemporal analysis. Each forest was analysed separately.

3.7 Image Differencing

Image differencing is a technique used to detect spectral changes between two images.

This requires subtraction of the values of cells of one image from the corresponding cells

of the other. The resulting image contains the difference values which may be negative,

positive or zero. The histogram of differences typically follows a symmetrical

distribution, and a normal distribution is assumed (Eastman, 1995). To determine areas of

real change, a threshold is set (Singh, 1989; Eastman, 1995). Values outside this

threshold are considered to represent extra-ordinary change while values within the

threshold are considered to be normal variations.

For this study, differences were calculated for the NDVI images 1988-1987, 1990-1988,

1994-1991, 1997-1994 and 1997-1987. Each forest was processed separately. The

threshold was set, in each case, to two standard deviations from the mean NDVI

difference.

To subtract the NDVI images, the background zero values were reclassed so that the subtraction process would not result in a background of zero change. This would compromise the true zero change values. For example, when subtracting the 1987 NDVI image from the 1988 NDVI image, the zero background values for 1987 were set to 100 and zero values for 1988 were set to -100. The OVERLAY module was used for subtracting the images. When subtracted, background values would be -200. These values were then removed from the final histogram plot that was used to determine differencing means and standard deviations.

With the NDVI difference images calculated, the images were further reclassed to indicate areas of negative change, no change and positive change. A threshold of two standard deviations (SD) was set. Classes were assigned as follows:

0 = Background values

1 = minimum value up to (Mean - 2 * SD)

2 = values between (Mean - 2 * SD) and (Mean + 2 * SD)

3 = values above (Mean + 2 * SD)

Class 1 indicates negative NDVI change, class 2 indicates no change and class 3 suggests positive NDVI change. A color palette was designed for these classes. Background values are shown in black, decreased NDVI values in red, no change pixels are shown in white and positive change is seen in green.

3.8 Ratio of band 5 : band 4

The ratio of Landsat TM band 5 to band 4 is also called the Moisture Stress Index (Hunt and Rock, 1989) and is intended to detect decreased vegetation vigor caused by decreased water content in foliage. Liquid water absorbs strongly in the mid- to far-infrared range, and only weakly at shorter wavelengths. As the water content of leaves decreases, less absorption of energy occurs in this range, and reflectance increases. These changes are less in the near-infrared range and hence an increase in the ratio of band 5 to band 4 should suggest decreasing water content of the tree canopy.

For this process, the OVERLAY module of *Idrisi* was used to calculate the ratio of band 5 to band 4 for years 1987 to 1992, 1994 and 1997. For the 1989 image, the RECLASS module of Idrisi was used to remove clouds and cloud shadows. As with the 1989 NDVI image, a value of 0 was assigned to pixels that represent these features. To determine the ratio for the isolated forests, the 5:4 ratio for the whole scene, for each year, was then multiplied by the 1987 mask for the hardwood and cottonwood forests, separately.

The band 5:4 ratio plots (Fig. 40) indicate that the forests follow parallel curves, both with a shallow negative trend, over the study period. The hardwood forest is almost linear except for small variations in 1989 and 1994. The cottonwood forest shows slightly larger peaks, also in 1989 and 1994. In order to unmask the fluctuations in the ratio values, the trend was removed by linear regression analysis using the "least squares" method. The residuals obtained from this process were used for further analysis and interpretation.

Ratio of band 5 to band 4 for hardwood and cottonwood forests

	1987	1988	1989	1990	1991	1992	1994	1997
Hardwood	0.85	0.84	0.83	0.77	0.74	0.71	0.69	0.62
Cottonwood	0.71	0.66	0.72	0.64	0.59	0.57	0.61	0.56
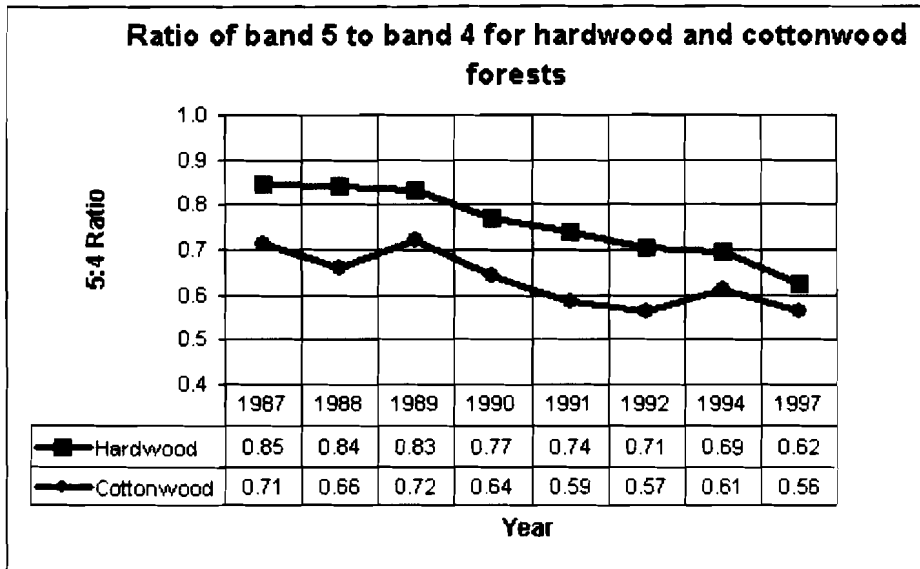
Fig. 40. Ratios of band 5 to band 4 for hardwood and cottonwood forests. The graph shows a decreasing trend over the study period. The ratios for each forest are distinctly separate but parallel.

Chapter 4

Results

4.1 Introduction

This chapter presents the results obtained from the analytical methods used in this study. Tables and graphs of mean NDVI for each image dataset are first presented. This is followed by the PCA component loadings and images of the time-integrated NDVI data, and then mean NDVI difference of pairs of images. Finally, the results of residual data from the band 5: band 4 ratios are displayed. The results of each method are discussed in conjunction with climatic data.

4.2 Mean NDVI

The mean NDVI values for each forest and for the whole scene are shown in Tables 4 and 5. In order to determine the relative change in mean NDVI over the time of study, mean NDVI was calculated for each year as a percentage of the 1987 year. Mean NDVI for 1987 was assigned a value of 100% as the image for this year showed healthiest vegetation overall. These percentage values are also shown in Tables 4 and 5. Plots of mean NDVI percentages for each forest and the whole scene are shown in Fig. 41. These data show that the lowest mean NDVI for each forest and full scene occurred in 1990.

Year	Whole Scene Mean NDVI	Whole Scene Std. Dev	Whole Scene % NDVI
1987	201.1	28.6	100
1988	186.9	33.2	92.9
1989	179.2	21.1	89.1
1990	165.7	26.0	82.4
1991	173.4	25.0	86.3
1992	168.8	22.9	84.0
1994	190.4	25.0	94.7
1997	192.7	26.6	95.8

Table 4. Mean NDVI, Standard Deviation and NDVI percentage of full scene based on 1987 image representing 100% for whole scene.

Year	Hardwood Mean NDVI	Hardwood Std. Dev	Hardwood % NDVI	Cottonwood Mean NDVI	Cottonwood Std. Dev.	Cottonwood % NDVI
1987	227.7	4.6	100	223.7	4.8	100
1988	216.4	12.2	95.0	224.3	6.2	100.3
1989	191.2	6.4	83.9	192.8	7.8	86.2
1990	189.8	7.1	83.3	190.7	8.3	85.3
1991	195.1	7.4	85.7	199.2	6.0	89.1
1992	192.5	9.8	84.5	196.4	4.3	87.8
1994	211.7	9.1	93.0	211.0	8.7	94.3
1997	220.0	7.4	96.6	220.4	4.8	98.5

Table 5. Mean NDVI, Standard Deviation and NDVI percentage based on 1987 forest masks representing 100% for hardwood forest and cottonwood forest.

Relative NDVI based on 1987 as 100%

% of 1987 NDVI

	1987	1988	1989	1990	1991	1992	1994	1997
Hardwood	100.0	95.0	83.9	83.3	85.7	84.5	93.0	96.6
Cottonwood	100.0	100.3	86.2	85.3	89.1	87.8	94.3	98.5

% of 1987 NDVI

	1987	1988	1989	1990	1991	1992	1994	1997
Whole scene	100.0	92.9	89.1	82.4	86.3	84.0	94.7	95.8

Year
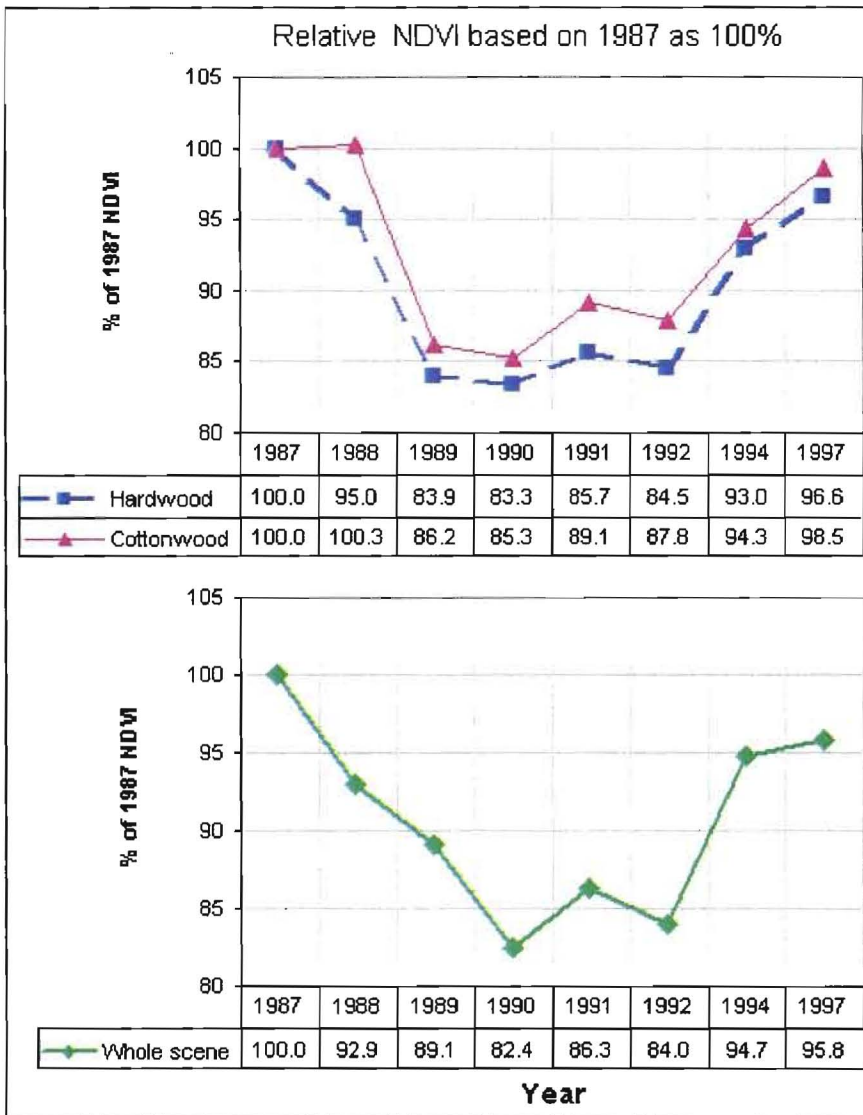
Fig. 41. Plots of relative changes in mean NDVI for the whole scene, hardwood forest, and cottonwood forest. The 1987 NDVI image for the whole scene and 1987 forest masks are assumed to represent 100%. Lowest values for all categories occur in 1990.

Table 6 presents several climatic variables for the Leavenworth region over the study period. The data include average 12-month precipitation, temperature, PDSI and annual tree-ring growth for the oak-hickory forest.

Fig. 42 shows plots of precipitation, PDSI and tree-ring residuals and temperature. The variations in precipitation and PDSI show the same pattern over time and correlate very well. The lowest values occur in 1989, and highest values in 1993. During the study period, mean 12-month temperature varied between $10.5°$ C to $13.0°$ C. The lowest value occurred in 1993 when heavy rains flooded the region, and the highest in 1987 and 1991.

The tree-ring residuals represent annual variations and there is a slight offset of the residual tree-ring data with precipitation and PDSI. This could be the result of the difference in the twelve months used for determining the averages. The patterns of variation, however, are very similar with the exception that the lowest tree-ring value occurred in 1988.

Year	Average July - June Precipitation (cm)	Average PDSI - July to June	Annual Residual Tree-ring Growth (10th mm)	Average July -June Temperature (^{o}C)
1987	100.8	3.46	3.64	13.0
1988	58.0	-0.28	-6.42	12.2
1989	43.2	-4.27	-2.22	12.2
1990	84.8	0.34	2.94	11.9
1991	64.7	-0.56	-2.59	13.0
1992	59.0	-0.58	0.67	12.7
1993	104.2	3.14	0.85	10.5
1994	93.1	1.69	-1.63	11.8
1995	81.8	-0.30	-0.41	11.8
1996	72.9	0.39	2.11	11.5
1997	72.9	1.91		11.0

Table 6. Average precipitation, Palmer Drought Severity Index, annual residual tree-ring growth and average temperature.

Fig. 42. Plots of annual precipitation (cm), PDSI, residual tree-ring data (10th mm) and temperature (^{o}C). Precipitation, PDSI and temperature were determined for the 12-month period, July to June, prior to the Landsat image capture.

Average 12-month (July to June) Precipitation

Average 12-month (July to June) Palmer Drought Severity Index (PDSI)

Residual Average Annual Residual Tree Ring Growth

Average 12-month temperature - June to July
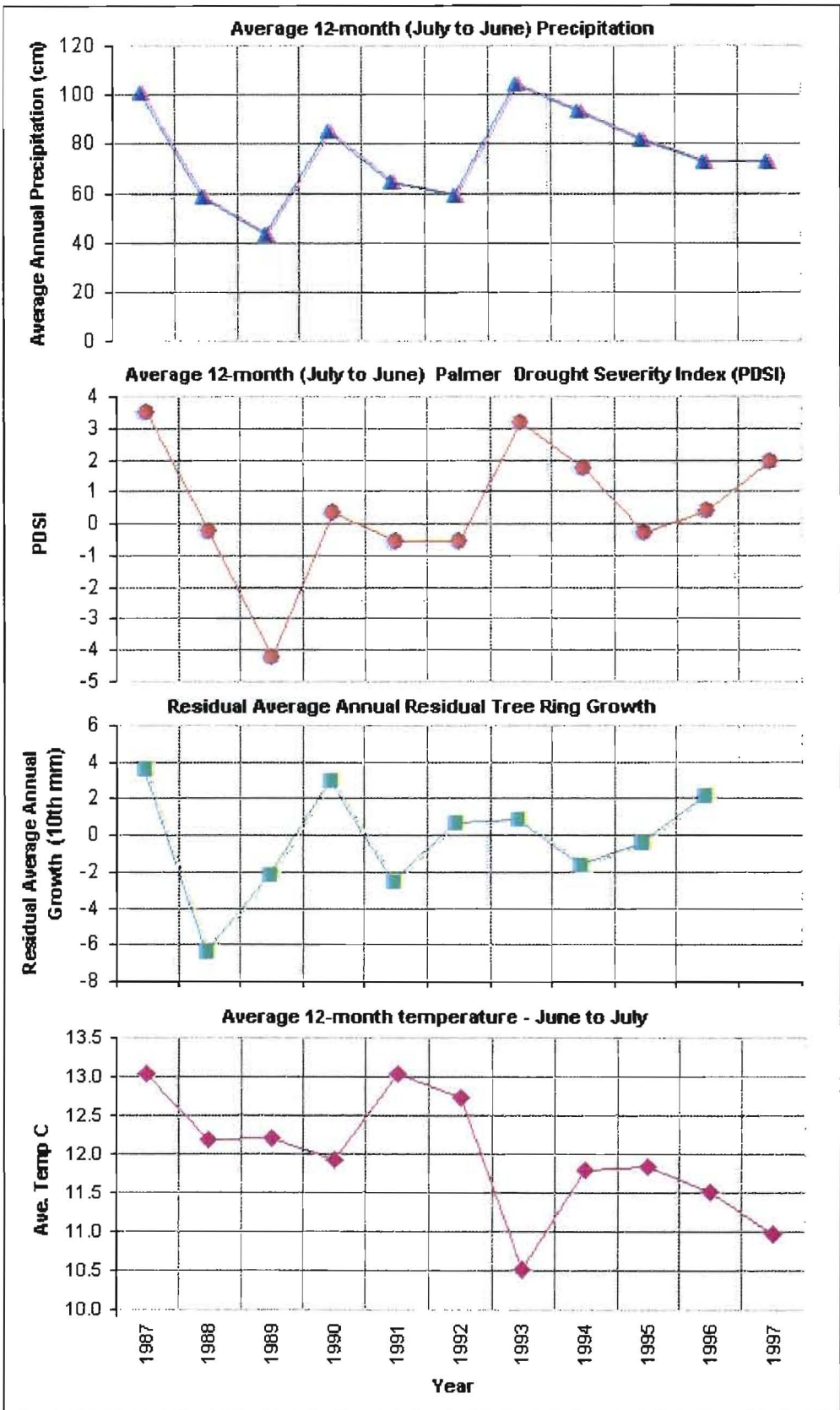
4.3 Principal Component Analysis (PCA)

The results of principal component analysis are presented as images showing the component NDVI values, as well as tabular data containing two elements of information. The first is the percent variance that each component derives from the total variance in the integrated dataset. The second contains the loadings or correlation of each original image with each component. The loadings vary from -1 (completely uncorrelated) to +1 (completely correlated). To assist with the interpretation of these analyses, data for precipitation, Palmer Drought Severity Index (PDSI), and annual tree-ring growth presented in Table 6 and Fig. 42, were integrated in this study.

4.3.1 Hardwood forest

Table 7 shows the percent variance that each component derived from the overall integrated images, as well as individual component loadings. Fig. 43 shows the plot of the percent variance of each component. The data show that more that 99.9% of the variation in the 6-image set is accounted for in component 1. This indicates that the images for all years are highly correlated and that there was not very much variation in NDVI over the study period. This is reflected in the component 1 image, which is similar in appearance to all July NDVI images. The small variations, however, can be significant and are of interest in this study.

	CMP 1	CMP 2	CMP 3	CMP 4	CMP 5	CMP 6
% Var	99.93196	0.02697	0.01378	0.01113	0.00914	0.00703
Loadings :	CMP 1	CMP 2	CMP 3	CMP 4	CMP 5	CMP 6
1987	0.999673	-0.0118	-0.0197	-0.0083	0.0031	-0.0081
1988	0.999344	0.0358	-0.0029	-0.0019	-0.0036	-0.0012
1990	0.999710	-0.0080	-0.0014	0.0206	-0.0088	-0.0025
1991	0.999781	0.0000	0.0017	0.0058	0.0185	0.0082
1994	0.999692	-0.0060	0.0206	-0.0065	0.0012	-0.0099
1997	0.999758	-0.0099	0.0017	-0.0097	-0.0104	0.0135

Table 7. Percent variance explained components 1 to 6 of NDVI images for the hardwood forest.

% Variance Contributed by Components of Hardwood Forest NDVI Images

	CMP 1	CMP 2	CMP 3	CMP 4	CMP 5	CMP 6
% variance	99.93196	0.026969	0.013779	0.01113	0.00914	0.007026

Year of Image
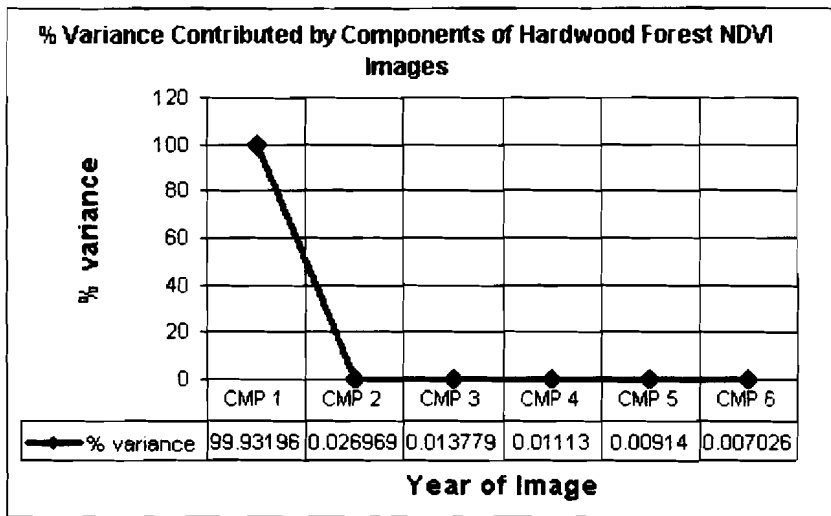
Fig. 43. Plot of percent variance contributed by 6 components derived from PCA analysis of NDVI images of the hardwood forest.

70

Fig. 44 shows the loadings plot and image for component 1. The graph shows the loadings of each component for each image in the dataset. Each NDVI image is identified by the year in which the Landsat data were obtained. The graph shows marked lower correlation for the 1988 NDVI and to a lesser extent, the 1994 NDVI image. On the component 1 image, this is represented by very slight variations in the color on the image. In 1988 and into 1989, the region suffered a severe drought as indicated by the reduced precipitation in Fig. 42.

The component 2 loadings graph and image are shown in Fig. 45. A strong positive correlation is present for the 1988 image, while the rest of the curve is relatively flat. Component 2 is, in effect, the first change component (Eastman, 1995), and the associated image shows where the areas of change are located. Generally, the background color represents no change and this serves as a guide in interpretation. Dark green colors indicate increasing NDVI and yellow to brown colors suggest negative change. Most of the forest is pale green, indicating little or modest change. Areas of decreased NDVI are concentrated around the outer edges of the forest, as well as along roads, horse trails and other areas of human activity. The forest edges in general are more open to the weather and climatic elements. The soil will dehydrate more quickly and the trees are more susceptible to damage from heat, wind and other climatic factors.

Fig. 44.

Above: Plot of loadings for component 1 of PCA analysis of hardwood forest.

Below: Image for component 1 of PCA analysis of hardwood forest.

Fig. 45.

Above: Plot of loadings for component 2 of PCA analysis of hardwood forest.

Below: Image for component 2 of PCA analysis of hardwood forest.

The third component plot (Fig. 46) shows a positive correlation for the 1994 NDVI image. The component 3 image shows NDVI reduction in parts of the interior and along the edges. These include an area west of Wagner Point, which is sparsely populated with trees, and also near the sanitary landfill in the north. Greening of some parts of the interior forest may be the result of heavy rains in 1993. The edges that show reduced NDVI have sparse tree cover and lower NDVI could be the result of flooding and other damage in 1993, as well as the reduction of temperature during that year.

The loadings and image for component 4 are shown in Fig. 47. This component shows a strong positive correlation for 1990. The component 4 image shows a general decline of the forest, as indicated by the pale green-yellow shades. Stronger reduction is evident along the eastern edge of the maple-basswood forest and near the edge of the sanitary landfill in the north. There was an increase in precipitation during 1990.

Component 5 loadings and image are shown in Fig. 48. This component shows a positive correlation in 1991 and the image indicates a decline of NDVI values in the northeast section of the forest but an increase in the southwest. Of the climatic variables considered in this study, this component may correlate with the average temperature for 1991 which had increased significantly over the previous year. Average precipitation for 1991 also decreased by 20 cm and tree-ring growth was lower than the previous year.
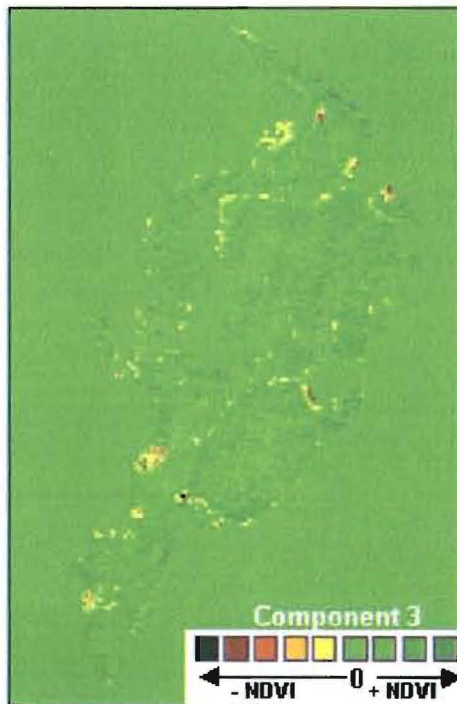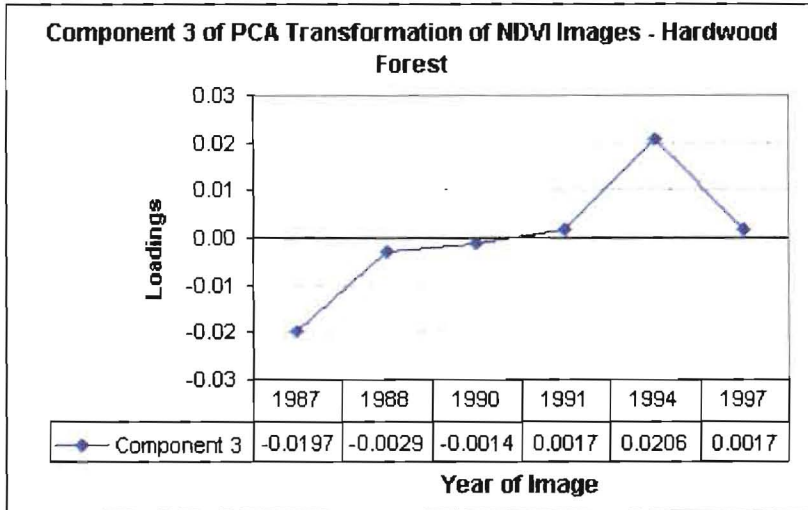
Fig. 46.

Above: Plot of loadings for component 3 of PCA analysis of hardwood forest.

Below: Image for component 3 of PCA analysis of hardwood forest.

Fig. 47.

Above: Plot of loadings for component 4 of PCA analysis of hardwood forest.

Below: Image for component 4 of PCA analysis of hardwood forest.

Fig. 48.

Above: Plot of loadings for component 5 of PCA analysis of hardwood forest.

Below: Image for component 5 of PCA analysis of hardwood forest.

Component 6 shows a small negative correlation for 1994 (Fig. 49). The image shows very small affected areas along the riverine forest west of Wagner Point and also near the sanitary landfill site.

For the higher order components such as 5 and 6, the patterns are more difficult to relate to the climatic factors. Some patterns may represent changes in spectral reflectance caused by differing atmospheric conditions, sun angles and sensor settings and may not be indicative of NDVI changes.

4.3.2 Cottonwood Forest

Table 8 shows the percent variance contributed by each of the 6 components of the PCA transformation of the cottonwood forest, as well as the individual loadings. As with the hardwood forest, the images are very highly correlated and component 1 represents over 99.9 percent of the total variance. Fig. 50 shows the associated percent variance plot.

The loadings for component 1 and associated component image are shown in Fig. 51. The loadings show changes in the correlation for the 1990 and 1994 NDVI images. The pattern is similar to the one for the hardwood forest, but with a 2-year difference between the first change component in 1988 for the hardwood forest and that in 1990 for the cottonwood forest. The decrease in 1994 may be representative of the effects of severe flooding of the in Missouri River 1993. This forest was inundated with floodwaters at that time.
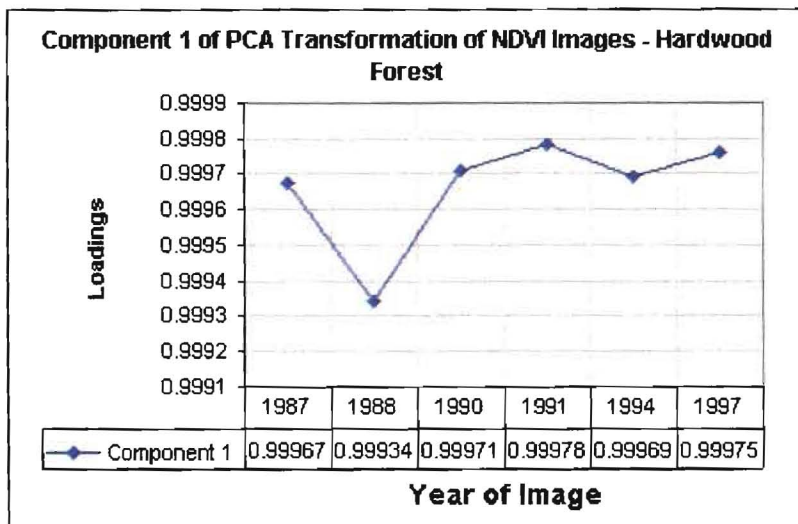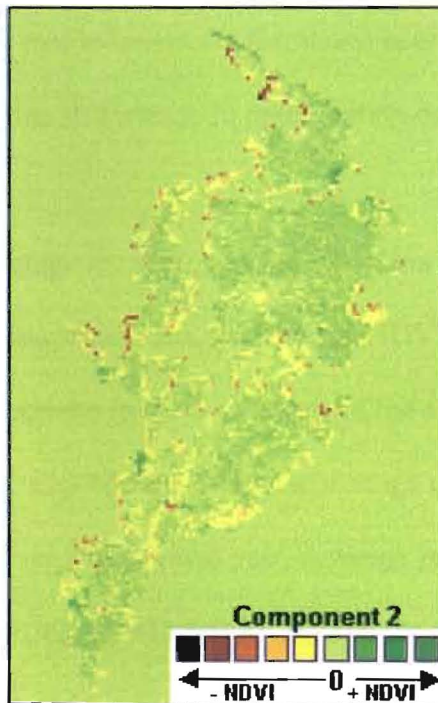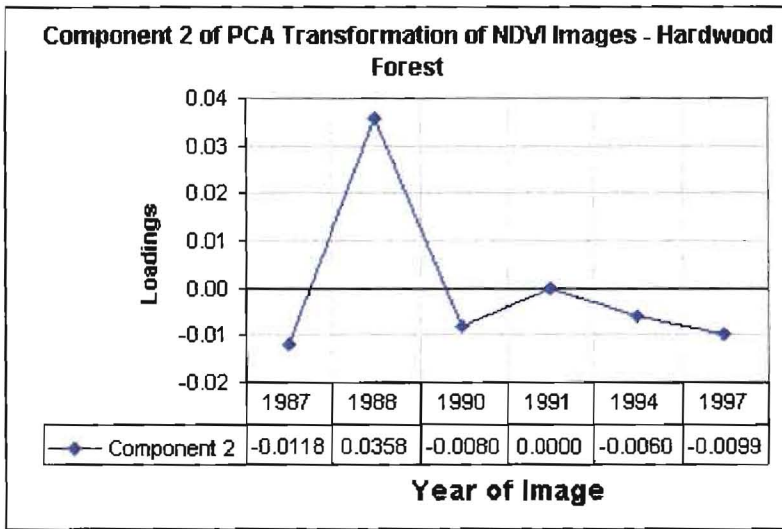
Fig. 49.

Above: Plot of loadings for component 6 of PCA analysis of hardwood forest.

Below:Image for component 6 of PCA analysis of hardwood forest.

	CMP 1	CMP 2	CMP 3	CMP 4	CMP 5	CMP 6
% Var	99.94922	0.01918	0.01312	0.00747	0.00648	0.00453
Loadings :	CMP 1	CMP 2	CMP 3	CMP 4	CMP 5	CMP 6
1987	0.999792	-0.0141	-0.0027	-0.0068	-0.0016	-0.0121
1988	0.999794	-0.0126	-0.0025	-0.0004	-0.0126	0.0087
1990	0.999599	0.0221	-0.0172	-0.0038	-0.0002	0.0003
1991	0.999814	0.0005	0.0006	0.0189	0.0014	-0.0030
1994	0.999651	0.0142	0.0219	-0.0044	-0.0019	-0.0002
1997	0.999826	-0.0101	0.0000	-0.0035	0.0149	0.0063

Table 8. Percent variance explained components 1 to 6 of NDVI images for the cottonwood forest.
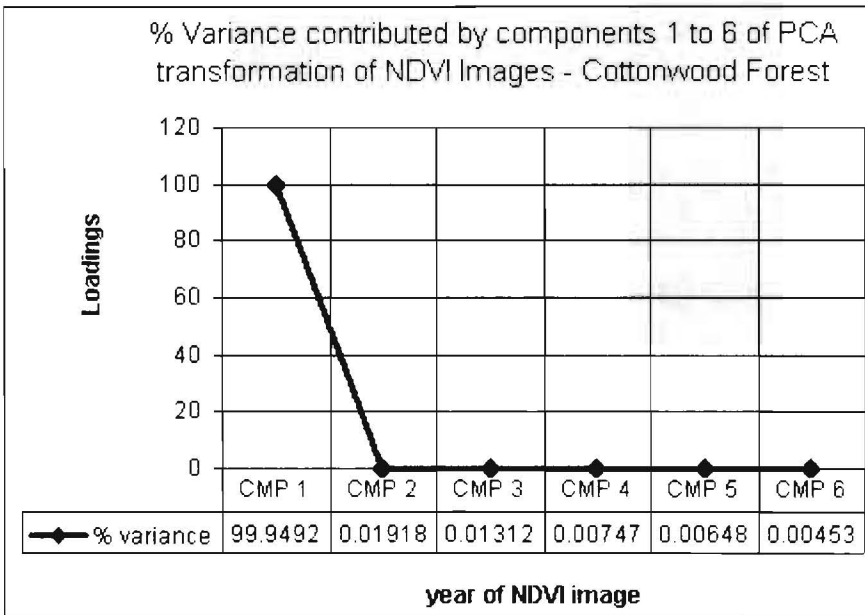
Fig. 50. Plot of percent variance contributed by 6 components derived from PCA analysis of NDVI images of the cottonwood forest.
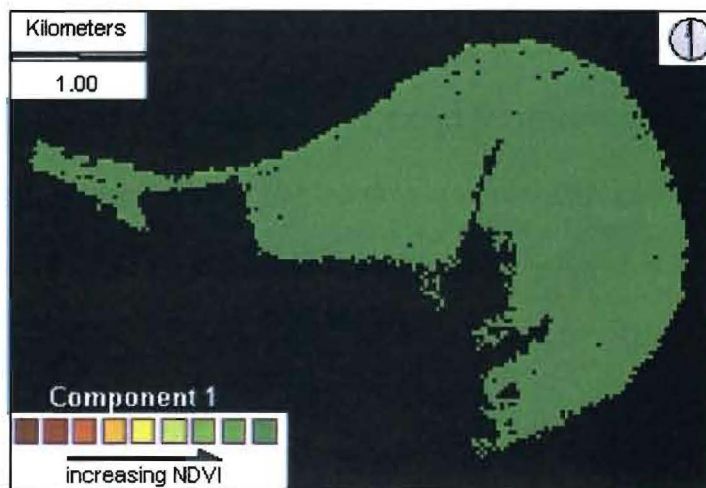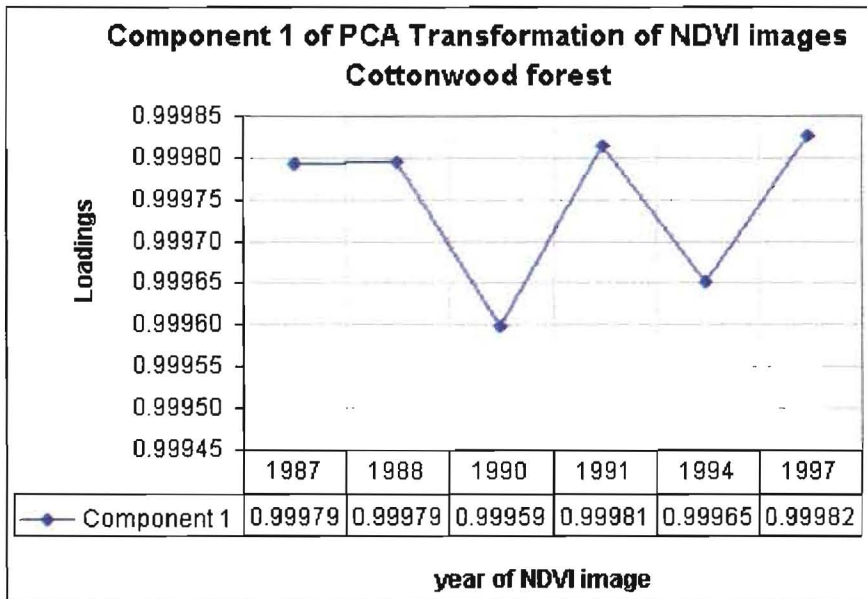
Fig. 51.

Above: Plot of loadings for component 1 of PCA analysis of cottonwood forest.

Below: Image for component 1 of PCA analysis of cottonwood forest.

The loadings graph and corresponding image for component 2 are shown in Fig. 52. The positive correlation of the 1990 and 1994 loadings with the component image indicate that the areas of decreased NDVI during those years occurred along the northern edge of the forest at Weston Bend and to the west. This is the first change component for the cottonwood forest and the lower NDVI of 1990 shows an offset from the 1988 hardwood forest response to the drought conditions. The 1994 decrease may be the result of destruction of parts of the forest by the severe flooding of the Missouri River in 1993.

Component 3 (Fig. 53) shows a negative correlation in 1990, suggesting an NDVI increase, and positive correlation in 1994, suggesting an NDVI decrease for images of those years. This component shows a response opposite to that of component 2 for 1990, and the same response for 1994, but the areas affected are the same. This component shows two broad spectral responses in the forest as a whole. The central section of the forest from Weston Bend and westward, is shown in one consistent shade, while to the north and south, another response is evident.

The loadings plot and image for component 4 are shown in Fig. 54. Component 4 shows a strong positive correlation with the 1991 NDVI image. This image indicates a general decline in NDVI over the forest as a whole, and an increase along the northern edge at Weston Bend and to the west. Some areas of decline are also evident along the western boundary with the airfield. This response is similar to that of component 5 for the

Component 2 of PCA Transformation of NDVI images
Cottonwood forest

|	1987	1988	1990	1991	1994	1997
Component 1	-0.0141	-0.0126	0.0221	0.0005	0.0142	-0.0101

year of NDVI image
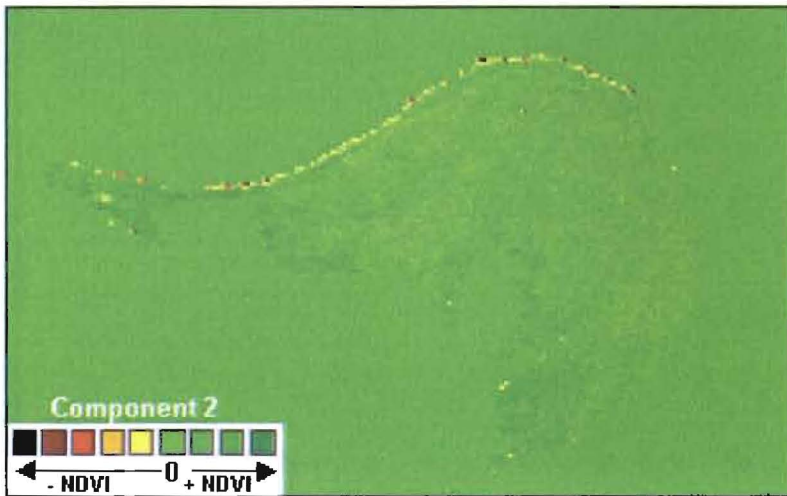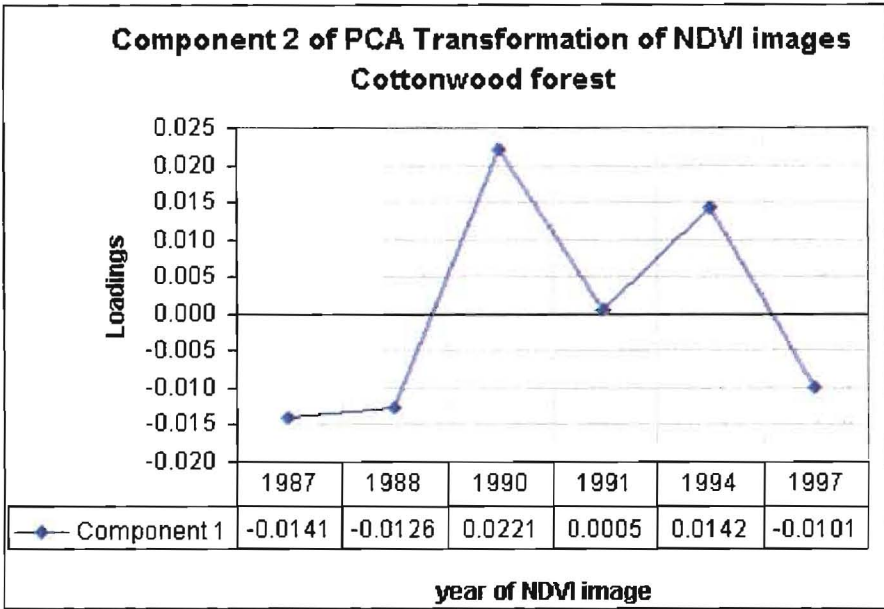
Fig. 52.

Above: Plot of loadings for component 2 of PCA analysis of cottonwood forest.

Below: Image for component 2 of PCA analysis of cottonwood forest.
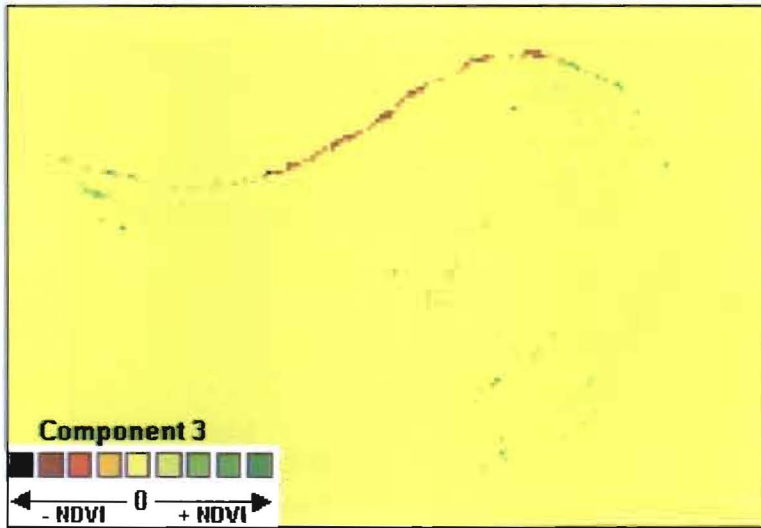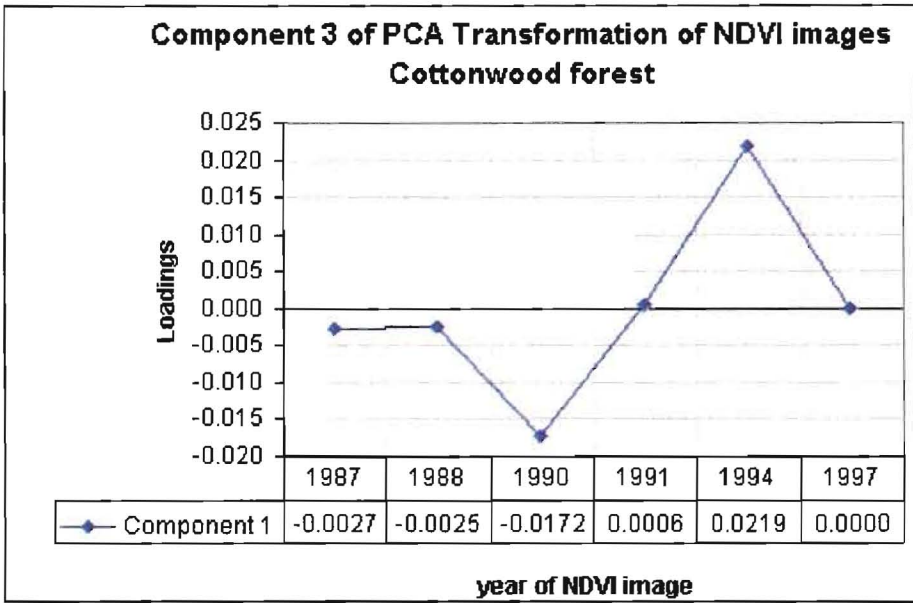
Fig. 53.

Above: Plot of loadings for component 3 of PCA analysis of cottonwood forest.

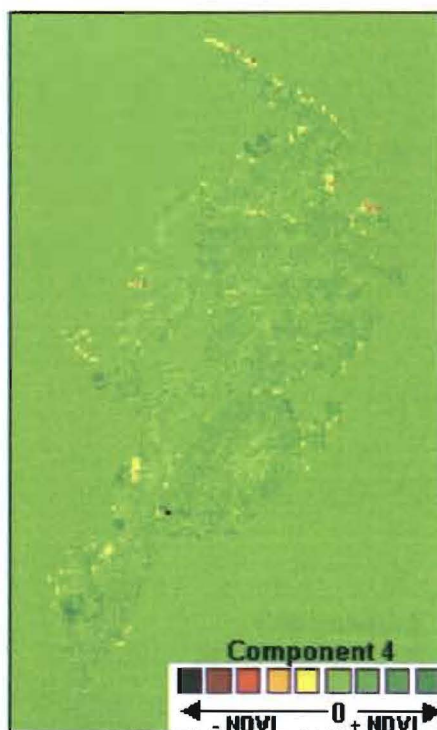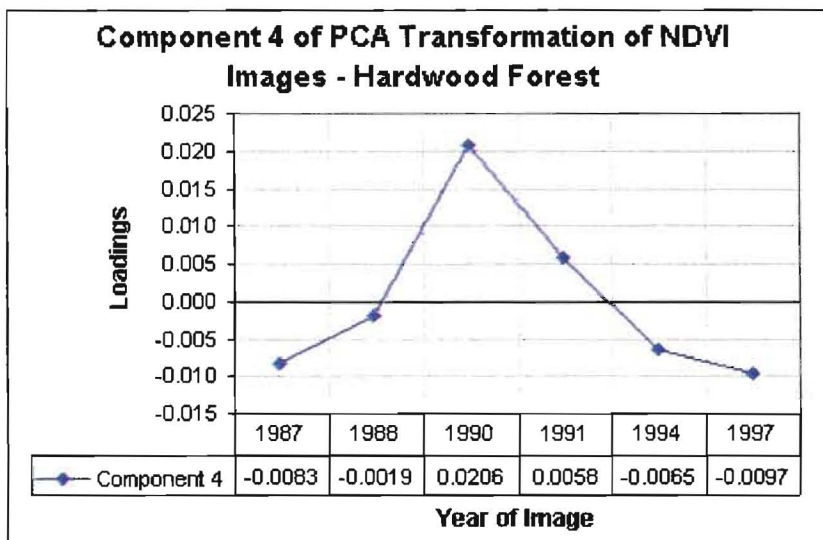Below: Image for component 3 of PCA analysis of cottonwood forest.
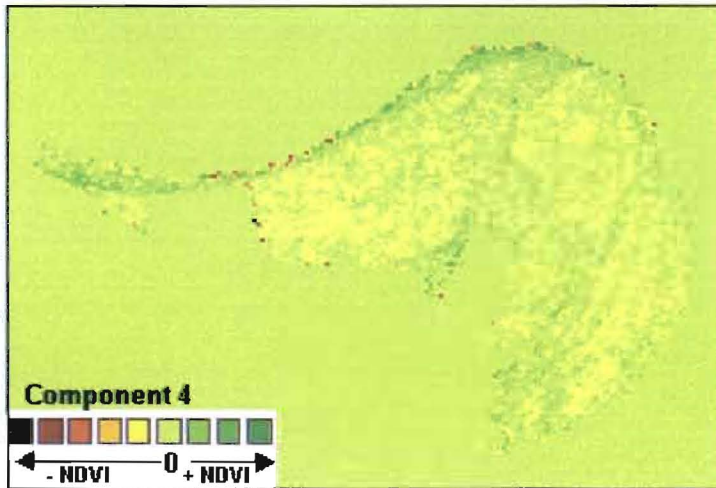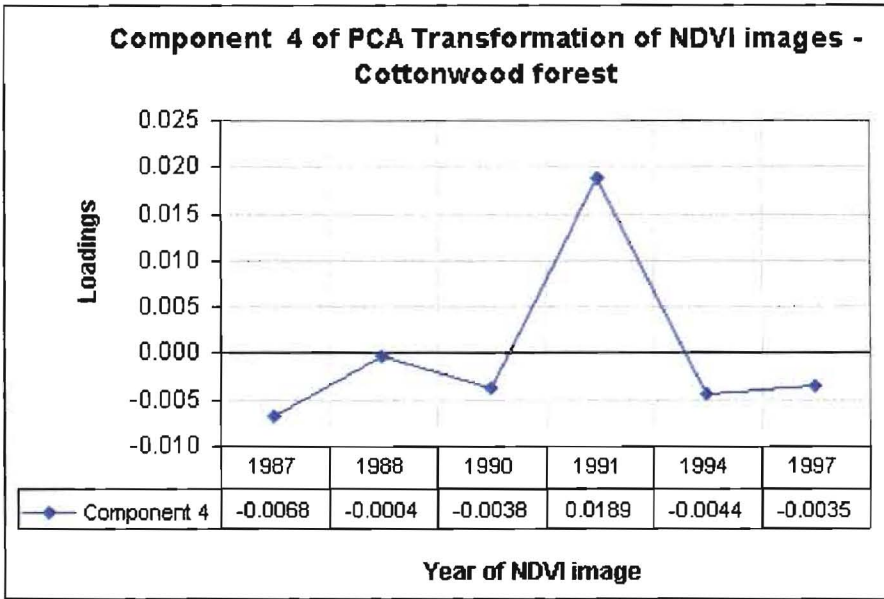
Fig. 54.

Above: Plot of loadings for component 4 of PCA analysis of cottonwood forest.

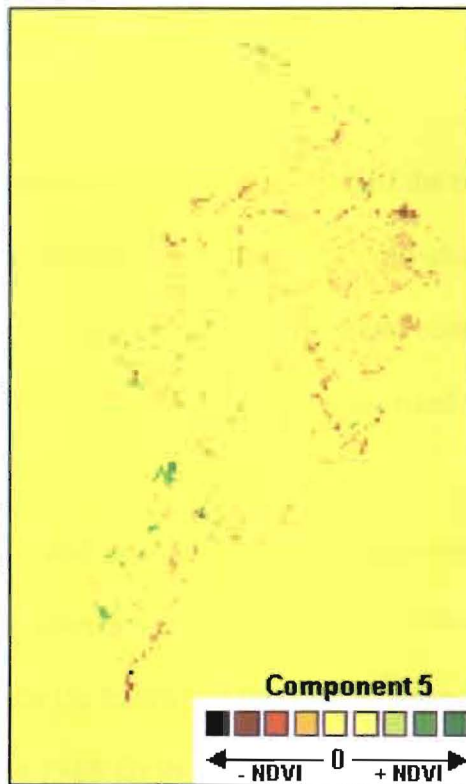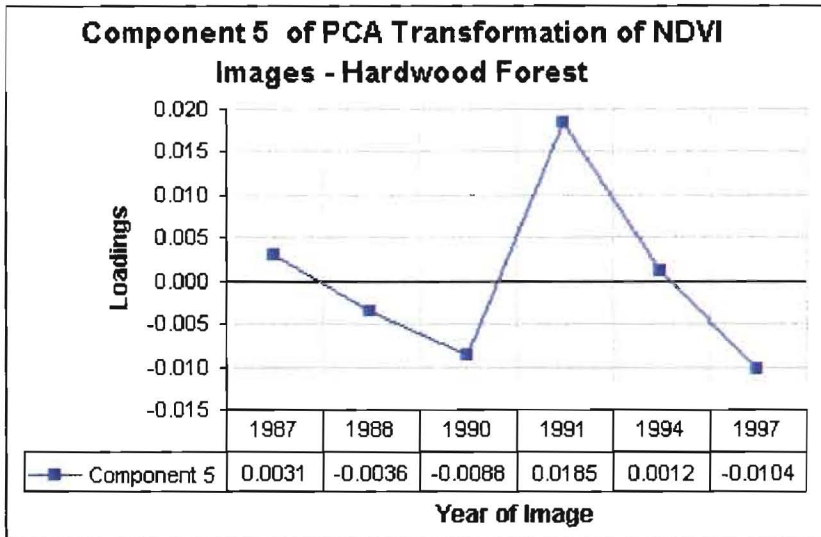Below: Image for component 4 of PCA analysis of cottonwood forest.

hardwood forest. As with the hardwood forest, the climatic factors that could be of some significance are an increase in average temperature and a decrease in precipitation in 1991.

Higher order components 5 and 6 (Figs. 55 and 56) both show responses in 1988. These could be associated with the drought conditions of that year and both components suggest an increase in NDVI for 1988. These components may represent spectral responses from the understory of this forest. The canopy cover is not full and the total radiance received by the Landsat sensor would include significant contribution from the forest understory. Other changes may relate to variations in atmospheric conditions, sun angles and sensor settings and may not necessarily relate to NDVI changes or vegetation response.
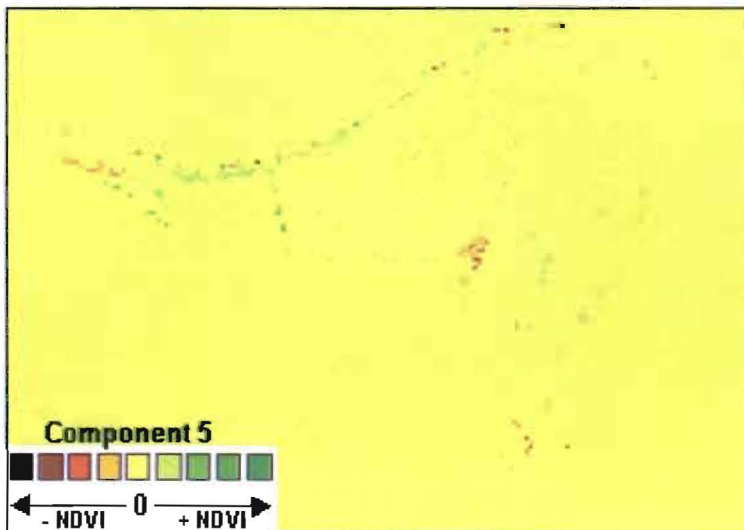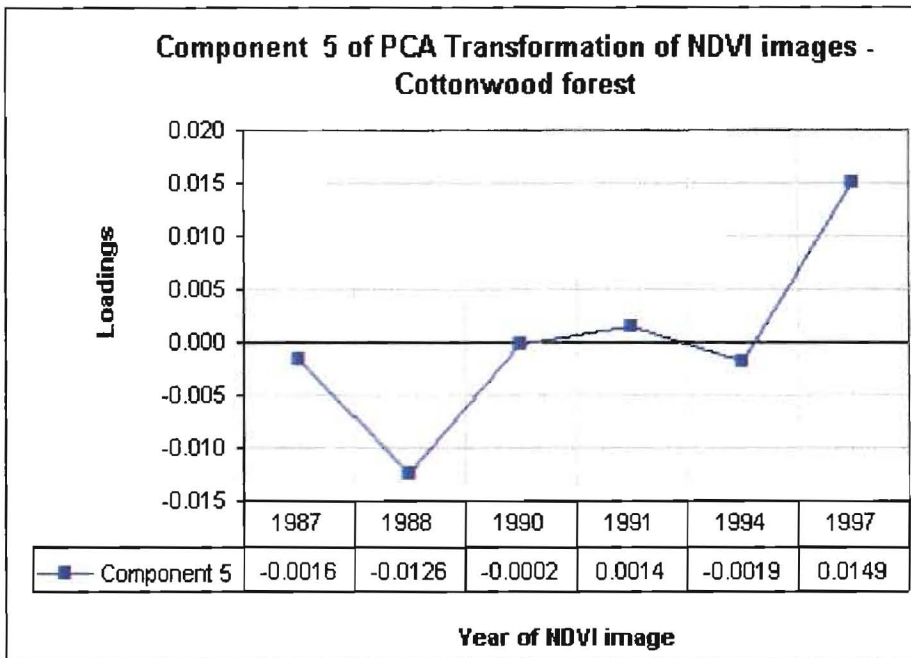
Fig. 55.

Above: Plot of loadings for component 5 of PCA analysis of cottonwood forest.

Below: Image for component 5 of PCA analysis of cottonwood forest.

Component 6 of PCA Transformation of NDVI images
- Cottonwood forest

	1987	1988	1990	1991	1994	1997
Component 6	-0.0121	0.0087	0.0003	-0.0030	-0.0002	0.0063

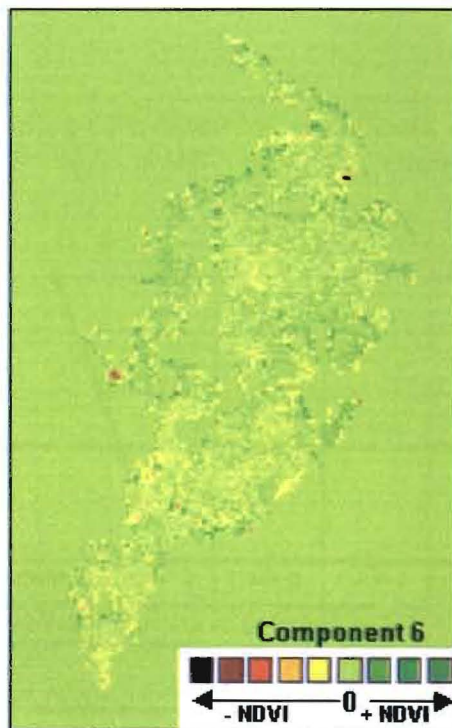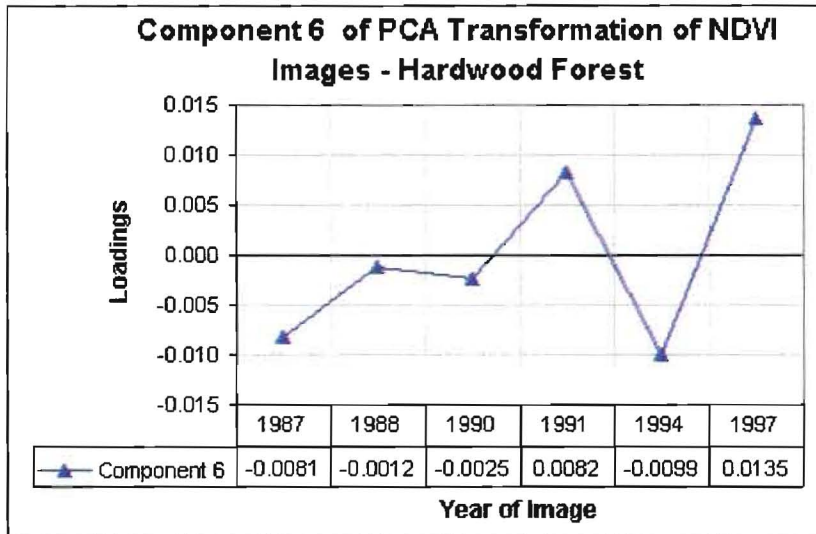Year of NDVI image

Component 6

- NDVI   0   + NDVI
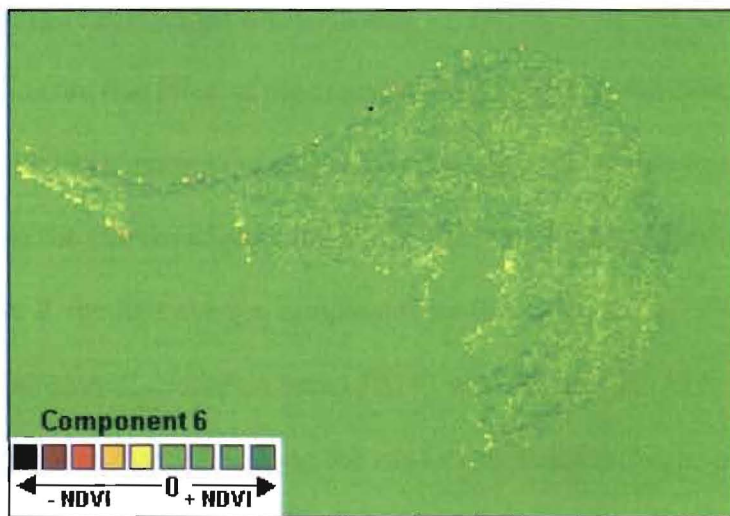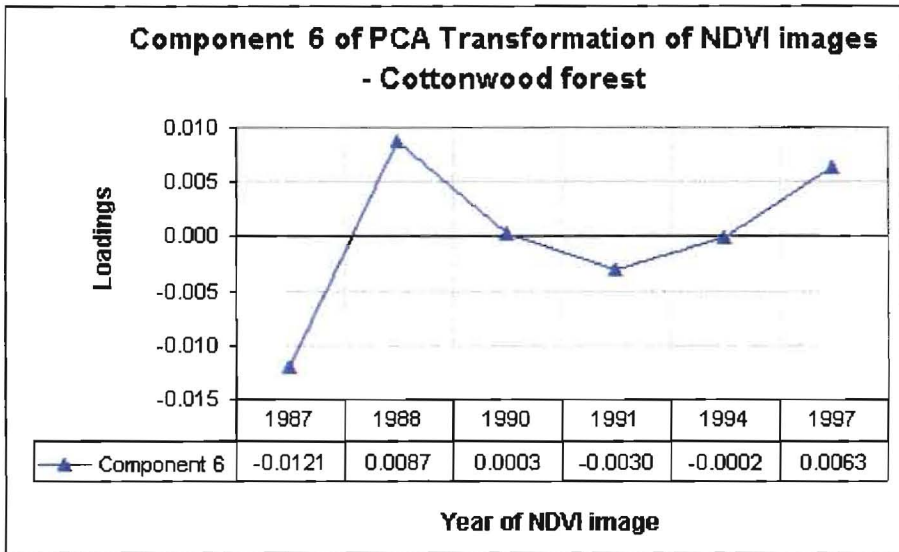
Fig. 56.

Above: Plot of loadings for component 6 of PCA analysis of cottonwood forest.

Below: Image for component 6 of PCA analysis of cottonwood forest.

88

4.4 Image Differencing

The image differencing method was also used to determine changes in NDVI by subtracting NDVI image pairs. Table 9 shows the mean NDVI differences for image pairs, including 1997-1987. Fig. 57 shows the plots of these difference values.

4.4.1 Hardwood forest

Figs. 58 to 62 show the histograms with mean and standard deviation of difference values for pairs of images for the hardwood forest.

The resulting difference images for the hardwood forest are consistent with PCA analyses, which indicate that most of the changes occurred along the exposed edges of the forest. The 1988-1987 image (Fig. 58) shows decline in NDVI along all edges of the forest, except along the eastern edge of the maple-basswood forest. This image is similar to PCA component 2, the first change component for this forest. The 1990-1988 values (Fig. 59) indicate an overall decline in mean NDVI with a value of -26.6, but there appeared to be some improvements along the western and eastern edges of the forest. By 1994, there was an overall NDVI increase over 1991, with a mean difference value of 16.6 for the 1994-1991 image (Fig. 60). However, the image indicates some decline along the western edges of the forest. Mean value for 1997-1994 was 8.4 (Fig. 61) and the image shows some positive changes along edges of the forest. The overall difference from 1987 to 1997 resulted in a slightly decreased NDVI mean of -2.7. Greatest decline is observed near Government Hill and along Sheridan Drive in the south, Wagner Point

	Hardwood Forest		Cottonwood Forest	
Year	NDVI Difference Mean	SD	NDVI Difference Mean	SD
88-87	-6.3	11.0	0.6	5.6
90-88	-26.6	10.5	-33.5	8.0
94-91	16.6	7.1	11.7	7.2
97-94	8.4	6.8	9.4	7.7
97-87	-2.7	7.3	-3.3	5.3

Table 9.   Mean and standard deviation of NDVI difference for pairs of images.

Mean NDVI Differences

	88-87	90-88	94-91	97-94
Hardwood	-6.3	-26.6	16.6	8.4
Cottonwood	0.6	-33.5	11.7	9.4
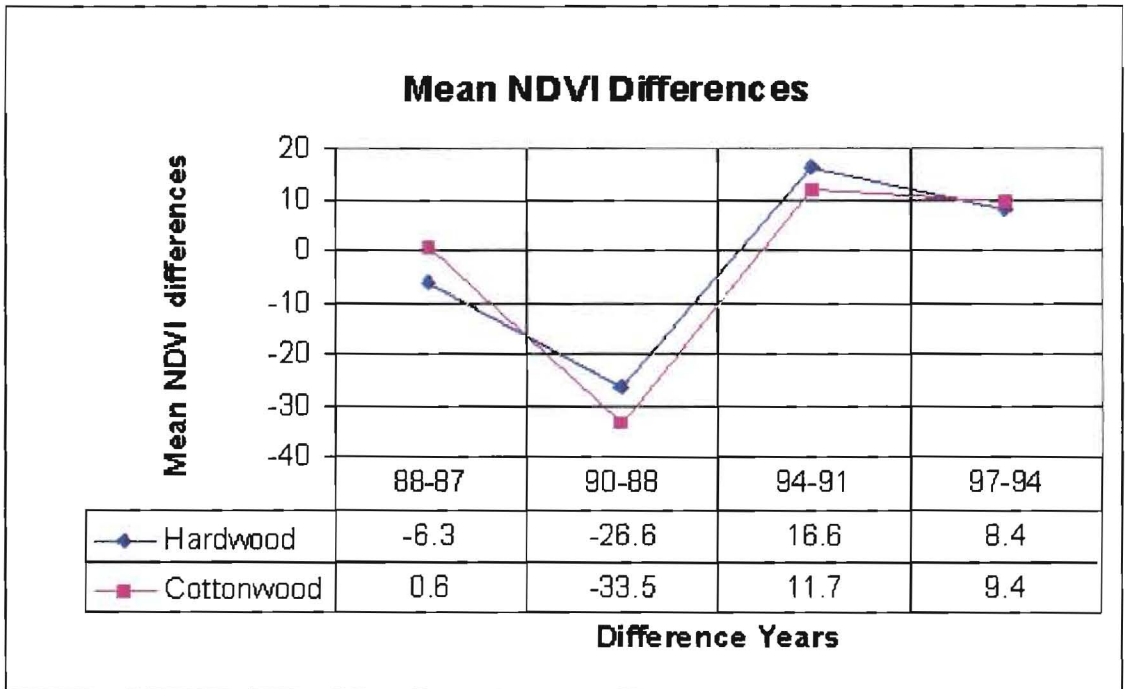
Fig. 57.   Mean NDVI differences for NDVI image pairs.
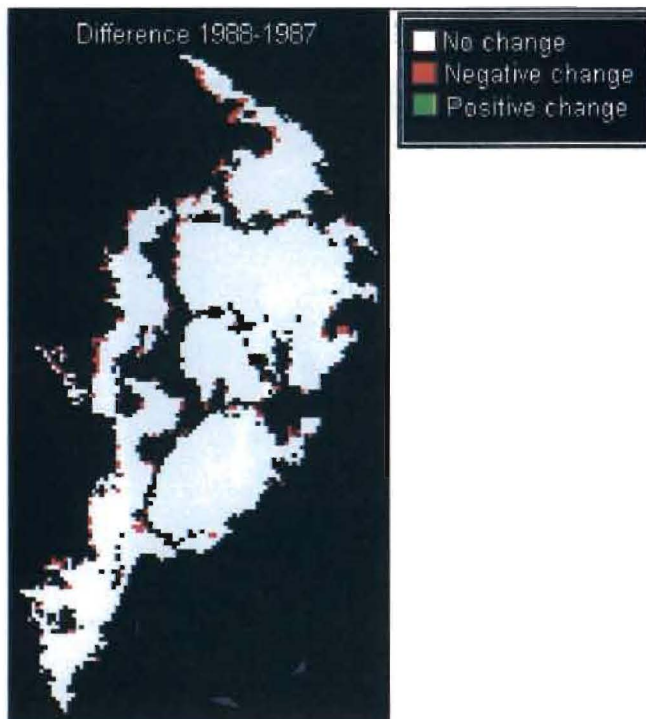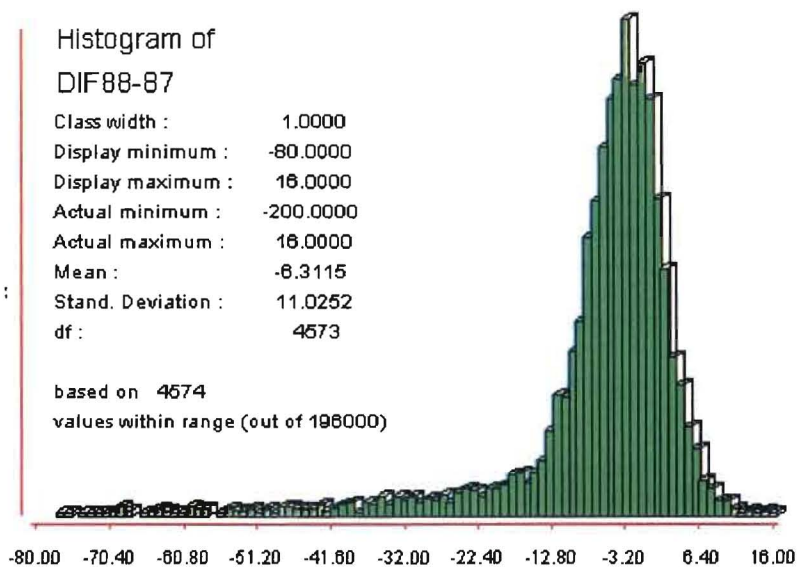
Fig. 58.

Above: Histogram of 1988-1987 hardwood forest NDVI difference.

Below: Image of NDVI difference, 1988-1987. The legend applies to

all difference images.

Histogram of
DIF90-88

Class width :	1.0000
Display minimum :	-91.0000
Display maximum :	50.0000
Actual minimum :	-91.0000
Actual maximum :	200.0000
Mean :	-26.6441
Stand. Deviation :	10.4667
df :	4573

based on   4574
values within range (out of 196000)

Difference 1990-1988
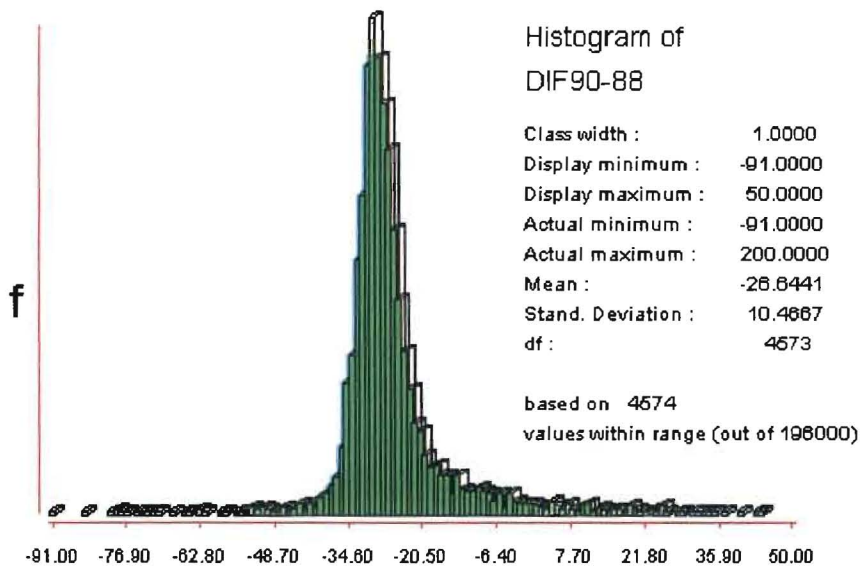
Fig. 59.

Above: Histogram of 1990-1988 hardwood forest NDVI difference.

Below: Image of NDVI difference, 1990-1988.

Histogram of
DIF94-91

Class width :	1.0000
Display minimum :	-50.0000
Display maximum :	66.0000
Actual minimum :	-200.0000
Actual maximum :	66.0000
Mean :	16.5619
Stand. Deviation :	7.1230
df :	4573

based on 4574
values within range (out of 196000)
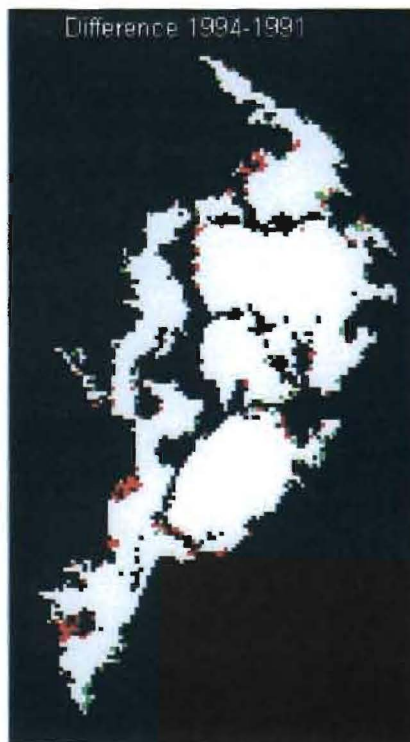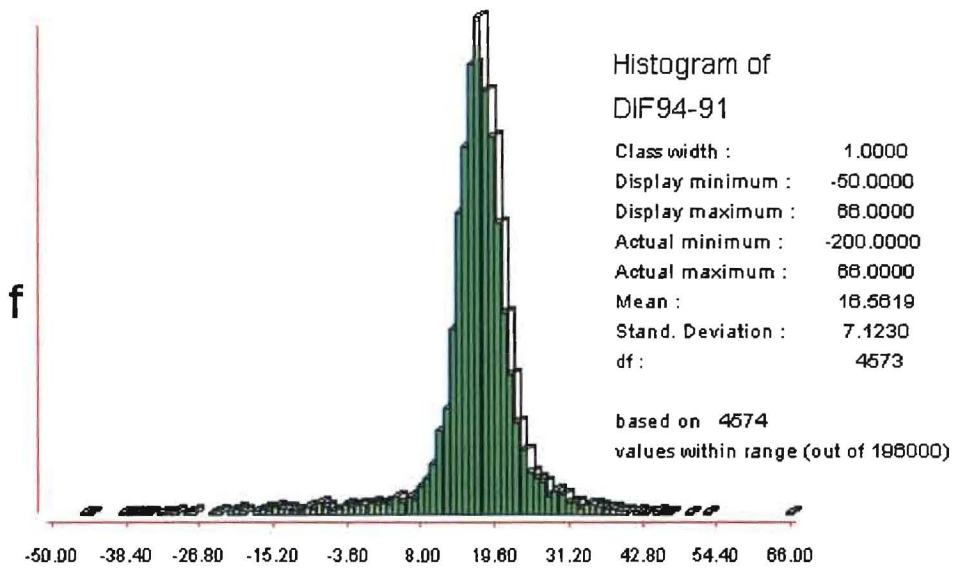
Fig. 60.

Above: Histogram of 1994-1991 hardwood forest NDVI difference.

Below: Image of NDVI difference, 1994-1991.
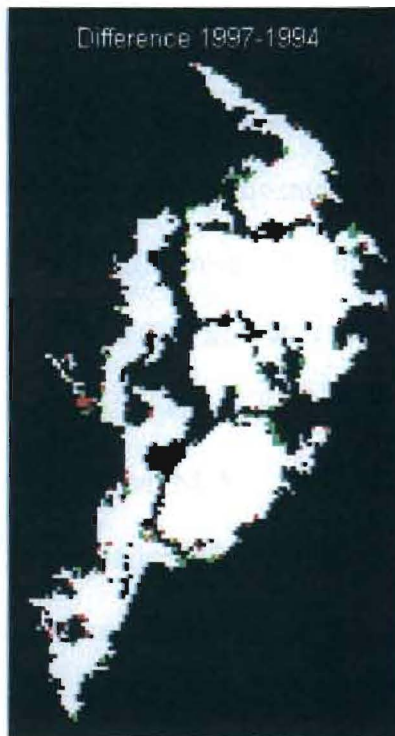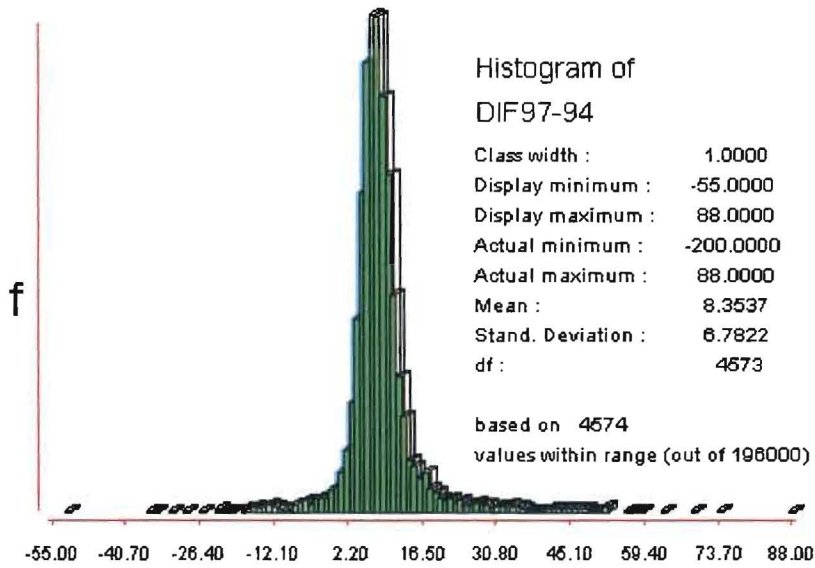
Fig. 61.

Above: Histogram of 1997-1994 hardwood forest NDVI difference.

Below: Image of NDVI difference, 1997-1994.

in the west, and near the sanitary landfill in the north. Some improvements along the forest edges for this period are evident in Fig. 62.

4.4.2 Cottonwood forest

Histograms and images of the mean NDVI differences for pairs of images for the cottonwood forest are shown in Figs. 63 to 67. The results for the cottonwood forest are also similar to the PCA transformation derived from NDVI images. The 1988-1987 image (Fig. 63) indicates very little change although some decreased NDVI values occur on the western interior edge of the forest, along the boundary with the airfield. 1990-1988 shows a large mean NDVI decrease of -33.5. Some areas of NDVI decline are found along the banks of the Missouri River at the northern edge of the meander (Fig. 64). The 1994-1991 difference image shows general improvement in the mean difference, with a mean value of 11.7 (Fig. 65). However, the image also suggests a decline in NDVI along Weston Bend and areas to the west. The data for 1997-1994 (Fig. 66) suggests a recovery of this area with a mean NDVI increase of 9.4. Over the ten-year period, 1997-1987, there was a decrease of -3.3 in mean NDVI. This is observed along its northern margin and also along the western boundary with the Sherman Army Airfield. Fig. 67 indicates a small area of positive change along the western end of the northern boundary of the forest.
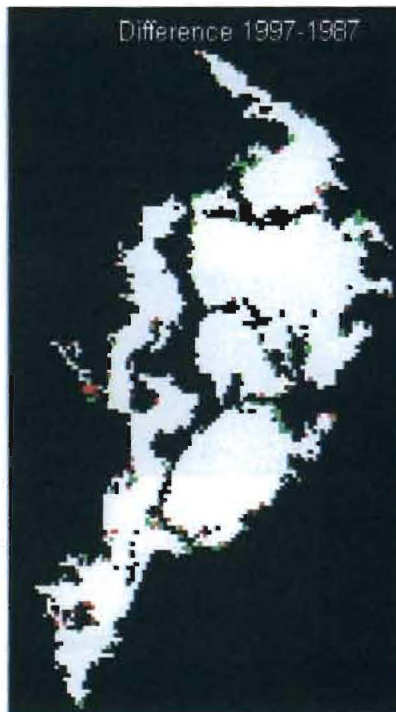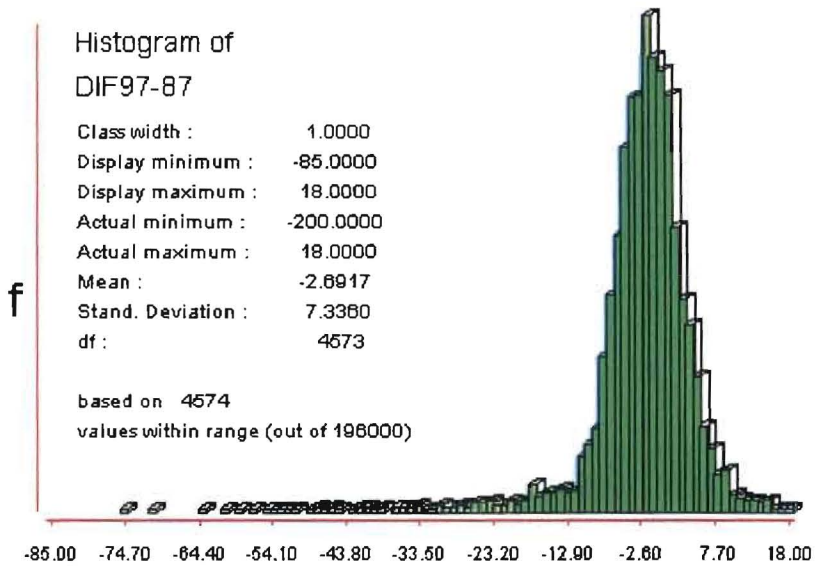
Fig. 62.

Above: Histogram of 1997-1987 hardwood forest NDVI difference.

Below: Image of NDVI difference, 1997-1987.

Histogram of
CT88-87

Class width :	1.0000
Display minimum :	-70.0000
Display maximum :	25.0000
Actual minimum :	-200.0000
Actual maximum :	25.0000
Mean :	0.5717
Stand. Deviation :	5.5919
df :	8181

based on 8182
values within range (out of 196000)

f

-70.00 -60.50 -51.00 -41.50 -32.00 -22.50 -13.00 -3.50 6.00 15.50 25.00

Difference 1988-1987
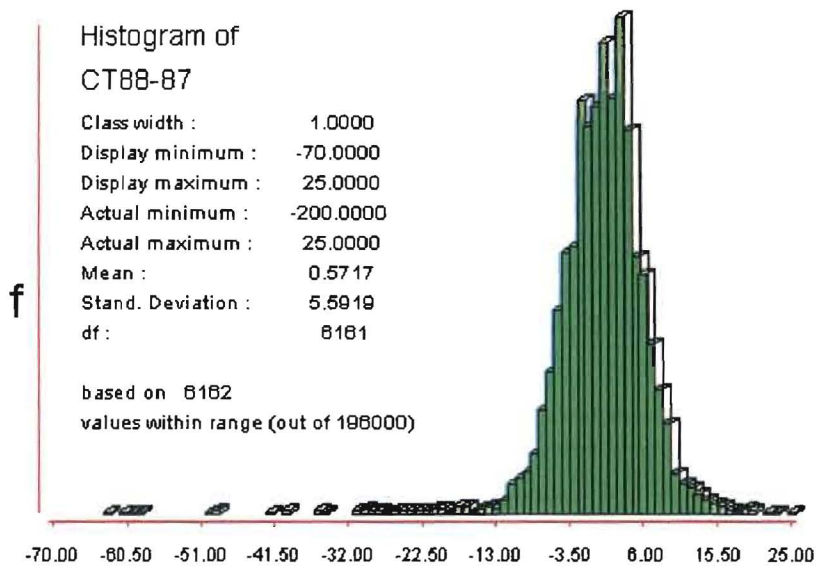
Fig. 63.

Above: Histogram of 1988-1987 cottonwood forest NDVI difference.

Below: Image of NDVI difference, 1988-1987.

Histogram of
CT90-88

Class width :	1.0000
Display minimum :	-137.0000
Display maximum :	50.0000
Actual minimum :	-137.0000
Actual maximum :	200.0000
Mean :	-33.5389
Stand. Deviation :	7.9537
df :	6161

based on   6162

values within range (out of 196000

-137.00 -118.30 -99.60 -80.90 -62.20 -43.50 -24.80 -6.10 12.60 31.30 50.00

Difference 1990-1988
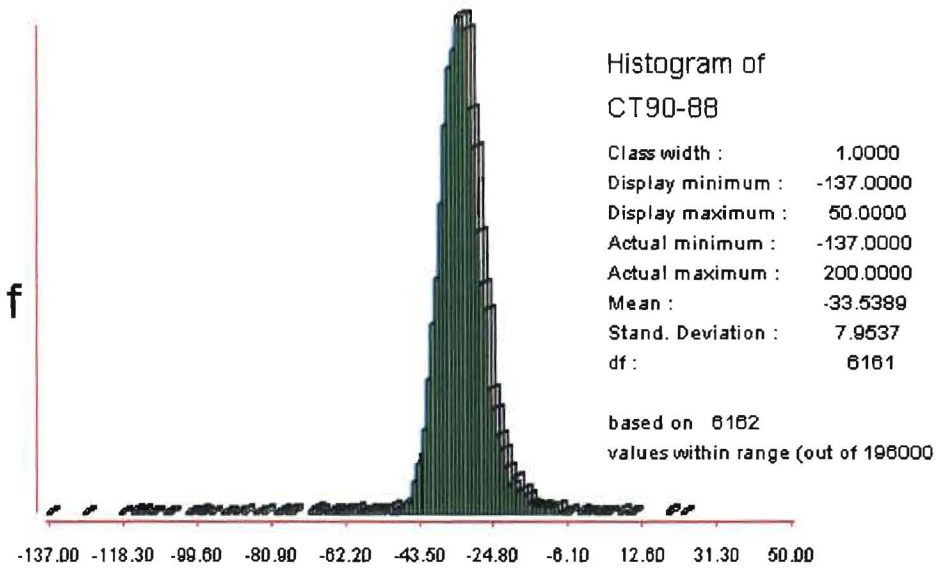
Fig. 64.

Above: Histogram of 1990-1988 cottonwood forest NDVI difference.

Below: Image of NDVI difference, 1990-1988.

Histogram of
CT94-91

Class width :	1.0000
Display minimum :	-80.0000
Display maximum :	74.0000
Actual minimum :	-200.0000
Actual maximum :	74.0000
Mean :	11.7379
Stand. Deviation :	7.1587
df :	6161

based on 6162
values within range (out of 196000)
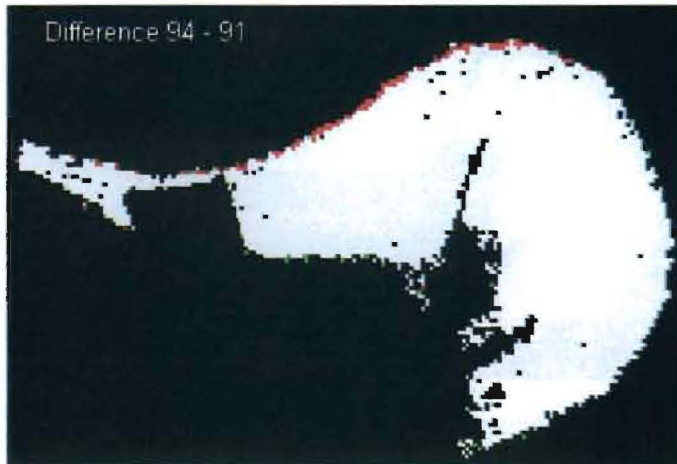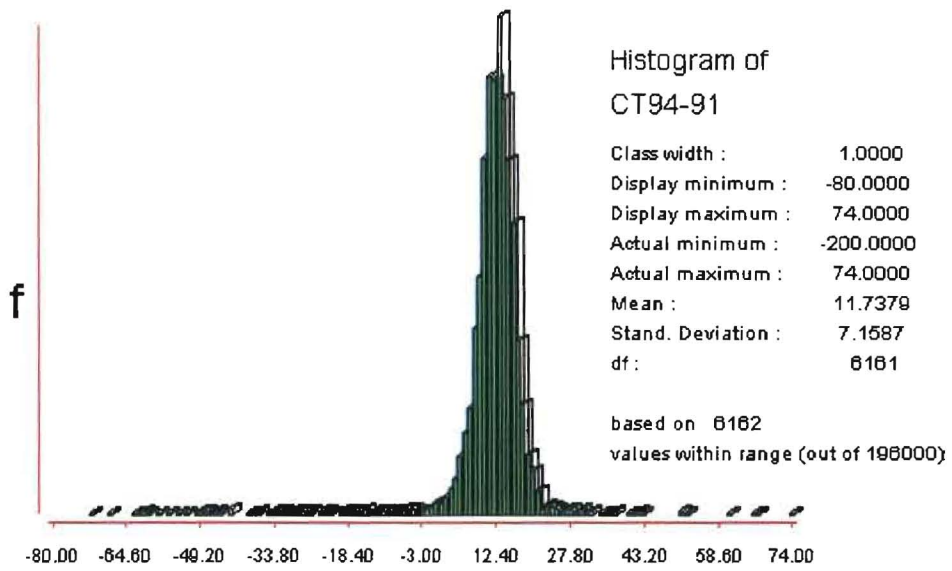
Fig. 65.

Above: Histogram of 1994-1991 cottonwood forest NDVI difference.

Below: Image of NDVI difference, 19948-1991.

Histogram of
CT97-94

Class width :   1.0000
Display minimum :   -55.0000
Display maximum :   89.0000
Actual minimum :   -200.0000
Actual maximum :   89.0000
Mean :   9.4049
Stand. Deviation :   7.6692
df :   6161

based on   6162
values within range (out of 198000)
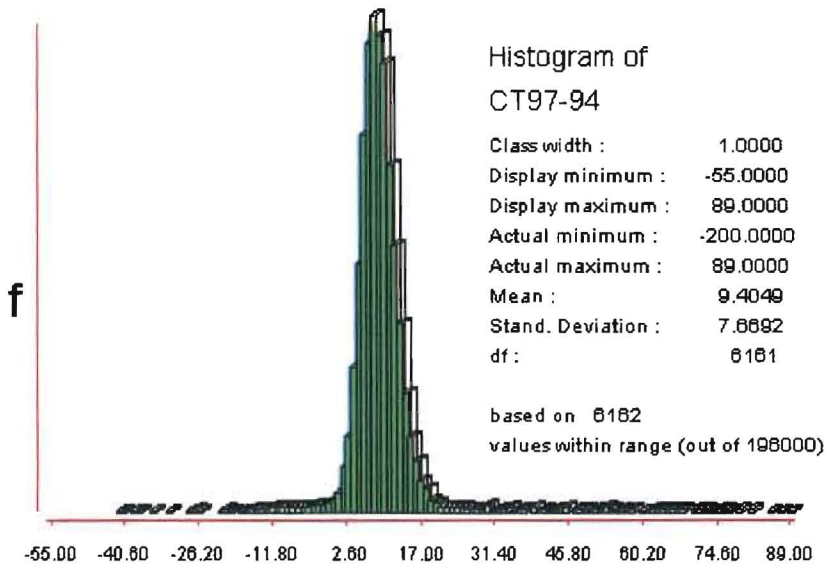
Fig. 66.

Above: Histogram of 1997-1994 cottonwood forest NDVI difference.

Below: Image of NDVI difference, 1997-1994.

Histogram of
CT97-87

Class width :	1.0000
Display minimum :	-85.0000
Display maximum :	20.0000
Actual minimum :	-200.0000
Actual maximum :	20.0000
Mean :	-3.3194
Stand. Deviation :	5.3260
df :	6161

based on 6162
values within range (out of 196000)

f

-85.00   -74.50   -64.00   -53.50   -43.00   -32.50   -22.00   -11.50   -1.00   9.50   20.00

Difference 1997-1987
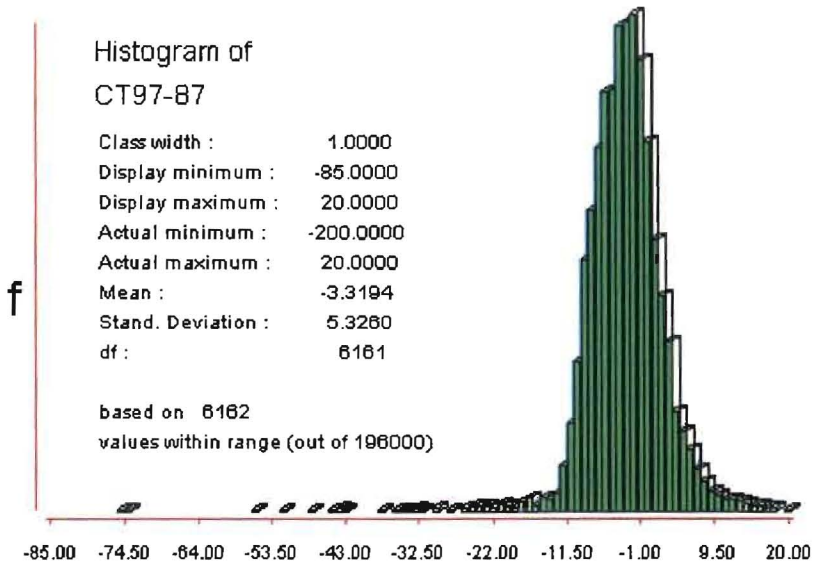
Fig. 67.

Above: Histogram of 1997-1987 cottonwood forest NDVI difference.

Below: Image of NDVI difference, 1997-1987.

4.5 Ratio of band 5: band 4

The ratio of Landsat TM band 5 to band 4 can be used to detect decreased vegetation vigor caused by decreased water content in the foliage. An increase in the ratio may suggest decreasing water content of the tree canopy.

The values for the ratios, trend lines and residuals for each forest are presented in Table 10. Fig. 68 shows the associated graph for the trend lines for the forests. The trend lines follow parallel curves and show a general declining trend with a shallow negative gradient between 1987 and 1997. Cottonwood forest values are consistently lower but parallel those of the hardwood forest.

The residual values are shown in Fig. 69. The ratio fluctuations for both forests are very similar, with the exception of opposite responses in 1988. During 1988, while the hardwood forest experienced an increase in the ratio, the cottonwood forest experienced a decline. Both forests indicate highest ratios in 1989, the year of lowest average 12-month precipitation during the ten-year period. These peak ratios also correspond to the period of greatest NDVI decline for both forests. With increased precipitation in 1990, the band 5:4 ratio decreased, and reached its lowest value in 1992. The ratios increased in 1994, possibly due to flooding and low temperatures in 1993.

Year	Hardwood forest			Cottonwood forest		
	Mean	**Trend**	**Residual**	**Mean**	**Trend**	**Residual**
1987	0.85	0.8512	-0.0048	0.71	0.6935	0.0197
1988	0.84	0.8274	0.0126	0.66	0.6785	-0.0188
1989	0.83	0.8037	0.0284	0.72	0.6636	0.0600
1990	0.77	0.7799	-0.0113	0.64	0.6487	-0.0039
1991	0.74	0.7561	-0.0186	0.59	0.6337	-0.0468
1992	0.71	0.7324	-0.0262	0.57	0.6188	-0.0535
1994	0.69	0.6848	0.0096	0.61	0.5889	0.0225
1997	0.62	0.6135	0.0103	0.56	0.5441	0.0207

Table 10. Mean ratios of band 5 to band 4, trend lines and residuals for hardwood and cottonwood forests.
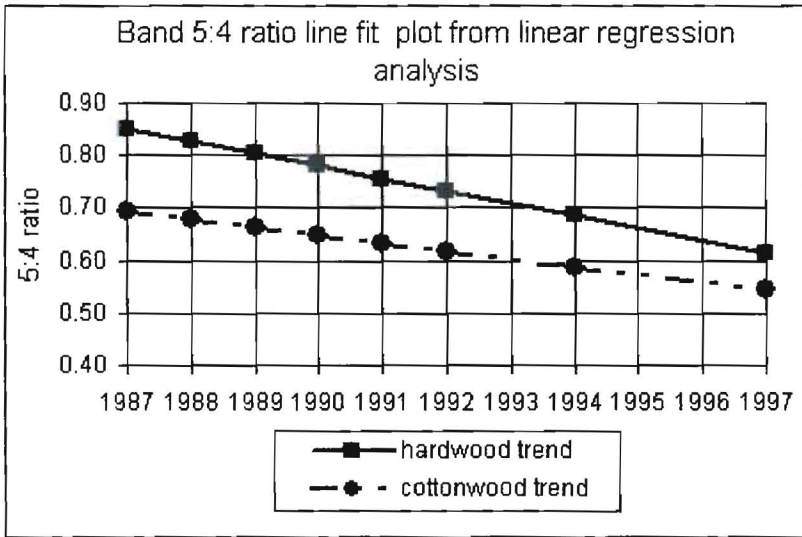
Fig. 68. Plots of trendlines obtained from linear regression analysis.
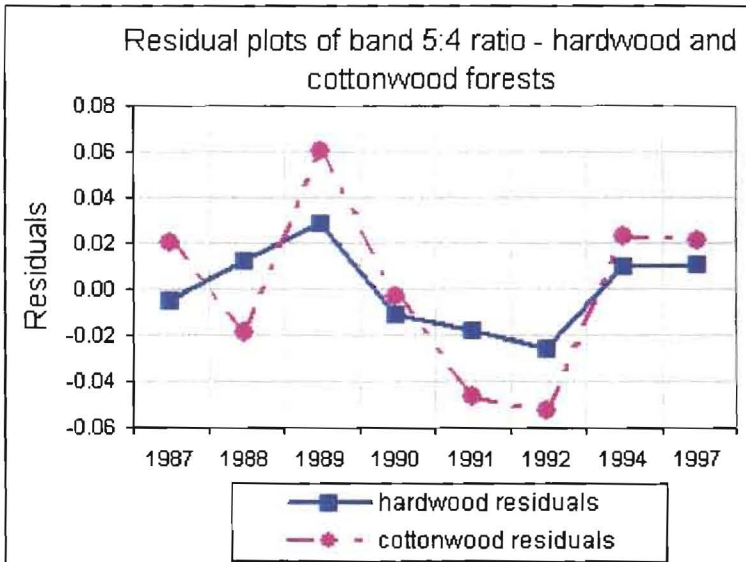
Fig. 69. Residual plots of 5:4 ratio for hardwood and cottonwood forests.

Chapter 5

Analysis of Results

5.1 Normalized Difference Vegetation Index (NDVI)

Drought conditions in northeastern Kansas began in winter 1987 and continued into 1988 and 1989. The data indicate that NDVI had been affected by the drought, but a time lag is apparent. Table 11 shows changes in precipitation and NDVI on a 12-month basis. The sharpest decline in precipitation (-42.8 cm) occurred from 1987 to 1988. However, only a moderate decline in NDVI is evident in the upland hardwood forest, and there is a slight NDVI increase for the floodplain cottonwood forest. The sharpest NDVI decline (-25.2 and -31.5) occurred the following year, between July 1988 and July 1989, for both hardwood and cottonwood forests. In addition, although precipitation increased substantially from 1989 to 1990, NDVI continued to show a small decline in both forests. These data suggest that while there is a response to the average precipitation of the previous 12-month period, the full response is not experienced until the following 12 to 24-month period. Hence, a delay period of approximately one to two years is required for the full effects of decreased precipitation to be echoed in forest vigor, as defined by NDVI, for both forests. This result is consistent with previous studies by Wilkins (1997) and Aber *et al.* (1998). Similar NDVI-precipitation lag responses have been noted for other forests in the Central Great Plains of the USA (Wang, 1999 a, c) and for forests in East Africa (Davenport and Nicholson, 1990).

	Precipitation change (cm)	Mean NDVI change	
year		hardwood	cottonwood
88-87	-42.80	-11.3	0.6
89-88	-14.71	-25.2	-31.5
90-89	41.55	-1.4	-1.2
91-90	-20.13	5.3	8.5
92-91	-5.67	-2.6	-2.8

Table 11. Changes in precipitation and NDVI for one-year periods from 1987 to 1991. Greatest precipitation decrease occurred between 1987 and 1988. However, the greatest NDVI decrease occurred between 1988 and 1989, one year after the most significant precipitation decline.

Of interest is the fact that the floodplain cottonwood forest experienced a slight increase in NDVI from 223.7 in 1987 to 224.3 in 1988, the drought year. It has been noted by J. S. Aber (personal communication, May 26, 2000) that at the beginning of drought periods, the standing water on the floor of the floodplain forest dries up and the areas are quickly overgrown by grasses. It is probable that at the start of a drought, there is enough moisture in this riparian environment to sustain hardy grasses. This would increase NDVI values as these grasses contribute to infrared reflectance. With continued depletion of moisture, stress sets in and the grasses would begin to decline in health and eventually die, thereby reducing NDVI. This observation may be important to consider in remote sensing analysis of similar wetland areas.

5.2 Principal Component Analysis (PCA)

PCA analyses of both forests indicate a high correlation among all NDVI images. Over 99.9 percent of the variance in the time-integrated dataset is extracted in component 1, indicating that only small changes have occurred over the 10-year study period. The reasons for this are twofold. First, the forests are relatively homogenous and largely undisturbed. Second, the Landsat images were all captured in the month of July and hence conditions of phenology and senescence are consistent. The data indicate that NDVI changes which have occurred have been most significant along edges of the forests.

For the hardwood forest, the first change component, component 2, shows strong decline along the forest edges in 1988. Among the areas most affected were Bell Point (Fig. 70), and the western margin of the maple-basswood forest (Fig. 71). Component 3 also shows a decline along the edges in 1994, likely due to the heavy rains and lower temperatures of 1993. Component 4 shows an overall decline in NDVI throughout the forest in 1990. Components 2 and 4 combined are likely to be responsible for the low NDVI values in 1990. The 1991 decline evident in component 5 may result from increased temperatures and decreased precipitation at that time.

Some areas of decline, such as those along Bell Point and Sheridan Drive, are subject to mild to moderate human activity (Matt Nowak, personal communication, February 24, 2000) which may have some impact on the general health of vegetation along those edges of the forest. However, the PCA results indicate that all edges are susceptible and the strong response during the drought period suggests that precipitation is the overriding factor on an annual basis.

For the cottonwood forest, the most significant change component, component 2, suggests decline in NDVI in 1990 and 1994. Component 3 also represents NDVI responses in these years. Changes consistently occur along the northern margin, along the banks of the Missouri River at Weston Bend, and to the west (Fig. 72).

Fig. 70. 1-meter DOQQ of the western margin of the upland hardwood forest near Bell Point. This edge showed significant decline in 1988 as seen in principal component analysis and image differencing.

Fig. 71. 1-meter DOQQ of northern section of upland hardwood forest, showing the maple-basswood strip along the Missouri River Bluffs. The western margin of this forest suffered decline in 1988 as seen in principal component analysis and image differencing.
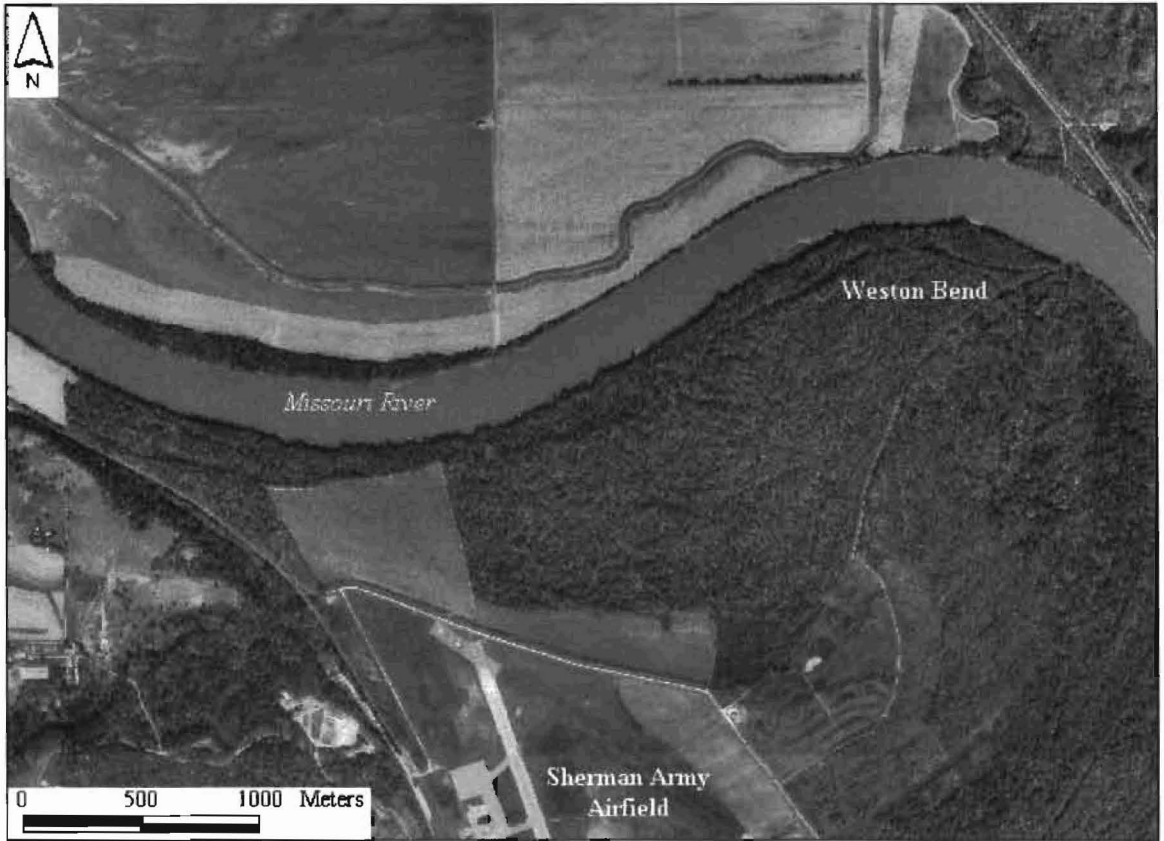
Fig. 72. 1-meter DOQQ of the floodplain cottonwood forest showing the northern edge along the Missouri River. This northern boundary is most susceptible to damage as seen in principal component analysis and image differencing. The western boundary with the airfield also shows decline over the 10-year study period.

The 1990 response compares with the low NDVI values for that year. The 1994 response is likely due to the severe flood conditions of 1993. The cottonwood forest was inundated by the high floodwaters of the Missouri River and average temperature was significantly lower during 1993. Component 5 for the cottonwood forest show a positive NDVI response in 1988. This could be associated with the temporary increase in vegetation in the understory as water which settles on the forest floor dissipates at the start of the drought.

Fig. 73 shows component 3 with a palette that emphasizes the contrast in spectral responses. The central area, shown predominantly in yellow, corresponds to the location of the pecan-sugarberry forest described by Freeman *et al.* (1997) and shown in Fig. 2. The darker orange-red shades correspond to the location of the cottonwood-sycamore forest also described by Freeman *et al.* (1997). Component 3 could therefore be the response of the separate forest stands in this floodplain.

5.3 Image Differencing

Image differencing analyses confirmed the results of principal component analyses with images showing that the greatest NDVI changes were consistently experienced along the all edges of the hardwood forest and along the northern edge of the cottonwood forest. The 1988-1987 image for the cottonwood forest shows areas of increased NDVI dotted throughout the forest. This could be indicative of grasses inhabiting the dried sloughs and ponds on the forest floor. The forests experienced a sharp decline in NDVI from 1988 to
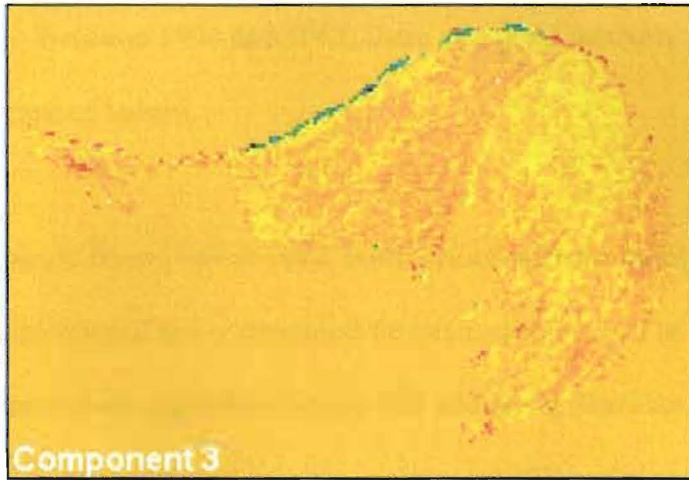
Fig. 73. Component 3 of the floodplain forest showing distinct spectral signatures that correspond to the cottonwood-sycamore stands in the north and south (orange-red) and the pecan-sugarberry forest in the central section (yellow).

1990 with decreases of -26.6 NDVI units and -33.5 units for hardwood and cottonwood forests respectively. Between 1994 and 1997, there was good recovery in places as indicated by the increased values.

Over the ten-year period from 1987 to 1997, both forests suffered small NDVI decreases of -2.7 and -3.3 for hardwood and cottonwood forests respectively. The oak-hickory forest shows greatest decline near Government Hill and along Sheridan Drive in the south, Wagner Point in the west, and near the sanitary landfill in the north. Ten-year decline for the cottonwood forest is observed along the northern margin and also along the western boundary with the Sherman Army Airfield. Some of these areas are subject to moderate human activity, which may be a factor in the long-term decline observed here.

5.4 Ratio of band 5: band 4 ratio

The residual plots show increased reflectance ratios for both forests in 1989 and 1994. The 1989 results are consistent with precipitation data, which indicate lowest average 12-month precipitation in 1989. This also corresponds to the period of sharpest NDVI decline for both forests. From 1990 to 1992, NDVI increased slightly and the band 5:4 ratio continued to decline. The inverse relation between precipitation, NDVI and the band 5:4 ratios is not persistent, however. While NDVI increased from 1992 to 1994, the ratios also increased. The increased ratio in 1994, however, is consistent with principal component analyses, which suggest that both forests experienced limiting growth effects after the flooding of 1993. The understory of the lowland cottonwood forest would have

been damaged. The average temperature had decreased sharply in 1993, and may also have had a negative effect on some aspects of growth in 1994.

The cottonwood forest experienced a decline in 5:4 ratio in 1988, a response opposite to that of the hardwood forest. This result is consistent with NDVI results, which indicate an increase in NDVI during 1988, followed by a decrease in 1990. This may be explained by the increase in the undergrowth at the start of the drought.

The declining trends experienced over the ten-year period are different for each forest. The separation of the trends may result, in part, from different spectral properties of the forest canopies themselves, or from the fact that canopy structure of each forest is different. The cottonwood forest has an open canopy, with a waterlogged, herbaceous understory and significant ponds of water are exposed on the forest floor. This water would absorb more energy in the mid-infrared band 5 range, causing lower reflectance values. As the forests are indistinguishable by visual inspection of the images, this ratio could be useful in distinguishing similar types of forests on Landsat or other remotely sensed images.

The band 5:4 ratio may also be affected by local conditions of temperature and atmospheric humidity at the time of image capture, as these would affect rates of evapotranspiration. In addition, soil moisture availability based on the level of the water table may be a contributing factor. These variables are not considered in this study but can be integrated into future studies.

Chapter 6

Conclusions

6.1 Summary

The main objective of this study was to determine changes in the state of health of two

forest stands on the Fort Leavenworth Military Reservation during the ten-year period

from 1987 to 1997. The data consisted of eight sets of Landsat TM data collected in the

month of July for selected years between 1987 and 1997. During this period, two

significant climatic events occurred in the study area. From late 1987 to 1989, a drought

ensued, and in 1993, high precipitation and severe flooding occurred.

The Normalized Difference Vegetation Index (NDVI) was used as the primary indicator

of forest health. Additionally, principal component analysis (PCA) was used to

temporally integrate the NDVI images in order to derive more detailed information.

Image differencing was also performed on pairs of NDVI images to determine changes.

The Moisture Stress Index (TM band 5:4 ratio) was used to determine the state of stress

caused by moisture deprivation. These methods are well documented in the literature

reviewed and have proved successful in many studies. For the present study, all methods

provided useful and unique information on the changes in vegetation over time and space.

In summary, the results of the study are as follows:

- NDVI results indicate that while there is a response to precipitation of the previous 12-month period, the most significant response is delayed by approximately one year and the full response may not be experienced until the second year.

- The floodplain cottonwood forest experienced a small increase in NDVI during the first year of the drought, likely due to increased undergrowth as wetland ponds and sloughs dried up on the forest floor. This response is opposite to that of the upland forest.

- Principal component analyses have identified the areas of the forests that have been most susceptible to change over the ten-year period. Indications are that the edges of the forests experience the most significant variations in NDVI and are most susceptible to damage. All edges of the upland hardwood forest are vulnerable and were most affected in 1988, at the beginning of the drought. More extensive but smaller changes were observed throughout the forest by 1990. The northern margin of the floodplain cottonwood forest experienced greatest change while the southern margin was most unaffected. This forest was most affected in 1990. The negative effects of the 1993 floods are also evident along the northern margin.

- PCA has also been useful in isolating different forest stands within the cottonwood forest. The third component for the floodplain forest separated the pecan-sugarberry stands from the cottonwood-sycamore stands.

- The results of image differencing are consistent with those of PCA in identifying forest edges as the areas responsible for most significant change. Areas of increased NDVI in the cottonwood forest during the first drought year, were also located on the 1988-1987 difference image. Small decreases in NDVI were observed for both forests over the ten years of study. At least some of these locations are subject to human activity, which may play a role in the long-term decline of the forests.

- The residuals for the band 5:4 ratios indicate stress in both forests in 1989 and 1994. The 1989 response is consistent with the lowest 12-month precipitation during the study period and with the sharp decline in NDVI for both forests during this period. The elevated ratios for 1994 may be the response to severe flooding and decreased temperature during 1993.

- The raw band 5:4 ratios for the forests plot as separate but parallel graphs, suggesting unique spectral responses.

6.2 Implications of the results

The one- to two-year NDVI-precipitation lag has previously been documented for the hardwood forest by Wilkins (1997) and Aber *et al.* (1998). The present study additionally identifies the lag in the floodplain forest. The results suggest that the biological processes that sustain the forests are such that the vegetation is able to retain its health for a one- to two-year period after a significant stressful event, such as the 1987-1989

drought. The implication is that NDVI may not always reflect current growth conditions and interpretation and analysis of NDVI data should always consider the climatic conditions of previous years. The NDVI lag results in general may be useful from a botanical perspective, in understanding the processes of food manufacture and storage is response to severe climatic conditions.

The NDVI data for the floodplain forest present an additional result not documented in the literature reviewed for this study. For this forest, NDVI increased during the first year of the drought, in response to a temporary increase in understory vegetation. This NDVI response is contrary to what would be expected and is very significant for NDVI interpretation for wetland areas. This type of forest exhibits a unique NDVI response, which should be considered in analysis of NDVI data. The result may have further implications for the study of biota in wetland habitats during periods of drought.

The principal decline of the forests occurred along edges as indicated by PCA and image differencing. These results have implications in the long-term management of the forests and may be useful in identifying areas that require particular attention. The data also suggest that NDVI changes are not uniform over the forests and this phenomenon of edge decline should be considered in studies of forests in general. In addition, forests with high edge to area ratio would be at greater risk of decline.

The correlation between the band 5:4 ratio and precipitation indicates that this is a useful method for assessing stress conditions for these forests. It is apparent that severe climatic

variations will produce stress in vegetation, measurable by this ratio. The ratio may be used to complement NDVI studies of similar forest types.

The separate graphs produced by the raw band 5:4 ratios could also be significant. The difference may result from the different spectral properties of the forest canopies, or from the different structures of the canopies. As the forests are indistinguishable by visual inspection of the images, this ratio may be useful in distinguishing similar types of forests on remotely sensed images.

6.3 Limitations of the study

The 1989 image contained some cloud cover over the study area and could not be used in the PCA transformations. This is unfortunate, as this image may have provided more precise data on the timing of NDVI changes. For other analytical methods, however, the removal of clouds and shadows through reclassification and clustering proved satisfactory.

The climatic variables considered in this study were precipitation, Palmer drought severity index (PDSI), temperature and tree-ring growth. The results may not relate exclusively to these variables. Soil moisture is a critical component of this study for both NDVI and moisture stress analysis, and precipitation has been used to reflect soil moisture content. Data on water table levels may prove to be useful. Other variables such as atmospheric humidity may also be important. In addition, this study does not include

detailed analyses of the human and animal activity in the forest, though it is known that human activity is moderate to low. However, a further look at these may explain some of the edge decline noted in the present analyses.

The structures of the forest canopies have not been studied in great detail, though this would be a significant factor in the spectral responses of these forests. More detailed information on the canopy structures could be useful.

6.4 Recommendations for future studies.

Future work may include ground observations along the forest edges that are subject to decline, to determine possible causes and remedies. More detailed information of specific uses of the forests, particularly in areas shown to be susceptible to damage, may contribute to long-term management plans.

A better understanding of the biological processes that lead to the NDVI lag is required. It is apparent that the mechanisms of the manufacture, storage and distribution of food within the forestry vegetation is of importance. A more detailed study of existing literature on these biological processes may help to explain how plants respond to limiting growth conditions.

The integration of additional climatic data may also prove useful. Data on water table levels may provide insight into the effects of ground water levels on leaf stress and

vegetation health overall. Atmospheric humidity affects the rate of evapo-transpiration, and could assist in analyses of moisture stress in vegetation.

To better understand the different responses of the forests, additional remote sensing studies may include hyperspectral analyses to provide more precise data on the chemistry and foliage characteristics of both forests. Imagery of high spatial resolution could be useful in determining the structure of the forest canopies and contribute to the understanding of the spectral responses of the forests. In addition, the areas of change are relatively small and data of high spatial resolution would help to define these areas more precisely.

In conclusion, the study has confirmed some previously documented results, and has provided some new data that have implications in remotely sensed studies of riparian and upland temperate deciduous forests. All analysis techniques used proved to be useful and contributed unique results that can be used in further studies of these and other similar forests.

References

Aber, J.S., Nang, K.M., Wilkins, N., Ye, H., Harrington, J., and Nowak, M.C., 1998, Remote sensing of forest growth and response to climatic variations in northeastern Kansas, *in* U.S.A. Proceedings 27th International Symposium On Remote Sensing of the Environment, June 8-12, Norway, p. 709-714.

Allen, W. A. and Richardson, A. J., 1968, Interaction of light with a plant canopy: Journal of the Optical Society of America, v. 58, no. 8, p 1023 - 1028.

Avery, T.E. and Berlin, L.B., 1992, Fundamentals of remote sensing and airphoto interpretation: Macmillan Publishing Company, 472 p.

Barbour, M.G., and Billings, D. W., 1988, North American terrestrial vegetation: Cambridge University Press, 434 p.

Bauer, M. E., Burk, T. E., Ek, A. R., Coppin, P. R., Lime, S. D., Walsh, T. A., Walters, D. K., Befort, W. and Heinzen, D. F., 1994, Satellite inventory of Minnesota forest resources: Photogrammetric Engineering and Remote Sensing, v. 60 no. 3, p 287-298.

Blasing, T. J. and Duvick, D., 1984, Reconstruction of precipitation history in North American corn belt using tree-rings: Nature, v. 307, January 1984, p. 143-145.

Brumwell, M.J., 1951, An ecological survey of the Fort Leavenworth Military Reservation: The American Midland Naturalist v. 45 no.1, p 187-231.

Byrne, G.F., Crapper, P.F., Mayo, K.K., 1980, Monitoring land-cover change by principal component analysis of multi-temporal Landsat data: Remote Sensing of Environment, v. 10 p.175-184.

Carter, G.A., 1991, Primary and secondary effects of water content on the spectral

reflectance of leaves: American Journal of Botany, v. 78 no. 7, p. 916-924.

Cibula, W.G., Zetka, E.F., and Rickman, D.L., 1992, Response of Thematic Mapper

bands to plant water stress: International Journal of Remote Sensing, v. 13, no. 10, p.

1869-1880.

Cohen, W.B., Fiorella, M., Gray, J., Helmer, E., and Anderson, K., 1998, An efficient

and accurate method for mapping forest clearcuts in the Pacific northwest using

Landsat imagery: Photogrammetric Engineering and Remote Sensing, v. 64, no. 4, p.

293-300

Cook, E.R., Kablack, M.A., and Jacoby, G.C., 1988, The 1986 drought in the

southeastern United States: How rare an event was it?: Journal of Geophysical

Research, v. 93 no. D11, p.14257-14260.

DASC, 1999, Kansas Data Access Support Center: Online,

http://gisdasc.kgs.ukans.edu/dasc_net.html

Davenport, M.L., and Nicholson, S.E., 1990, On the relation between rainfall and the

Normalized Difference Vegetation Index for diverse vegetation types in East Africa:

International Journal of Remote Sensing, vol. 14, no. 12, p. 2369-2389.

Eastman, J.R., and Fulk, M.A., 1993, Long sequence time series evaluations using

standardized principal components: Photogrammetric Engineering and Remote

Sensing, v. 59, no. 8, p.1307-1312.

Eastman, J.R., McKendry, J.E., and Fulk, M.A., 1995, UNITAR explorations in

geographic information systems technology, Volume 1, Change and time series

analysis: Clark Labs, Clark University, Massachusetts, 121 p.

Freeman, C.C., Busby, W. H., Lauver, L.L., Kindscher, K., Elliott, J., and Eifler, D.A., 1997, A natural areas inventory of the Ft. Leavenworth Military Reservation, Leavenworth County, Kansas: Report 77, State Biological Survey of Kansas. University of Kansas, 246 p.

Fritts, H. C., 1976, Tree rings and climate: New York, Academic Press, 567 p.

Gates, D.M., Keegan, H.J., Schleter, J.C., and Weidner, V.R.,1965, Spectral properties of plants: Applied Optics, v. 4, no. 1, p. 11-20.

Green, K., Kempka, D., and Lackey, L., 1994, Using remote sensing to detect and monitor land-cover and land-use change: Photogrammetric Engineering and Remote Sensing, v. 60, no. 3, p. 331-337.

Hunt, R.E. Jr., and Rock, B. N., 1989, Detection of changes in leaf water content using near- and middle-infrared reflectances: Remote Sensing of Environment, v. 30, p. 43-54.

Idrisi, 1997, Idrisi for Windows, version 2, users guide: Clark Labs, Clark University, Massachusetts, 387 p.

Idrisi, 1999, Idrisi 32 Guide to GIS and image processing, Volume 1: Clark Labs, Clark University, Massachusetts, 193 p.

Jano, A.P., Jefferies, R.L., and Rockwell, R.F., 1998, The detection of vegetational change by multitemporal analysis of Landsat data: the effects of goose foraging: Journal of Ecology, v. 86, p. 93-99.

KGS, 1999, Geology of Leavenworth County, Kansas Geological Survey: Online, http://www.kgs.ukans.edu/General/Geology/County/klm/leavenworth.html

Kuchler, A. W., 1974, A new vegetation map for Kansas: Ecology, v. 55, p. 586-604.

Lott, J.N., 1994, The U.S. Summer of 1993 a sharp contrast in weather extremes: Weather, v. 49, no. 11, p. 370-383.

Lu, J., 1988, Development of principal component analysis applied to multitemporal Landsat TM data: International Journal of Remote Sensing, v. 9, no. 12, p. 1895-1907.

Muchoney, D. M., and Haack, B. N., 1994, Change detection for monitoring forest defoliation: Photogrammetric Engineering and Remote Sensing, v. 60, no. 10, p. 1243 - 1251.

Nang, K. N., 1998, Remote sensing and tree-ring study of forest conditions in northeastern Kansas [MSc. Thesis]: Emporia State University, Kansas, 67 p.

NASA, 1999, Nasa's Observatorium: Online, http://observe.ivv.nasa.gov/nasa/gallery/landsatapp/landsatapp.html

NCDC, 1999, Get/View Online Climate Data: Online, http://www.ncdc.noaa.gov/ol/climate/climatedata.html

Pinder, J. E. III, and McLeod, K.W., 1999, Indications of relative drought stress in longleaf pine from Thematic Mapper data: Photogrammetric Engineering and Remote Sensing, v. 65, no. 4, p. 495-501.

Rock, B. N., Vogelmann, J. E., Williams, D. L., Vogelmann, A. F. and Hoshizaki, T., 1986, Remote detection of forest damage. Bioscience, v. 36, no. 7, p. 439-445.

Rouse, J. W. Jr., Haas, R. H., Deering, D. W., Schell, J. A., and Harlan, J. C., 1974, Monitoring the vernal advancement and retrogradation (green wave effect) of natural vegetation: NASA/GSFC Type III Final Report, Greenbelt, MD., p. 371.

Singh, A., and Harrison, A., 1985, Standardized principal components: International Journal of Remote Sensing, v. 6, no. 6, p. 883-896.

Singh, A., 1989, Digital change detection techniques using remotely sensed data: International Journal of Remote Sensing, v. 10, p. 989 - 1003.

Stockton, C. W., and Meko, M.M., 1975, A long-term history of drought occurrence in Western United States as inferred from tree rings: Weatherwise, v. 28, no. 6. p. 244-250.

Thomas, J.R., Namken, L.N., Oerther, G.F. and Brown, R.G., 1971, Estimating leaf water content by reflectance measurements: Agronomy Journal, vol. 63, p. 845-847.

Townshend, J. R. G., Goff, T.E., and Tucker, C.J, 1985, Multitemporal dimensionality of images of Normalised Difference Vegetation Index at continental scales: IEEE Transactions on Geoscience and Remote Sensing, vol. GE-23, No. 6, p. 888-895

Tucker, C.J., 1980, Remote sensing of leaf water content in the near infrared: Remote Sensing of Environment, vol. 10, p. 23-32.

Wang, J., Rich, P. M., Price, K. P., and Kettle, D. W., 1999 a, Relations between NDVI and tree productivity in the Central Great Plains: submitted to Ecology.

Wang, J., Price, K. P., and Rich, P. M., 1999 b, Spatial patterns of NDVI response to precipitation and temperatures in the Central Great Plains: Submitted to International Journal of Remote Sensing.

Wang, J., Rich, P. M. and Price, K. P., 1999 c, Temporal response of NDVI to precipitation and temperatures in the Central Great Plains: Submitted to Remote Sensing of Environment.

Wilkins, N.H., 1997, Analysis of forest change at Fort Leavenworth, Kansas, using Landsat Thematic Mapper data [MSc. Thesis]: Emporia State University, Kansas, 83p.

Appendix 1

Documentation and Header File Example

Header File for July 2, 1997 scene

NDF_REVISION=0.00;

PRODUCT_NUMBER=01198012601040002;

DATA_FILE_INTERLEAVING=BSQ;

TAPE_SPANNING_FLAG=1/1;

START_LINE_NUMBER=1;

START_DATA_FILE=1;

BLOCKING_FACTOR=1;

MAP_PROJECTION_NAME=UTM;

USGS_PROJECTION_NUMBER=1;

USGS_MAP_ZONE=15;

USGS_PROJECTION_PARAMETERS=6378137.000000000000000,6356752.314140000400000,0.000000000000000,0.00000000000
0000,0.000000000000000,0.000000000000000,0.000000000000000,0.000000000000000,0.000000000000000,0.000000000000000,0.
000000000000000,0.000000000000000,0.000000000000000,0.000000000000000,0.000000000000000;

HORIZONTAL_DATUM=WGS84;

EARTH_ELLIPSOID_SEMI-MAJOR_AXIS=6378137.000;

EARTH_ELLIPSOID_SEMI-MINOR_AXIS=6356752.314;

EARTH_ELLIPSOID_ORIGIN_OFFSET=0.000,0.000,0.000;

EARTH_ELLIPSOID_ROTATION_OFFSET=0.000000,0.000000,0.000000;

PRODUCT_SIZE=FULL_SCENE;

RESAMPLING=CC;

PROCESSING_DATE/TIME=012798/03071500;

PROCESSING_SOFTWARE=NLAPS_3_0_4E;

DATA_SET_TYPE=EDC_TM;

PIXEL_FORMAT=BYTE;

PIXEL_ORDER=NOT_INVERTED;

BITS_PER_PIXEL=8;

PIXELS PER LINE=6858;

LINES PER DATA FILE=6499;

DATA_ORIENTATION=UPPER_LEFT/RIGHT;

NUMBER_OF_DATA_FILES=7;

LINES_PER_VOLUME=45493;

RECORD_SIZE=6858;

UPPER_LEFT_CORNER=0961538.8286W,0395156.2381N,221088.343,4417933.025;

UPPER_RIGHT_CORNER=0940121.3952W,0393208.8629N,412121.241,4376736.336;

LOWER_RIGHT_CORNER=0942636.9257W,0375400.0915N,373081.415,4195705.015;

LOWER_LEFT_CORNER=0963754.9272W,0381326.1739N,182048.516,4236901.704;

REFERENCE_POINT=SCENE_CENTER;

REFERENCE_POSITION=0952022.1716W,0385312.5680N,297084.879,4306819.020,3429.50,3250.00;

REFERENCE_OFFSET=-340.13.11.82;

ORIENTATION=12.169600;

WRS=027/033.0;

ACQUISITION DATE/TIME=070297/16303935;

SATELLITE=LANDSAT_5;

SATELLITE_INSTRUMENT=TM;

PIXEL SPACING=28.5000,28.5000;

PIXEL SPACING UNITS=METERS;

PROCESSING_LEVEL=08;

SUN_ELEVATION=61.76;

SUN_AZIMUTH=115.48;

NUMBER_OF_BANDS_IN_VOLUME=7;

BAND1_NAME=TM_BAND_1;

BAND1_WAVELENGTHS=0.45,0.52;

BAND1_RADIOMETRIC_GAINS/BIAS=0.6024314,-1.5200000;

BAND2_NAME=TM_BAND_2;

BAND2_WAVELENGTHS=0.52,0.60;

BAND2_RADIOMETRIC_GAINS/BIAS=1.1750981,-2.8399999;

BAND3_NAME=TM_BAND_3;

BAND3_WAVELENGTHS=0.63,0.69;

BAND3_RADIOMETRIC_GAINS/BIAS=0.8057647,-1.1700000;

BAND4_NAME=TM_BAND_4;

BAND4_WAVELENGTHS=0.76,0.90;

BAND4_RADIOMETRIC_GAINS/BIAS=0.8145490,-1.5100000;

BAND5_NAME=TM_BAND_5;

BAND5_WAVELENGTHS=1.55,1.75;

BAND5_RADIOMETRIC_GAINS/BIAS=0.1080784,-0.3700000;

BAND6_NAME=TM_BAND_6;

BAND6_WAVELENGTHS=10.40,12.50;

BAND6_RADIOMETRIC_GAINS/BIAS=0.0551582,1.2377996;

BAND7_NAME=TM_BAND_7;

BAND7_WAVELENGTHS=2.08,2.35;

BAND7_RADIOMETRIC_GAINS/BIAS=0.0569804,-0.1500000;

END_OF_HDR;

Documentation File for Band 1

```
file title  : Leavenworth - Full Scene July 02, 1997

data type   : byte

file type   : binary

columns     : 6858

rows        : 6499

ref. system : plane

ref. units  : km

unit dist.  : 1.0000000

min. X      : 0

max. X      : 205.74

min. Y      : 0

max. Y      : 194.97

pos'n error : unknown

resolution  : .03

min. value  : 0

max. value  : 255

value units : TM1

value error : unknown

flag value  : none
```

```
flag def'n  : none

legend cats : 0
```

- ❖ Columns = Pixels per line

- ❖ Rows = Lines per data file

- ❖ Ref. System set to **Plane**

- ❖ Reference Units were chosen to be kilometers

- ❖ Resolution of each cell rounded to 0.03 km

- ❖ Min X and Y set to 0

- ❖ Max X and Y calculated –

  - ➢ Max X = No. of columns * Resolution

  - ➢ Max Y = No. of rows * Resolution

Min. and Max values set to 0 and 255 respectively

Appendix 2

Old and New X, Y Coordinates and RMS Error for Resampling of

each Landsat TM Image

1987

Resample : Summary of Transformation

Computed polynomial surface : Linear   (based on 13 control points)

Coefficient	X	Y
b0	752.6578641568194140	-4460.3733879181090700
b1	1.0370557390843072	0.1987150170286789
b2	-0.2228156082681494	1.0441227543613678

Control points used in the transformation :

Old X	Old Y	New X	New Y	Residual
126.759500	156.039300	332.840000	4357.995000	0.043704
126.582900	156.753000	332.758000	4358.725000	0.050353
126.825200	155.442300	332.746000	4357.513000	0.085425
129.283500	157.178100	335.355000	4358.549000	0.051342
128.289900	158.746400	334.762000	4360.249000	0.037787
129.466200	158.710400	335.820000	4359.953000	0.027037
126.489400	158.416200	333.051000	4360.251000	0.041631
127.033000	157.278200	333.293000	4359.133000	0.050829
129.412200	154.274600	334.880000	4355.844000	0.068171
127.995800	153.098100	333.373000	4355.055000	0.019431
123.224500	160.427000	330.379000	4362.602000	0.057112
122.116800	155.512600	328.372000	4358.286000	0.049692
116.775800	151.314400	322.620000	4355.415000	0.009890

Overall RMS =   0.049387

1988

Resample : Summary of Transformation

Computed polynomial surface : Linear   (based on 13 control points)

Coefficient	X	Y
b0	761.7488271520123820	-4436.5860272830468600
b1	1.0342120361891674	0.1987402782371923
b2	-0.2218021204204490	1.0386880427501524

Control points used in the transformation :

Old X	Old Y	New X	New Y	Residual
139.337100	156.133300	332.840000	4357.995000	0.037487
139.155100	156.882000	332.758000	4358.725000	0.043256
139.365300	155.595000	332.746000	4357.513000	0.046320
141.853300	157.248100	335.355000	4358.549000	0.017383
140.866200	158.864500	334.762000	4360.249000	0.023919
142.003400	158.838600	335.820000	4359.953000	0.053178
139.035100	158.471500	333.051000	4360.251000	0.086962
139.605300	157.395700	333.293000	4359.133000	0.044558
141.975700	154.394700	334.880000	4355.844000	0.068388
140.531200	153.220000	333.373000	4355.055000	0.036415
135.791300	160.519400	330.379000	4362.602000	0.063485
134.686200	155.593100	328.372000	4358.286000	0.020527
129.370300	151.451100	322.620000	4355.415000	0.004738

Overall RMS =   0.047352

1989

Resample : Summary of Transformation

Computed polynomial surface : Linear   (based on 13 control points)

Coefficient	X	Y
b0	799.9532949600252320	-4428.8350949865416600
b1	1.0380387422929118	0.1997633996827943
b2	-0.2297794207197796	1.0368531707372455

Control points used in the transformation :

Old X	Old Y	New X	New Y	Residual
144.039500	156.189300	332.840000	4357.995000	0.075501
143.861800	156.972000	332.758000	4358.725000	0.044835
144.105500	155.679100	332.746000	4357.513000	0.059575
146.530200	157.365700	335.355000	4358.549000	0.044996
145.515900	158.950400	334.762000	4360.249000	0.045735
146.710300	158.896300	335.820000	4359.953000	0.018499
143.793400	158.596200	333.051000	4360.251000	0.043327
144.282000	157.482200	333.293000	4359.133000	0.043445
146.785700	154.611600	334.880000	4355.844000	0.203970
145.239600	153.230200	333.373000	4355.055000	0.105910
140.474100	160.598400	330.379000	4362.602000	0.059134
139.388200	155.715100	328.372000	4358.286000	0.053435
134.049300	151.539700	322.620000	4355.415000	0.011390

Overall RMS =   0.077849

1990

Resample : Summary of Transformation

Computed polynomial surface : Linear   (based on 13 control points)

Coefficient	X	Y
b0	752.6497059012181130	-4484.3897768690949300
b1	1.0365325213654515	0.1947413795394830
b2	-0.2195957587679089	1.0499408811094639

Control points used in the transformation :

Old X	Old Y	New X	New Y	Residual
140.623400	156.062900	332.840000	4357.995000	0.028653
140.438600	156.748000	332.758000	4358.725000	0.074709
140.687200	155.492900	332.746000	4357.513000	0.054789
143.143500	157.142400	335.355000	4358.549000	0.008638
142.151400	158.820600	334.762000	4360.249000	0.014847
143.295900	158.730600	335.820000	4359.953000	0.033021
140.355400	158.435200	333.051000	4360.251000	0.044316
140.859600	157.265000	333.293000	4359.133000	0.083970
143.266200	154.264600	334.880000	4355.844000	0.066574
141.825800	153.118500	333.373000	4355.055000	0.043803
137.103100	160.494800	330.379000	4362.602000	0.073222
135.946800	155.527300	328.372000	4358.286000	0.028636
130.626600	151.360200	322.620000	4355.415000	0.005926

Overall RMS =   0.049901

1991

Resample : Summary of Transformation

Computed polynomial surface : Linear   (based on 13 control points)

Coefficient	X	Y
b0	791.2149472861783580	-4456.8821813458926000
b1	1.0387512414151452	0.1957883811643324
b2	-0.2282968760033413	1.0436409136101617

Control points used in the transformation :

Old X	Old Y	New X	New Y	Residual
141.975300	156.435200	332.840000	4357.995000	0.068263
141.821000	157.151100	332.758000	4358.725000	0.070787
142.039600	155.925100	332.746000	4357.513000	0.021383
144.523500	157.548100	335.355000	4358.549000	0.011676
143.505600	159.166000	334.762000	4360.249000	0.031219
144.675900	159.110300	335.820000	4359.953000	0.019601
141.739600	158.835900	333.051000	4360.251000	0.025785
142.243000	157.693200	333.293000	4359.133000	0.049227
144.618500	154.692200	334.880000	4355.844000	0.076984
143.325600	153.524400	333.373000	4355.055000	0.068280
138.445600	160.866300	330.379000	4362.602000	0.076203
137.356800	155.927600	328.372000	4358.286000	0.043178
131.985500	151.756200	322.620000	4355.415000	0.028711

Overall RMS =   0.050987

1992

Resample : Summary of Transformation

Computed polynomial surface : Linear   (based on 13 control points)

Coefficient	X	Y
b0	777.3679389568860640	-4446.4994962428463600
b1	1.0332420603553914	0.1974636858800825
b2	-0.2239937098789824	1.0412287608200614

Control points used in the transformation :

Old X	Old Y	New X	New Y	Residual
145.063700	156.853700	332.840000	4357.995000	0.060485
144.880700	157.597800	332.758000	4358.725000	0.044942
145.127200	156.343000	332.746000	4357.513000	0.031546
147.568900	157.993600	335.355000	4358.549000	0.029784
146.592200	159.579100	334.762000	4360.249000	0.041477
147.735700	159.555800	335.820000	4359.953000	0.037138
144.789700	159.252900	333.051000	4360.251000	0.044951
145.331200	158.115200	333.293000	4359.133000	0.054024
147.670200	155.084600	334.880000	4355.844000	0.039312
146.385900	153.998200	333.373000	4355.055000	0.090673
141.565600	161.278800	330.379000	4362.602000	0.080246
140.446800	156.347600	328.372000	4358.286000	0.038303
135.101100	152.172400	322.620000	4355.415000	0.031032

Overall RMS =   0.051318

1994

Resample : Summary of Transformation

Computed polynomial surface : Linear   (based on 13 control points)

Coefficient	X	Y
b0	802.5320316194556650	-4456.0714236693456800
b1	1.0373324383005311	0.1977174026858588
b2	-0.2303476542495417	1.0433721804889160

Control points used in the transformation :

Old X	Old Y	New X	New Y	Residual
143.894100	156.706200	332.840000	4357.995000	0.064700
143.710700	157.450800	332.758000	4358.725000	0.046762
143.956500	156.195000	332.746000	4357.513000	0.031103
146.445900	157.841200	335.355000	4358.549000	0.027714
145.395600	159.453100	334.762000	4360.249000	0.034764
146.566200	159.406400	335.820000	4359.953000	0.032123
143.652800	159.103500	333.051000	4360.251000	0.040830
144.163000	157.968200	333.293000	4359.133000	0.057446
146.536200	154.964600	334.880000	4355.844000	0.061087
145.215900	153.818100	333.373000	4355.055000	0.053153
140.348500	161.135100	330.379000	4362.602000	0.069849
139.238100	156.225100	328.372000	4358.286000	0.057430
133.928300	152.011700	322.620000	4355.415000	0.024742

Overall RMS =   0.048566

1997

Resample : Summary of Transformation

Computed polynomial surface : Linear   (based on 13 control points)

Coefficient	X	Y
b0	774.5360570720513350	-4452.9534113972331400
b1	1.0331144934355407	0.1978436018228074
b2	-0.2269860607676293	1.0427903481306373

Control points used in the transformation :

Old X	Old Y	New X	New Y	Residual
129.165200	157.362800	332.840000	4357.995000	0.030005
128.955200	158.082500	332.758000	4358.725000	0.036468
129.223400	156.856900	332.746000	4357.513000	0.018395
131.685900	158.445500	335.355000	4358.549000	0.019679
130.670000	160.070300	334.762000	4360.249000	0.032457
131.805900	160.040300	335.820000	4359.953000	0.043074
128.895700	159.697100	333.051000	4360.251000	0.069270
129.402000	158.595400	333.293000	4359.133000	0.052915
131.777100	155.564300	334.880000	4355.844000	0.034124
130.425600	154.450100	333.373000	4355.055000	0.040891
125.613100	161.766300	330.379000	4362.602000	0.077451
124.514200	156.825100	328.372000	4358.286000	0.033725
119.214700	152.635400	322.620000	4355.415000	0.025012

Overall RMS =   0.043022

Appendix 3

Examples of Macro used in Resampling Images

Example of macro used for RESAMPLE (georeferencing images)

resample x i hz9702-1 re9702-1 9702 us27tm15 km 1.0 0.0 319.6 342.5 4348.0 4366.9 763 630 1 1

resample x i hz9702-2 re9702-2 9702 us27tm15 km 1.0 0.0 319.6 342.5 4348.0 4366.9 763 630 1 1

resample x i hz9702-3 re9702-3 9702 us27tm15 km 1.0 0.0 319.6 342.5 4348.0 4366.9 763 630 1 1

resample x i hz9702-4 re9702-4 9702 us27tm15 km 1.0 0.0 319.6 342.5 4348.0 4366.9 763 630 1 1

resample x i hz9702-5 re9702-5 9702 us27tm15 km 1.0 0.0 319.6 342.5 4348.0 4366.9 763 630 1 1

resample x i hz9702-7 re9702-7 9702 us27tm15 km 1.0 0.0 319.6 342.5 4348.0 4366.9 763 630 1 1

The arguments for this macro are:

x batch mode, i image file, input file name, output file name, correspondence file name, new reference system, new reference units, new unit distance, background value, minimum X, maximum X, minimum Y, maximum Y, number of columns, number of rows, mapping function (1=linear / 2=quadratic / 3=cubic), resampling type (1=nearest neighbor / 2=bilinear)

This macro can easily be modified for other image sets.

Appendix 4

Principal Component Analyses with 1989 Cloud Covered Image

The plots of precipitation and PDSI shown in Fig. 42 indicate that the lowest values over the study period, occurred in the 12-month period from July 1988 to June 1989. For analysing these NDVI images, the contribution of the 1989 image was therefore of interest. However, because of the cloud cover on the 1989 image, there was difficulty in working with this dataset. PCA analyses were carried out separately with two datasets. One dataset included the 1989 NDVI image while the other did not. The 1992 image was excluded from both.

The results are displayed in Figs. 74 and 75. These show similar results for both forests. Dark brown areas indicate lowest NDVI values increasing to the highest values in dark green. Background color is zero. The loadings and images for components 1 and 2 show a significantly lower value in 1989. The component 1 images show the typical high NDVI values common to all images in the dataset. Pale green areas represent the parts of the forest covered by clouds and shadows. Component 2 shows positive loadings for 1989 and the images show the clouds and shadows in dark brown. This component isolates the clouds and shadows.

With the removal of the clouds and shadows in component 2, component 3 therefore becomes the first real change component. A comparison with the loadings and images of components 3 and 4 for both forests indicate that these are equivalent to components 2 and 3 of the dataset without the 1989 images which are discussed in Chapter 4.
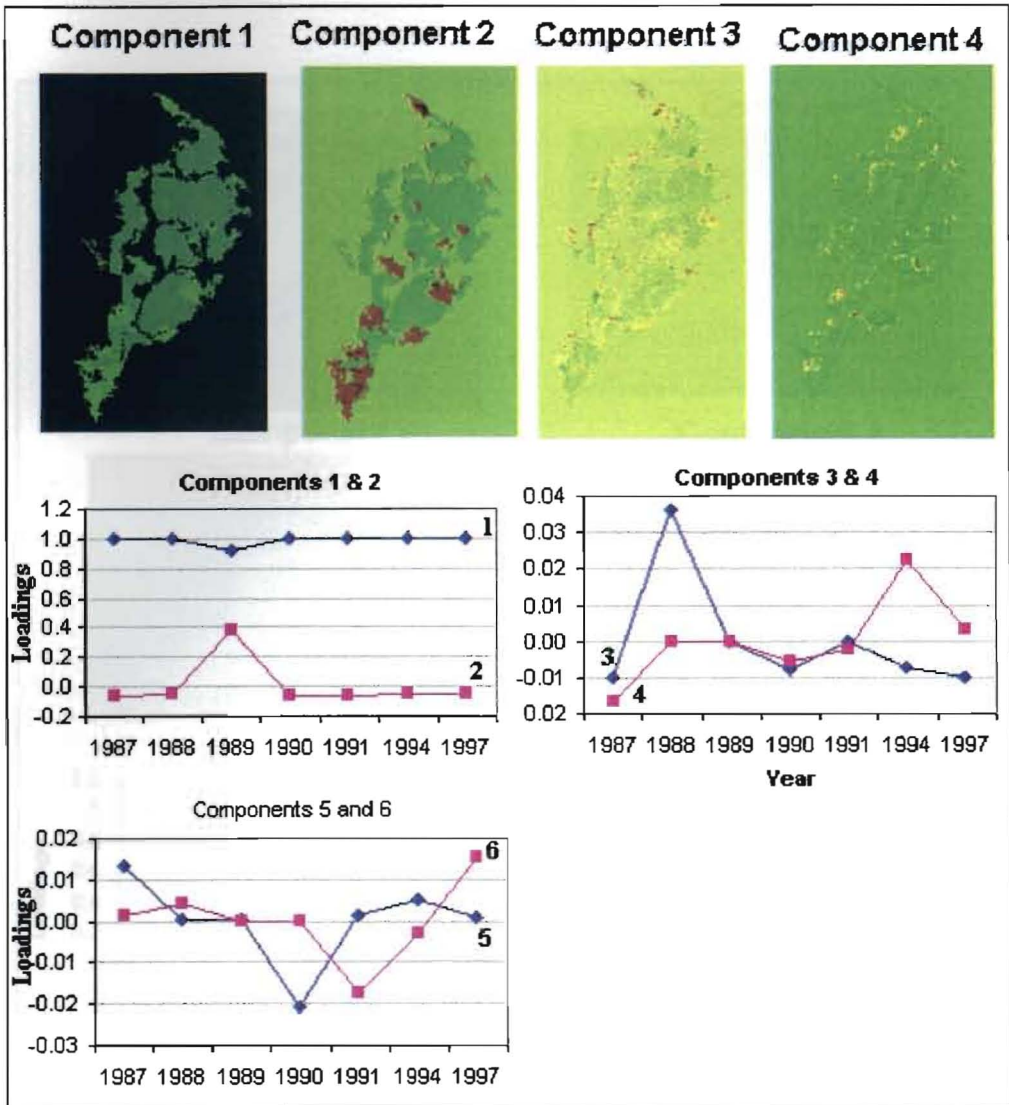
Fig. 74. Loadings and images for components of PCA analysis of the upland hardwood forest, using the 1989 NDVI image.
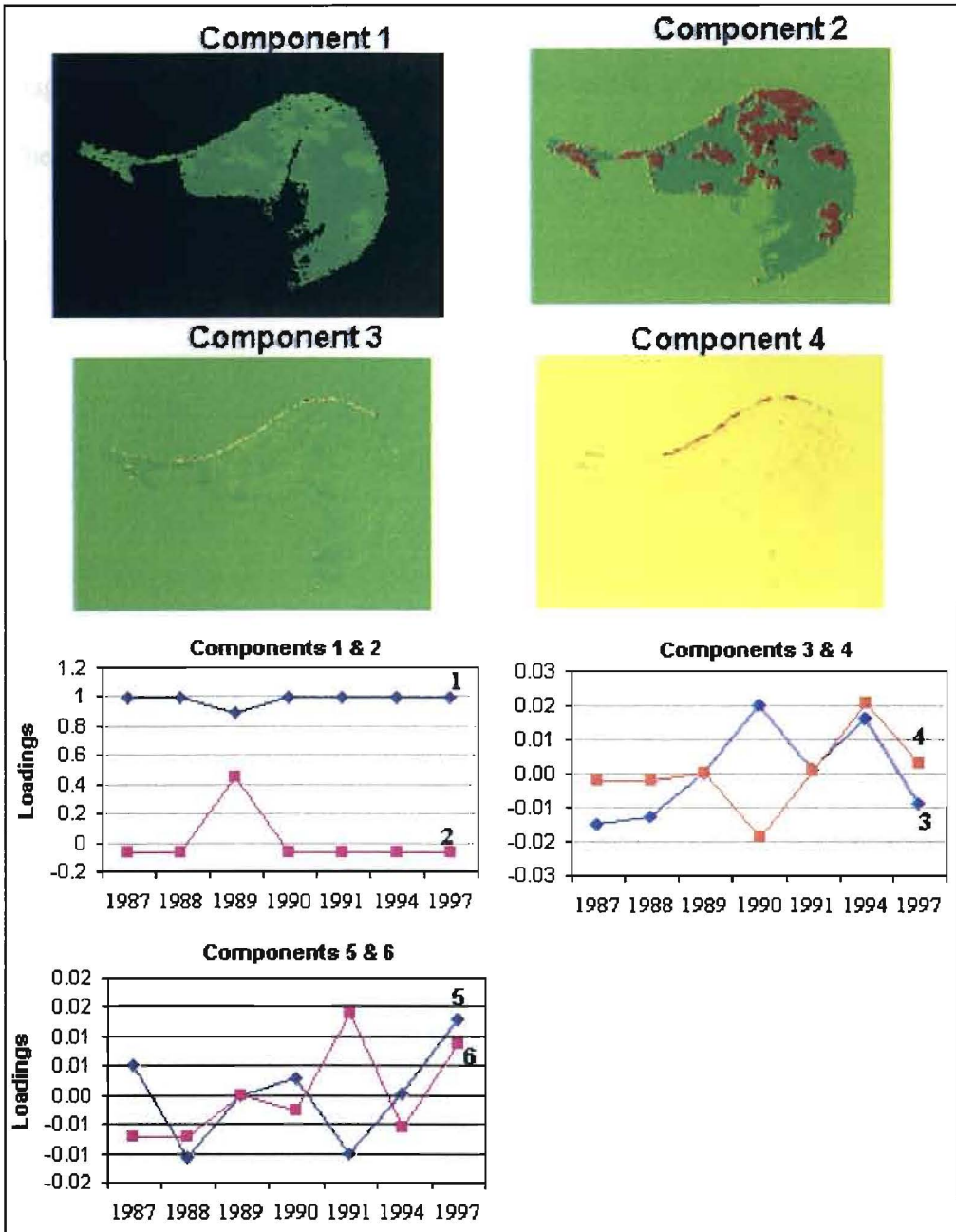
Fig. 75. Loadings and images for components of PCA analysis of the floodplain cottonwood forest, using the 1989 NDVI image.

Apart from component 2, no other component had a significant correlation with the 1989 NDVI image. It was therefore decide to complete the studies of principal components without the 1989 image, with no effect on the final results.

Publication Rights

I, _Juliet A. Wallace_ , hereby submit this thesis to Emporia State University as partial fulfillment of the requirements for an advanced degree. I agree that the library of the University may make it available for use in accordance with its regulations governing materials of this type. I further agree that quoting, photocopying, or other reproduction of this document is allowed for private study, scholarship (including teaching), and research purposes of a nonprofit nature. No copying which involves potential financial gain will be allowed without written permission of the author.

_____
Signature of Author

_____
Date

Temporal Studies of Deciduous Forests in
Northeastern Kansas Using Landsat
Thematic Mapper Images

_____
Title of Thesis/Research Project
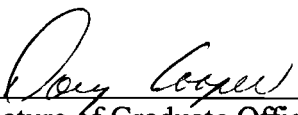
_____
Signature of Graduate Office Staff Member

_____
Date Received

Distribution: Director, William Allen White Library
                Graduate School Office
                Author